SCHOOL OF CIVIL ENGINEERING

JOINT HIGHWAY RESEARCH PROJECT

FHWA/IN/JHRP-81/4

PREDICTION AND CONTROL OF FIELD SWELL PRESSURES OF COMPACTED MEDIUM PLASTIC CLAY

Gregory M. Terdich

PURDUE UNIVERSITY
INDIANA STATE HIGHWAY COMMISSION

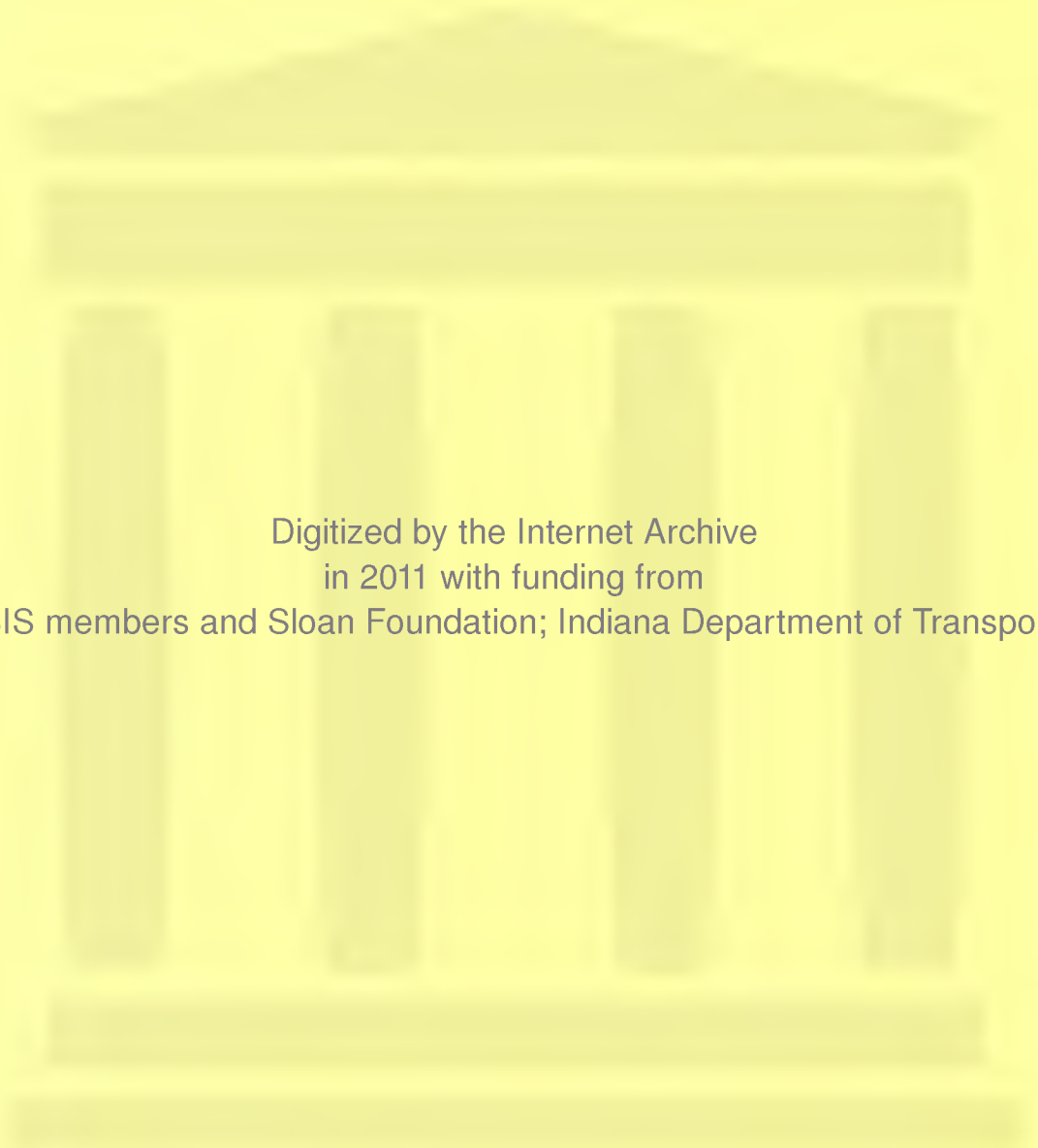

Interim Report

PREDICTION AND CONTROL OF FIELD SWELL PRESSURES OF COMPACTED MEDIUM PLASTIC CLAY

TO: H. L. Michael, Director
Joint Highway Research Project

March 17, 1981

Project: C-36-5M

FROM: A. G. Altschaeffl, Research Engineer
Joint Highway Research Project

File: 6-6-13

The attached Interim Report is submitted on the HPR Part II Study titled "Improving Embankment Design and Performance". This is the 8th Interim Report and is titled, "Prediction and Control of Field Swell Pressures of Compacted Medium Plastic Clay." It has been authored by Gregory M. Terdich of our staff.

This report addresses the swelling pressure response of a medium plastic clay compacted both in the laboratory and in the field. A procedure is developed which enables the engineers to select compaction variables to control the swelling pressure to a desired maximum value. Additionally, a procedure is presented to allow prediction of maximum swelling pressure for a field soil knowing inspection test results. Research continues on the project to develop similar procedures for the field behavior properties of compressibility and strength for this soil. In addition research is being conducted into the validation of these prediction procedures as well as their inclusion into conventional engineering embankment analysis.

The report is submitted in partial fulfillment of the objectives of this study, and completes Tasks FF and GG of the project's work plan. Following acceptances by the JHRP Board, it will be forwarded to ISHC and FHWA for review, comment, and similar acceptance.

Respectfully submitted,

A. G. Altschaeffl

A. G. Altschaeffl
Research Engineer

AGAmag

cc: A. G. Altschaeffl
W. L. Dolch
R. L. Eskew
G. D. Gibson
W. H. Goetz
M. J. Gutzwiller
G. K. Hallock
D. E. Hancher
K. R. Hoover
J. F. McLaughlin
R. D. Miles
P. L. Owens
G. T. Satterly
C. F. Scholer
K. C. Sinha
C. A. Venable
H. P. Wehrenberg
L. E. Wood
E. J. Yoder
S. R. Yoder

Interim Report

PREDICTION AND CONTROL OF FIELD SWELL PRESSURES OF COMPACTED MEDIUM PLASTIC CLAY

by

Gregory M. Terdich
Graduate Instructor in Research

Joint Highway Research Project

Project No.: C-36-5M

File No.: 6-6-13

Prepared as Part of an Investigation

Conducted by

Joint Highway Research Project
Engineering Experiment Station
Purdue University

in cooperation with the

Indiana State Highway Commission

and the

U.S. Department of Transportation
Federal Highway Administration

Purdue University
West Lafayette, Indiana
March 17, 1981

TECHNICAL REPORT STANDARD TITLE PAGE

1. Report No.	2. Government Accession No.	3. Recipient's Catalog No.
FHWA/IN/JHRP-81/4		

4. Title and Subtitle	5. Report Date
PREDICTION AND CONTROL OF FIELD SWELL PRESSURES OF COMPACTED MEDIUM PLASTIC CLAY	March 17, 1981
	6. Performing Organization Code
7. Author(s)	8. Performing Organization Report No.
Gregory M. Terdich	JHRP-81-4
9. Performing Organization Name and Address Joint Highway Research Project Civil Engineering Building Purdue University West Lafayette, Indiana 47907	10. Work Unit No.
	11. Contract or Grant No. HPR-1(18), Part II
12. Sponsoring Agency Name and Address Indiana State Highway Commission State Office Building 100 North Senate Avenue Indianapolis, Indiana 46204	13. Type of Report and Period Covered Interim Report
	14. Sponsoring Agency Code

15. Supplementary Notes

Prepared in Cooperation with the U.S. Department of Transportation, Federal Highway Administration. From research study titled, "Improving Embankment Design and Performance."

16. Abstract

This study investigates the swelling pressure response of a medium plastic clay (AASHTO A-6) compacted both in the field and in the laboratory. Correlation was attempted to provide a prediction process for the field result.

Swelling pressure was controlled by water content deviation from optimum, compactive effort, dry density, and various interactions among these terms. Regression models for laboratory and field results are different.

Variability in dry density and swelling pressure was sizeable but predictable, with the field variability being larger.

Prediction models were developed for expected average and maximum swelling pressure. Charts enable the engineer to select the compaction variables that will control the swelling pressure to a desired maximum value.

A computer program creates tabulations allowing the prediction of maximum swelling pressure for a field soil knowing inspection testing results.

17. Key Words	18. Distribution Statement
soil compaction; swelling pressure; compacted soil; soil variability; field behavior prediction; specification procedure	No restriction. This document is available to the public through the National Technical Information Service, Springfield, Virginia 22161

19. Security Classif. (of this report)	20. Security Classif. (of this page)	21. No. of Pages	22. Price
Unclassified	Unclassified	186	

Form DOT F 1700.7 (8-69)

ACKNOWLEDGMENTS

The author would like to express his sincere thanks and appreciation to Prof. A. G. Altschaeffl for his constructive advice and guidance during the course of this investigation. Special thanks goes to Prof. R. D. Holtz for his counsel and helpful review of the manuscript.

Thanks are due to Prof. George McCabe and graduate student Terry Dailey for their help and recommendations in developing the statistical analysis used in this study.

The assistance of Dr. R. Aubrey Abeyesekera in the Laboratory and at the St. Croix test pad is greatly appreciated. The author is grateful for the time and effort offered at the test pad site by fellow graduate students M. Suri Surendra, Albert DiBernardo, Barney Hale, James Johnson, Robert Stetkar, David Weitzel, and Gary Witsman.

Mr. Dean White is specially thanked for his assistance as a research partner. His companionship, and that of Mr. M. Suri Surendra, will not be forgotten.

Special thanks are in order for the secretarial work done by Mrs. Edith Vanderwerp and Ms. Cathy Minth. Mrs. Carole Montgomery typed the thesis and Mr. Donald Hogancamp did the drafting work.

The author appreciates the financial support provided by the Joint Highway Research Project of Purdue University, the Indiana State Highway Commission, and the Federal Highway Administration.

TABLE OF CONTENTS

LIST OF TABLES

LIST OF FIGURES

LIST OF SYMBOLS AND ABBREVIATIONS

AASHTO	American Association of State Highway and Transportation Officials
ASTM	American Society for Testing and Materials
cm	centimeter
CVS	constant volume swell
E_R	energy ratio
ft	foot
in	inch
I_p	plasticity index
ISHC	Indiana State Highway Commission
kg	kilogram
kPa	kilopascal
lb	pound
m	meter
mm	milimeter
mph	miles per hour
MSE	error mean square (or mean square error)
OMC	optimum moisture content
OMC_p	predicted field optimum moisture content
pcf	pounds per cubic foot
psi	pounds per square inch
R^2	coefficient of multiple determination

SP	swell pressure
SP_{max}	maximum swell pressure
$\hat{SP}$	expected swell pressure
$\hat{SP}_{max}$	expected maximum swell pressure
SPSS	Statistical Package for the Social Sciences
$V(\hat{SP})$	expected variability of swell pressure
$V(\Delta w)$	variability of water content deviation from OMC
$V(\hat{\gamma}_d)$	expected variability of dry density
w	absolute water content
Δw	water content deviation from optimum moisture content
w_L	liquid limit
w_p	Plastic limit
w_S	shrinkage limit
γ_d	dry density
γ_{dmax}	maximum dry density
$\hat{\gamma}_d$	expected dry density
γ_p	predicted field dry density
γ_{pmax}	predicted field maximum dry density

HIGHLIGHT SUMMARY

Compaction, the mechanical densification of soil, is an effective means of improving the behavior properties of soil in the field. While it improves the overall integrity of the soil mass, compaction can also induce the tendency to swell in many fine grained soils. This swelling can result in a lowered soil strength or damage to structures placed on or in the fill.

It is the desire of the geotechnical engineer to quantitatively predict and control the overall performance of field compacted soil. The state-of-the-art suggests that the behavior of laboratory compacted soil can be extrapolated to field soil compacted at a similar water content (relative to optimum water content) and to a similar dry density. Data indicate that such extrapolations are often poor. As an alternative to this method, test embankments can be constructed, but these are usually too costly for small scale projects.

This study investigates the swell pressure response of a medium plastic clay (AASHTO A-6) compacted both in the field and in the laboratory. Field compaction was achieved using a Caterpillar Model 825 compactor and a RayGo Rascal Model 420C vibratory roller; Proctor impact and Hveem-type kneading procedures were employed in the laboratory. Three energy levels and various molding water contents were used for each compactor type to study their effects on swell pressure behavior.

Constant volume swell tests were performed in two benchtop consolidometers.

Statistical regression models were found for dry density and swell pressure response for each compactor type. In general, these relationships were influenced by water content deviation from optimum moisture content, compactive effort, dry density (swell pressure models only), and various interactions of these terms. The field compactors produced dissimilar swell pressure models; the laboratory methods produced very similar models, but these were quite different from the field models.

Variability of the dry density and swell pressure magnitudes was found to be sizeable but predictable. Field samples exhibited larger variabilities than laboratory compacted samples. Larger uncertainty in the independent regression variables caused an increase in the dry density and swell pressure variabilities.

Prediction models were designed to provide expected average and maximum values for field swell pressure response. The expected maximum swell pressure is the sum of the expected mean and the expected variability of swell pressure. The prediction models are presented in graphical form for use by the design engineer. These charts enable the engineer to select compaction variables that will ultimately control the field swell pressure to a predetermined maximum value.

The prediction models are also presented in computer tabulation format. The tables contain values of the compaction variables and their uncertainty, the expected mean swell pressure, and the variability associated with it. This format is more suitable for quality

control work and evaluation of swell pressure behavior for compaction projects under construction.

A user's guide was developed and is entitled "Application of Results." By use of an example and commentary, it indicates how the results of this study can be used in both engineering design and quality control work. Also, a method is proposed for applying the results of this study to A-6 soils that may have somewhat different compaction characteristics.

INTRODUCTION

The design of many engineering structures incorporates the use of compacted soil. Some projects utilize compacted fills to improve foundation conditions; others, such as dams and highways, rely on earth embankments to achieve their intended purpose. Proper use of compacted soil ensures both safe and economical design of long-life structures.

The compaction process itself mechanically densifies soil by expelling air from the voids at an essentially constant water content. The most readily apparent product of this process is an increase in soil density. However, this increased density is not the sole or ultimate goal of the engineer. Rather, he intends to improve the in-service behavior of the soil. This improvement may require an increase in the soil strength, a decrease of its compressibility or, possibly, a reduction in the permeability of the soil mass.

In current practice the compaction specification is written in terms of the end result, i.e., the required, as-compacted soil density achieved within a limited range of water content. Characteristics of the field compaction equipment are also sometimes specified. In most cases, these specified requirements are based on results of standard laboratory compaction tests; these tests provide the basis for quality control. Unfortunately, the state-of-the-art practice

does not specify the actual behavior properties to be achieved. Instead the engineer must infer these properties through proper selection of as-compacted density, water content range, and field compactor type.

The foregoing specification controls only the as-compacted nature of the soil. It is only by additional inference that the engineer includes the environmental changes which occur over the life of the structure. Such service-life changes include the consolidation of the soil mass under the weight of successive lifts as well as additional volume changes induced by an increased saturation of the soil (i.e., swell or collapse).

An effort is being made to better predict the behavior of the field compacted soil. This endeavor includes the testing of the same soil compacted both in the laboratory and in the field. The samples are tested for strength, compressibility, and volume change behavior, and a correlation between the results obtained from lab and field compacted samples is then produced for each type of behavior. It is intended to quantitatively predict the field behavior, with data acquired from laboratory compacted samples, by using these correlations. In addition, an effort is made to enable the selection of the correct state-of-the-art compaction specification which produces a field mass exhibiting the desired behavior parameters.

Several studies have already been undertaken on a silty clay and a medium plastic clay. Essigmann (1976), Scott (1977), and Price (1978) have conducted studies of soil strength for the silty clay. For the more plastic clay (St. Croix clay), DiBernardo (1979) has studied

the compressibility in both the as-compacted state and after saturation. As-compacted shear behavior has been investigated by Weitzel (1979), while Johnson (1979) has examined the shear behavior after saturation and consolidation; both of these studies were conducted at various confining pressures. The compressibility and as-compacted shear behavior for field compacted samples are currently under investigation. White (1980) has recently completed a study of the effects of field and laboratory compaction on the differences produced in the soil fabric, as suggested by pore-size distribution parameters.

The study reported herein concerns itself with the soil's tendency to swell, a behavior which the compaction process induces. This phenomenon has been described by Ladd (1959) and it definitely affects the long-term behavior of the compacted mass. The tendency to swell is measured in terms of the swelling pressure that develops while the soil remains at a constant total volume in the presence of free water. This investigation examines both laboratory and field compacted material. Statistical correlation techniques relate the tendency to swell with the respective compaction procedures and variables.

The ultimate goal of this investigation is to predict the field behavior of the compacted mass, i.e., its tendency to swell. It also investigates the selection of compaction specifications which explicitly control the swelling phenomenon to tolerable levels. It is hoped that the engineer can use these results to quantitatively specify a compacted soil mass which exhibits the desired behavior. For specifications which have not been prepared in this manner, results

are presented that can be used for quality control testing and for prediction of swell pressures induced by the compaction process.

1 - LITERATURE REVIEW

Mechanisms of Compaction and As-Compacted Soil Structure

Proctor (1933) gave one of the first descriptions of the compaction process, the variables which affect this process, and the changes in soil structure that result from it. He postulated that densification occurred when the compacting force overcame the frictional resistance between soil particles. His concept of structure dealt with particle spacing, rather than degree of particle orientation. In his theory water acted as a lubricant between particles; a change in water content resulted in a different particle spacing for a given method of compaction.

Proctor also noted the influence of compactive effort on particle spacing. He stated the need to select the proper type of construction equipment, as well as an appropriate moisture content, to ensure proper performance of a compacted soil mass. Proctor developed procedures for standard compaction tests and the penetration resistance needle that are still used in engineering practice today.

Physico-chemical concepts were used by Lambe (1960) to explain the structure and engineering behavior of compacted clays. Under this theory, individual clay particles govern the behavior of the compacted soil. Because of their minute size, clay particles are

dominated by electrical forces rather than mass forces. The negatively charged clay particles attract cations and polar water molecules to them. The swarm of counterions and water is called the diffuse double layer,* and the clay particle plus the double layer is termed the micelle.

In his theory of compaction, Lambe (1960) introduced the concept of water deficiency. This idea stated that, "Any given soil particle under any given state of stress requires a certain amount of water to develop fully its double layer." This deficiency gives rise to negative pore water pressures in compacted soil, and the soil will try to imbibe enough water to satisfy its deficiency.

For compaction at low moisture contents the double layers are depressed. This reduces interparticle repulsions and flocculation occurs. Therefore, a flocculated structure with a low degree of particle orientation characterizes clay soils compacted at low moisture contents. As the molding water content is increased, Lambe postulates that double layers expand and interparticle repulsions increase. This causes a more orderly (parallel) arrangement of particles and therefore a higher density. Above OMC the particles achieve an even more orderly arrangement, but the double layers are large enough to reduce the concentration of soil particles per unit of volume. This causes a decrease in dry density.

An increase in compactive effort results in higher densities by causing a more parallel arrangement and closer spacing of the clay particles. At high molding water contents, however, the effect may

---

*Diffuse double layer, diffuse layer, and double layer are used interchangeably in the literature and also in this report.

be to merely align the particles without significantly changing the particle spacing.

The descriptions and hypotheses given above are based on the Gouy-Chapman theory for electrical potential in the double layer. Lambe (1960) noted that real soils do not conform to assumptions made in the Gouy-Chapman theory, and this limits its application. He also pointed out that the variation of structure with molding water content depends on the particular soil. Some soils may exhibit only a slight improvement of orientation with increasing water content, while others may become fully dispersed at low moisture. Soils with intermediate responses also exist.

Seed and Chan (1961) agreed in principle to Lambe's (1960) hypotheses about the effects of a soil's structure on its engineering behavior and to his theory of compaction. After conducting their own testing programs, however, Seed and Chan offered some additions and modifications to Lambe's proposals. For compaction at low moisture contents, they agreed with Lambe's hypothesis. At higher water contents, however, Seed and Chan stated that, "In many cases it is the progressive increase in shear deformation (for a constant compaction effort) as the water content is increased which is largely responsible for the progressive increase in the degree of orientation of the clay particles."

The results of their testing program led to the following conclusions:

1) For samples prepared dry of OMC, all methods of compaction produced no appreciable shear deformations, and essentially flocculated structures resulted in all cases.

2) For samples of the same composition prepared wet of OMC, the method of compaction had a pronounced influence on the resulting structure.

3) Kneading compaction wet of OMC produced the highest shear strain during compaction and, therefore, the most dispersed structure. An increase in the foot penetrations resulted in an even higher degree of orientation.

4) Impact compaction wet of OMC caused slightly less shear strain and a lower degree of dispersion than kneading compaction. However, these differences were small.

5) Static compaction produced little shear deformation during compaction both wet and dry of optimum. A relatively flocculated structure resulted in all cases.

6) Vibratory compaction also produced small shear strains during compaction. The structure was similar to that for static compaction, but slightly more dispersed. Apparently the vibrations enabled the particle to achieve a higher degree of orientation.

7) The magnitude of structural changes resulting from an increase in molding water content was dependent on the soil type. Lambe (1960) also noted this.

An effective stress theory of compaction has been proposed by Olson (1963) for kneading compaction. This theory successfully explained the densification process in terms of changes in effective stresses, pore water pressures, and shearing strength of the soil. Olson believed that physico-chemical variables controlled the shape of the compaction curve, and therefore the resulting as-compacted soil structure. He also noted reasons why impact compaction can be used well above OMC but kneading methods cannot; this latter effect was observed in this study.

Nalezny and Li (1967), Barden and Sides (1970), and Hodek (1972) offer a deformable aggregate model to explain the compaction process. Due to electric forces between individual clay particles,

the particles combine to form aggregates.* These authors state that the behavior of these aggregates governs the soil's response to the compaction process. The particles within each aggregate may assume a flocculated or dispersed structure, however, depending on water content, type of soil, type of compaction, and other factors previously mentioned.

At low moisture contents, the individual aggregates are quite strong and do not readily deform into the available pore space when the compactive effort is applied. This results in many large pores between the aggregates (macropores). As the water content is increased, the aggregates become softer and can deform more easily into the spaces between them. This increases the density and the macropores become smaller. Near optimum moisture content these factors produce their maximum effect; maximum dry density is achieved, the macropores are nearly filled with water, and the air voids become discontinuous. Above OMC an increase in water content enlarges the pore volume and dry density decreases.

The authors postulate that the structure within aggregates changes from a flocculated to a more dispersed structure as water content is increased. Barden and Sides (1970) used the scanning electron microscope to study this concept for kaolin and a naturally occurring clay. For both clays at low magnifications (110X), individual peds were visible at moisture contents below optimum but were not observable at water contents above OMC. At high magnifications (9500X)

---

*The literature also refers to these groups of particles as clusters, peds, macropeds, and soil crumbs.

both clays exhibited an essentially dispersed structure both wet and dry of OMC; the natural clay appeared to be somewhat more flocculated dry of OMC, however.

Young and Sheeran (1973) stated that "Examination of electron micrographs and soil performance shows that individual particles rarely act as single particle units. . . . The different sizes and arrangements of particle groups observed in fabric viewing suggest that response behavior might be controlled by the kinds and arrangements of these particle groups." These observations lend support to the deformable aggregate model of soil.

Pore size distribution measurements of laboratory compacted clays were conducted by Diamond (1970 and 1971), Sridharan et al. (1971), Ahmed et al. (1974), Bhasin (1975), Reed et al. (1979), and Garcia-Bengochea et al. (1979). These tests were performed on kaolin, illite, Boston blue clay, and other types of clay. Results from these studies were in general agreement and found that dry of OMC, more pore space is found in the relatively large pores. Bhasin (1975) found that an increase in compactive effort dry of OMC decreased the porosity and quantity of large pores, while wet of OMC it had little effect on the porosity or pore size distribution. These results are in agreement with the deformable aggregate soil model.

White (1980) conducted pore size distribution measurements on the St. Croix clay used in this study. Laboratory samples were prepared by impact and kneading compaction, and field samples were compacted using a Caterpillar Model 825 roller and a RayGo Rascal Model 420C roller. The following conclusions were made from his study:

1) More pore space is found in the relative large pores dry of OMC for all compactors.

2) Laboratory fabric and field fabric are different.

3) Impact and kneading compaction produce the same fabric. Ahmed et al. (1974) also found this to be true for Grundite samples.

4) Differences in fabric exist on the dry side only between the Rascal and Caterpillar field compacted samples.

These conclusions are in general agreement with the deformable aggregate model. It should also be pointed out that White (1980) conducted the first known study of pore size distributions in field compacted soil.

From the literature it can be seen that every compaction variable can have an effect on the resulting soil structure. The micro- and macrostructure of compacted clay appear to be intimately related to each other, as well as to the subsequent behavior of the compacted soil. Factors causing changes in structure should ultimately be observed to cause changes in the measured behavior response.

The molding water content is very important in controlling the as-compacted structure. Differences in structure have been shown to be most pronounced when dry-side structures are compared with those produced by wet-side compaction. Therefore, it is reasonable to expect different swell pressure relationships for samples compacted dry of OMC when compared to those for wet-side samples.

Seed and Chan (1961) found that different methods of laboratory compaction can result in different structures and behavior. Based on this, one can expect field and laboratory compaction to likewise produce different structures and behavior. White (1980) found this to be true for soil fabric.

Based on the information presented in the literature, a comprehensive study of field swell pressure behavior should contain several features. The range in water content should produce sufficient data for wet-side and dry-side relationships to be investigated. As noted by Price (1978) variations in compaction variables and behavior response should be measured and accounted for in the analysis. The effects of different types of field compaction equipment should be investigated. Field relationships should be compared with those of laboratory samples to determine if a large difference in their as-compacted structures exists.

Mechanisms of Swelling

Theories of swelling usually account for this phenomenon at the particle level. For a saturated clay, Ladd (1959) proposed that osmotic pressures between clay particles are largely responsible for clay swelling. Osmotic pressures exist when an aqueous solution is separated from pure water (or a solution of different concentration) by a semi-permeable membrane. The water tends to pass through the membrane to dilute the solution. The pressure required to prevent this flow in termed the "osmotic pressure" of the solution.

For clay particles, the concentration of cations in the double layer is higher than in the surrounding free water. These cations are held in the double layer by the negative charge on the clay particles. This negative electric field acts as a semi-permeable membrane by allowing water to enter the double layer and by preventing the ions from leaving it.

Free water, if present, attempts to enter the double layer in order to neutralize the difference in ion concentration. If water enters, the double layer expands and the interparticle spacing increases; i.e., swelling occurs. An effective stress equal to the osmotic pressure is required to prevent this swelling, and is termed the swelling pressure. The osmotic pressure can be calculated from the van't Hoff equation

$$P_o = RT(C_c - C_o)^2$$

where P_o = osmotic pressure, R = gas constant, T = absolute temperature, C_o = ion concentration in the free pore water, and C_c = ion concentration in the central plane between particles. Bolt (1956) used this equation and the Gouy-Chapman theory of the electric double layer to calculate interparticle spacings for illite and montmorillonite suspensions. Ladd (1959) cautioned that real soils are far from the ideal system used in these theories, and the theories should be used only in a qualitative manner for real soils. He noted that the influence of the negative electric field and van der Waals forces on the double layer water could also be partially responsible for swelling in clay-water systems.

Seed, Mitchell, and Chan (1961) observed that mechanical components of swelling can also exist. While the elastic compression of solid clay particles is probably insignificant within the practical range of loadings, volume changes resulting from the bending of platy clay particles may be appreciable. They stated that, "By making reasonable assumptions concerning moduli of elasticity, it may be shown

that a typical clay plate, acting as a simple beam between other particles, may be held by menisci in a deformed state where the deflection is about 10 percent of the span."

To prove the existence of these effects, they compacted several identical samples at a high water content and allowed them to swell in calcium acetate solutions of various concentrations. At high electrolyte concentrations a constant value of about 1.1% swell occurred. This swelling was attributed to mechanical factors since osmotic pressures and water adsorptive forces were negligible for these test conditions.

Ladd (1959) and Seed et al. (1961) suggested that air can also play a role in the swelling behavior of compacted clays. If the air is initially at atmospheric pressure and there are many interconnected tubular air voids, water entering the soil from all directions will cause the air to compress and exert a pressure along the walls of the voids. If the soil structure cannot withstand this pressure an expansion may occur. These conditions can exist for clays compacted dry of OMC. Terzaghi and Peck (1967) explained that this increase in air pressure is at least partially responsible for slaking of dry soils immersed in water.

From this discussion it appears that the physico-chemical model provides a better explanation of mechanisms of swelling than does the deformable aggregate model. However, the interaction between micro- and macrostructure can become important at low molding water contents.

Compositional Factors Affecting the Swelling Behavior of Compacted Clays

Because swelling is governed primarily by physico-chemical forces, many factors indeed can influence the magnitude of swell or swell pressure induced in the soil. The composition of the clay and its adsorbed cations is of fundamental importance. Mitchell (1976) noted that water can be adsorbed between structural sheets in montmorillonite. This results in larger amounts of swell than for minerals in which this does not occur (e.g., illite). He also noted that, since clay minerals govern swelling behavior, an increase in clay content will logically increase the amount of swell.

Lambe (1960) stated that, ". . . a decrease in the double layer thickness reduces the electrical repulsion, which, in turn, causes a tendency toward flocculation," and, ". . . that a tendency toward flocculation is usually caused by increasing electrolyte concentration, ion valence, and temperature; and decreasing dielectric constant, size of hydrated ion, pH, and anion adsorption." If any of these variables in the soil-water system changed, as would occur in the presence of free water, Mitchell (1976) stated that, "In general, the thicker the double layer the less the tendency for particles in suspension to flocculate and the higher the swelling pressure in cohesive soils." Since a flocculated structure results in more particle-to-particle contacts and smaller, more depressed double layers, it is logical to expect a higher degree of swelling from this type of particle arrangement. That is, a highly depressed double layer can undergo a larger expansion to an equilibrium condition in the

presence of free water than a double layer that was initially less depressed.

Seed et al. (1961) and Ladd (1959) demonstrated that an increase in the pore fluid electrolyte concentration caused a decrease in swelling. This is consistent with the osmotic pressure and double layer theories previously discussed.

In addition to these purely physico-chemical factors, the compaction variables also play an important role in the swelling behavior of compacted clays. These variables include the molding water content, type and amount of compaction, dry density, degree of saturation, and the resulting as-compacted soil structure. It must be remembered, however, that these variables are not completely separable from physico-chemical influences.

Several investigators have shown that molding water content has a dominant influence on the swelling behavior of compacted clays. These investigators include Holtz and Gibbs (1956), Ladd (1959), Seed and Chan (1961), Seed et al. (1961), Parcher and Liu (1965), and others. This should be expected since it has previously been shown that molding water content controls the double layer size, as-compacted soil structure, and dry density for a given method of compaction. These investigatiors have shown that, in general, a decrease in molding water content causes an increase in the magnitude of swelling or swell pressure induced by a given method of comapction.

This occurrence can be attributed to the following factors. At low moisture contents the double layer is quite depressed and a large water deficiency exists according to Lambe (1960). In the

presence of free water this results in a larger intake of water, larger expansion of the double layer, and larger magnitude of swelling or swell pressure than for samples compacted at a higher water content. Ladd (1959) noted that pore water tensions exist in compacted clay, particularly if compacted dry of OMC. As water enters the compacted soil it destroys the capillary menisci, thus decreasing the effective stresses. This permits the double layers to expand until a new equilibrium condition is reached. Over-all swelling of the sample can be prevented by applying an effective stress equal to the swell pressue.

Molding water content also has an influence on the as-compacted soil structure which, in turn, has an effect on the swelling behavior of compacted clays. Seed and Chan (1961) concluded that "Samples compacted dry of optimum (tending to have more flocculated structures) exhibited greater swell pressures than samples of the same final composition compacted wet of optimum (tending to have more dispersed structures)."

Seed and Chan (1961) also studied the effects of different methods of compaction on swelling behavior. For samples compacted to the same composition dry of OMC, kneading and static compaction produced essentially flocculated structures and exhibited similar swelling characteristics. Wet of OMC, however, statically compacted samples retained an essentially flocculated structure and produced considerably higher swell pressures than did the relatively dispersed samples prepared by kneading compaction.

Holtz and Gibbs (1956), Seed et al. (1961), and others have shown that an increase in dry density for a constant water content

results in larger magnitudes of swelling and swell pressure. This, in effect, states that an increase in compactive effort at a constant water content results in higher tendencies to swell. Changes in particle spacings and soil structure are responsible for the increased swelling.

In this investigation, compaction variables were the only compositional factors that were allowed to vary. The effects of purely physico-chemical factors was reduced substantially by maintaining a nearly constant temperature during testing and by using only demineralized water. In this way, the effects of the compaction variables on swell pressure were not clouded by unrelated factors.

The Influence of Test Conditions on Swelling Behavior

Several methods of evaluating the swelling characteristics of expansive soils have been proposed in the literature. Holtz and Gibbs (1956) showed that free-swell tests, colloid content, plasticity index, and shrinkage limit are good indicators of the degree of expansion that can be anticipated from different soils. Seed, Woodward, and Lundgren (1962) used clay content, plasticity index, shrinkage limit, and activity to predict the swelling potential of compacted clays.

These tests work well for their intended purpose; that is, to identify potentially expansive soils. However, these methods cannot measure the effects of different compaction conditions on the induced tendency to swell. Because of this they are not applicable to the intended purposes of this research.

In recent years, several investigators have studied soil suction as a means of predicting the swelling behavior of clays. Measured values of suction must be correlated with meaningful engineering behavior, such as swelling or swell pressure, before they can be used. These correlations can be quite inaccurate at low suctions according to Johnson (1977). For these reasons, measurement of soil suction was not employed in this study.

Tests that measure swell pressure or the magnitude of swelling have been used by many investigators. Meaningful information about the swelling characteristics of a soil can be obtained directly from the data produced by these tests. Seed et al. (1961), Fredlund (1969), and others have shown that test conditions can have a large influence on the interpretation of data obtained from these tests. The following is a discussion of procedural factors that affect swell pressure and swelling tests.

Lambe (1960) demonstrated the effects of temperature changes on a sample under constant load. An increase in temperature depressed the double layer and the sample compressed. The effects were reversed for a temperature decrease. Seed et al. (1961) showed that temperature changes can influence the components of the measuring system. Temperature variations of 10° to 15° F can change the observed swelling by 0.5 percent. Therefore, temperature conditions must be held constant.

Time can have significant effects on the measured value of swell response. Seed et al. (1961), Fredlund (1969), and many others have shown that several days may be required for the full swelling response to develop. Sample size and method of introducing free water

have an influence on the time required for testing. By using a relatively small sample size and allowing water to enter both ends, testing time was dramatically reduced for this study.

Barber (1956) observed that as the time between compaction and testing increased, the measured swell under loading decreased. Nalezny and Li (1967) observed that samples stored for three days exhibited less swelling and lower swell pressures than samples tested immediately after compaction. They attributed this to thixotropic hardening that occurred during storage.

Kassif and Baker (1971) studied the aging effects of compacted clay samples stored for as long as 90 days. They noted that thixotropy in a compacted clay is associated with an increase of the negative pore water pressures (i.e., they become more negative), and the formation with time of electrochemical bonds between clay particles. Their test results showed that swell pressures increased for short storage durations (less than about 10 days) then decreased with storage time. The effects of increased negative pore water pressures dominated the swelling behavior for short periods of storage. As storage time increased, more bonds formed between particles and swell pressures were lower. To minimize these time-dependent effects, storage time should be the same for all samples tested. This time should be sufficient to permit elastic rebound and water equilibration of the compacted sample.

The amount of expansion measured in a swelling test is dependent on the surcharge load and stress history during the test. Gibbs and Holtz (1956) showed a systematic variation between swelling and

surcharge load. As would be expected, lighter surcharge loads permitted more swelling, but the relationship between swelling and surcharge was not linear. Gibbs and Holtz used these relationships to estimate actual movements that might occur under various load conditions in the field.

Seed et al. (1961) showed the effects of varying the stress history during a swelling test. Samples placed under a constant 1 psi surcharge load swelled more than those subjected to an initially higher load that was subsequently decreased to 1 psi. This effect can be explained in terms of particle reorientations that occur in the sample. Under low surcharge loads, sample expansion can take place with ease. Higher surcharge pressures cause more internal particle reorientations to occur. Lambe (1960) suggested that the particles tend to align with their flat surfaces perpendicular to the direction of applied stress. This rearrangement results in an essentially more dispersed structure; Seed and Chan (1961) have shown this type of structure to exhibit lower swelling characteristics than the initially more flocculated one. Because of these particle reorientations, samples used in constant volume swell tests were not subsequently used to measure the magnitude of swelling.

Seed et al. (1961) have demonstrated that a volume expansion of as little as 0.1 percent can cause a large error in the magnitude of the observed swell pressure. A larger amount of expansion will obviously result in a lower observed swell pressure. This phenomenon is conversely related to the amount of swelling that will occur under different static surcharge loads.

In order to obtain more consistent measurements of swell pressures, constant volume swell (CVS) tests should be conducted. Several factors must be considered in order to minimize volume changes. Seed et al. (1961) observed that the faces of compacted samples developed a curvature after being trimmed. They attributed this to elastic rebound. When these samples were placed in the testing apparatus, only a small portion of each face was in contact with the loading platens. This permitted a volume expansion to occur before an entire face was in contact with the end plates. As a result of this expansion, measured swell pressures were considerably lower for these samples than for samples trimmed flush immediately before testing.

Most CVS tests are conducted in ordinary consolidometers. Fredlund (1969) outlined the many procedural factors that can affect the results of such tests. Of these factors, compressibility of the apparatus can result in the largest measurement errors. Fredlund noted that the loading mechanism, porous stones, and filter paper all contribute to the apparatus compressibility. Filter paper can contribute a significant proportion of this compressibility; it not only has an instantaneous compression, but also a time-dependent component. He suggested that calibration tests be conducted by replacing the soil specimen with a steel block. Results of these tests can then be used to ensure that a constant volume is indeed maintained during CVS tests on soil. He also cautioned that machine parts (porous stones, loading platens, etc.) should never be interchanged. If this occurs, calibration tests should be conducted using the new parts.

Seating of the porous stones and the soil sample must also be accounted for. Fredlund noted that most seating occurs under low pressures. Therefore, a small initial seating load should be used in order to get a representative initial deflection reading. He also observed that friction in the mechanical components of the apparatus is negligible for most consolidometers.

For the intended purposes of his study, it is believed that CVS tests provide the most reliable measurement of swelling behavior and also the most meaningful data. The procedures set forth by Fredlund (1969) were followed in this investigation, and filter paper was replaced with thin, polycarbonate film.

Escario (1969), Gromko (1969), and others have attempted to measure the in situ swelling behavior of expansive clays. However, the soil samples compacted in the field and collected for the swell pressure measurements presented in this report are, to the author's knowledge, the first data of this type reported.

As can be seen from this literature review, the mechanisms controlling the compaction, structure, and swelling behavior of fine-grained soils are very complex and not completely understood. It is hoped that future research will result in clearer, more comprehensive, and better substantiated theories regarding these mechanisms.

2 - APPARATUS AND EXPERIMENTAL PROCEDURE

Soil Studied

The soil used in both the field and laboratory phases of this investigation was a medium plastic clay called St. Croix clay. It was obtained from a cut and fill area made as part of a realignment project of State Road 37, approximately four miles south of St. Croix, Indiana. It was a shale and sandstone residual of tan color with gray and red mottling. Other pertinent data are given in Table 2.1 and the grain size distribution curve is shown in Figure 2.1

Test Pad Construction

In June of 1978, test pads were constructed in the fill area of the previously mentioned SR 37 realignment project. The purpose of the test pad was to create field-compacted soil for subsequent investigations of mechanical properties and fabric descriptors.

Ten test pads were constructed 14 ft (4.3 m) wide and 116 ft (35.4 m) long. Their layout is shown in Figure 2.2. A subbase of varying thickness (4 to 5 ft or more) was constructed to provide a level base for the test pads. The pads were placed as 8 in (20 cm) loose lifts and a tractor-drawn disk was used to break up large clumps of soil.

Five test pads were compacted by a Caterpillar Model 825 tamping foot roller and five were rolled with a RayGo Rascal Model 420C

Table 2.1 Index Properties and Classification of St. Croix Clay

		Field	Laboratory
Atterberg Limits (%) Mean (low, high)	w_L	40.1 (30.0, 53.2)	38.3 (37.0, 39.2)
	w_P	18.4 (16.7, 21.3)	16.3 (15.6, 16.7)
	I_P	22.2 (16.7, 29.0)	22.0 (20.9, 22.7)
Shrinkage Limit, w_s (%)		11.8	
Specific Gravity, G_s		2.78	
Percent Finer Than 0.002 mm (clay content)		34	
Percent Finer Than 0.001 mm (colloid content)		30	
Skempton's Activity, A		0.65	
Unified Soil Classification		CL	
AASHTO Classification		A-6	
Swell Potential (Based on Gibbs and Holtz, 1956)		High	

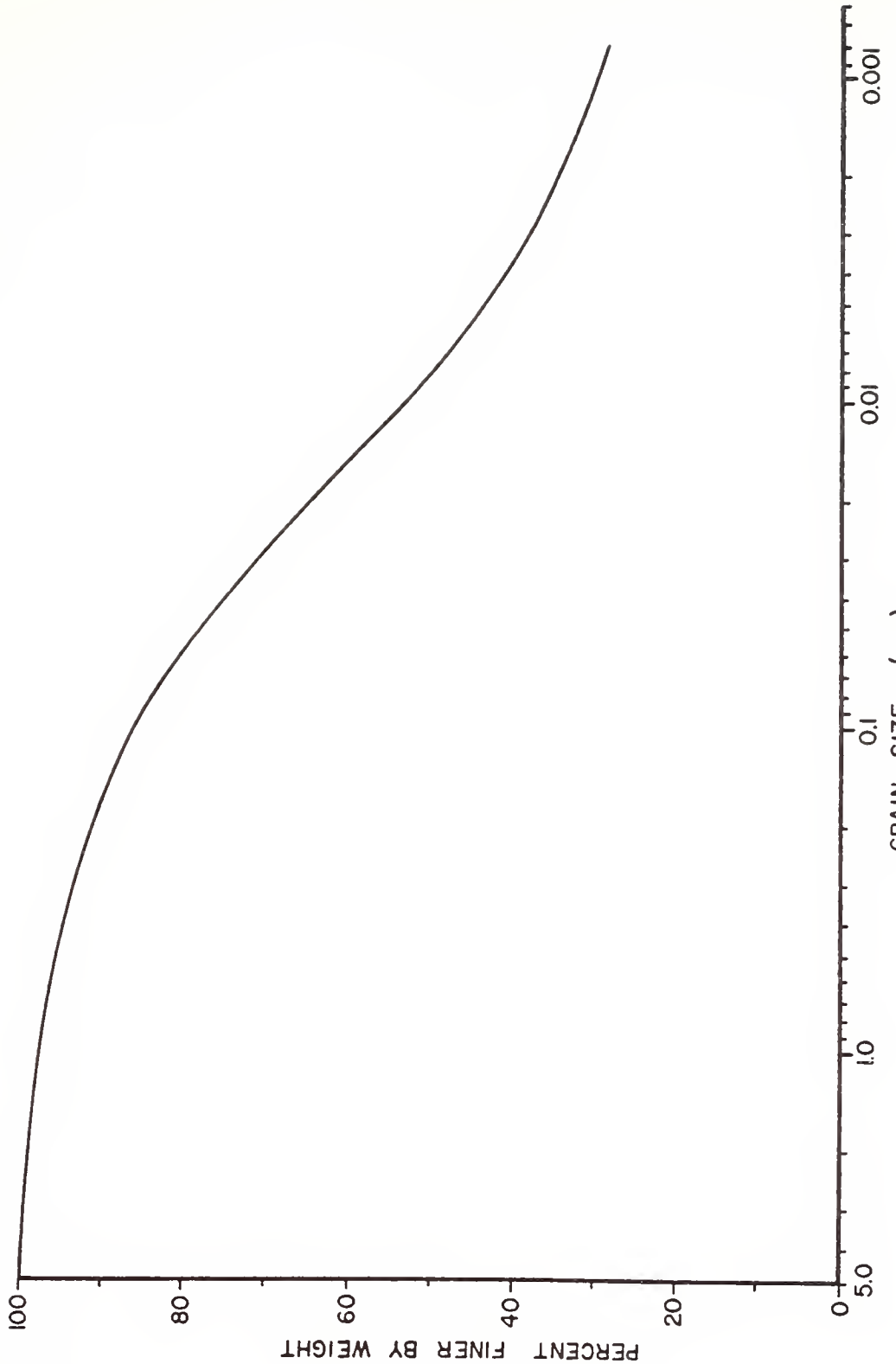

Figure 2.1 Grain Size Distribution for Laboratory Soil

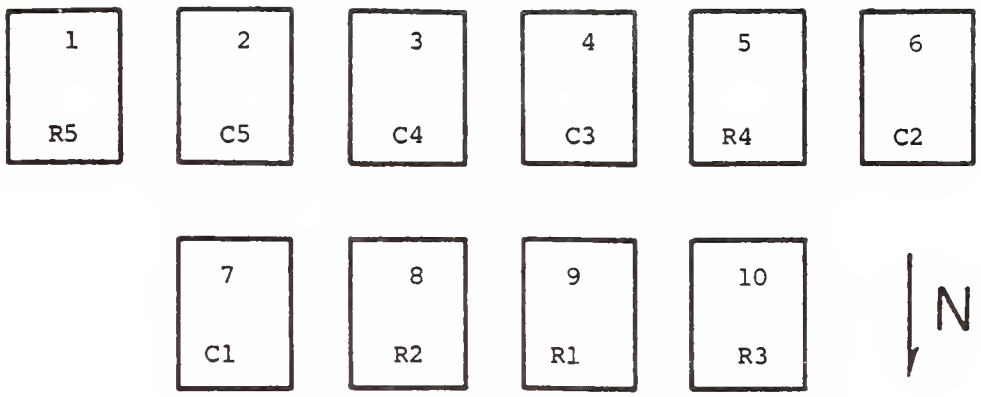

Figure 2.2 Test Pad Layout Showing Pad Number, Compactor Type, and Water Content Level

Table 2.2 Field Compaction Equipment Specification

Caterpillar Model 825			
Length	23 ft - 4 in	No. of Drums	4
Width	13 ft - 8 in	No. of Pads/Drum	65
Wheelbase	11 ft - 8 in	Drum Length	44.5 in
Weight	63,000 lb	Top Speed in 1st Gear	3 mph
RayGo Rascal Model 420C			
Length	18 ft - 9 in	No. of Drums	1
Width	9 ft - 0 in	No. of Pads/Drums	140
Wheelbase	9 ft - 0 in	Drum Length	84 in
Weight	25,160 lb	Top Speed in 1st Gear	4 mph
Vibration	hydraulic, direct drive		
Frequency	1100 - 1500 vpm		
Dynamic Force	32,000 lb		

padded vibratory drum compactor.* These compactor types were designated "C" and "R" respectively for sample identification purposes; their specifications are given in Table 2.2. These rollers were selected by the contractor because of their capability to perform satisfactorily with the intended soil.

For each roller type, the five test pads were brought to different average water contents prior to compaction. The range in water contents from pad to pad was selected to include points both wet and dry of what was believed to be the optimum moisture content for the respective rollers. For identification these were designated "1" to "5" from lowest to highest moisture level. Within each pad a uniform moisture distribution was desired. Although special measures were taken in the field, it can be seen from Table 2.3 that some variation did result. A sizeable variation appears to be inherent in compaction projects, and control of the water content variation has been associated with proper performance of the embankment (Price, 1978).

The desired water content for each test pad was achieved in the field in different ways. First, moisture contents were taken at four different locations in the loose pad using the Speedy Moisture Tester apparatus, and the average was tabulated. If the pad was initially too wet, the tractor-drawn disk was employed to facilitate drying and to help produce moisture uniformity. Additional water contents were taken periodically during disking until the desired magnitude was achieved. If the pads were initially too dry then water

---

*Unless otherwise noted, future references to "tamping foot", "padded drum", and "segmented pad" will be used interchangeably and will apply to both compactor types.

Table 2.3 Density and Moisture Content Values Obtained from Field Nuclear Gage Measurements

No. of Passes			4		8		16	
Pad No.	Compactor Type	Moisture Level	γ_d	w	γ_d	w	γ_d	w
1	R	5	108.2	22.5	106.9	23.6	111.9	17.0
			95.0	26.0	106.3	19.4	102.6	28.1
			101.7	23.1	103.4	19.2	105.7	21.8
			R5A		R5B		R5C	
2	C	5	97.2	26.1	101.2	25.1	106.0	22.6
			106.9	23.8	97.7	27.4	106.5	21.8
			100.0	20.0	103.8	21.1	106.3	20.7
			C5A		C5B		C5C	
3	C	4	103.1	21.2	106.6	20.5	111.6	17.0
			108.0	19.2	100.0	22.7	104.0	21.2
			100.0	22.1	105.5	19.4	99.4	21.4
			C4A		C4B		C4C	
4	C	3	105.0	10.3	109.1	14.7	107.4	15.4
			104.9	16.3	110.3	12.4	105.9	15.6
			107.4	12.7	103.8	41.0	107.5	14.0
			C3A		C3 B		C3C	
5	R	4	99.5	20.6	101.2	17.9	103.3	19.0
			99.4	21.1	102.5	25.7	95.6	22.8
			96.9	19.2	101.2	17.9	105.9	17.0
			R4A		R4B		R4C	
6	C	2	103.2	17.1	108.4	13.7	102.1	15.2
			105.3	15.7	111.5	16.1	108.4	17.2
			105.8	13.9	114.2	14.7	103.9	15.5
			C2A		C2B		C2C	
7	C	1	98.0	14.8	113.2	15.4	110.2	15.6
			104.0	14.9	109.3	14.5	112.5	16.0
			96.0	16.9	111.1	16.5	112.8	16.8
			C1A		C1B		C1C	
8	R	2	104.3	17.7	111.9	13.8	105.9	15.1
			98.0	16.6	106.8	12.5	110.7	14.2
			101.8	14.2	102.3	14.9	108.7	15.6
			R2A		R2B		R2C	

Table 2.3 (continued)

No. of Passes			4		8		16	
Pad No.	Compactor Type	Moisture Level	γ_d	w	γ_d	w	γ_d	w
9	R	1	98.9	15.7	103.2	16.8	114.5	13.6
			101.7	16.4	107.6	12.9	112.5	14.7
			104.2	14.6	107.4	14.4	106.3	14.5
			R1A		R1B		R1C	
10	R	3	103.5	14.0	107.6	17.0	111.9	16.5
			98.3	13.0	104.8	15.7	105.8	15.0
			95.9	14.6	106.4	12.9	108.6	15.9
			R3A		R3B		R3C	

was added by passage of a calibrated water truck; the soil was then mixed again by disking. Those pads which were at the desired water content were briefly disked for mixing purposes and then compacted.

Once the desired average water content was achieved in a pad, soil compaction began immediately. Each pad was sampled after 4, 8, and 16 passes of the compaction equipment (see section titled "Field Sampling" for discussion of sampling techniques). These samples were labeled "A", "B", and "C", respectively, for identification of energy levels. Several steps were taken during the compaction process to reduce variability in applied energy. Equipment was operated at top speed in first gear (about 3 mph) for all passes. Ample room was allowed for the roller to reach this top speed before entering the actual test pad area, and equipment was carefully guided to prevent overlap at the interface of adjacent coverages. The same equipment operator was used for all compaction work.

Despite these precautions, it appeared that the segmented pad roller itself provided a major source of input energy variability. During a single pass of the roller drum only the soil under the raised pads received the maximum applied energy; areas surrounding the pads might have had no compaction at all. On subsequent passes the compactor pads could have run over either previously compacted soil or relatively uncompacted areas. As the number of passes increased, so did the overall uniformity for the entire test pad. The variation in applied energy was believed to be one cause of the variability in field dry density as shown in Table 2.3 and the resulting compaction curves presented in Figures 2.3 and 2.4.

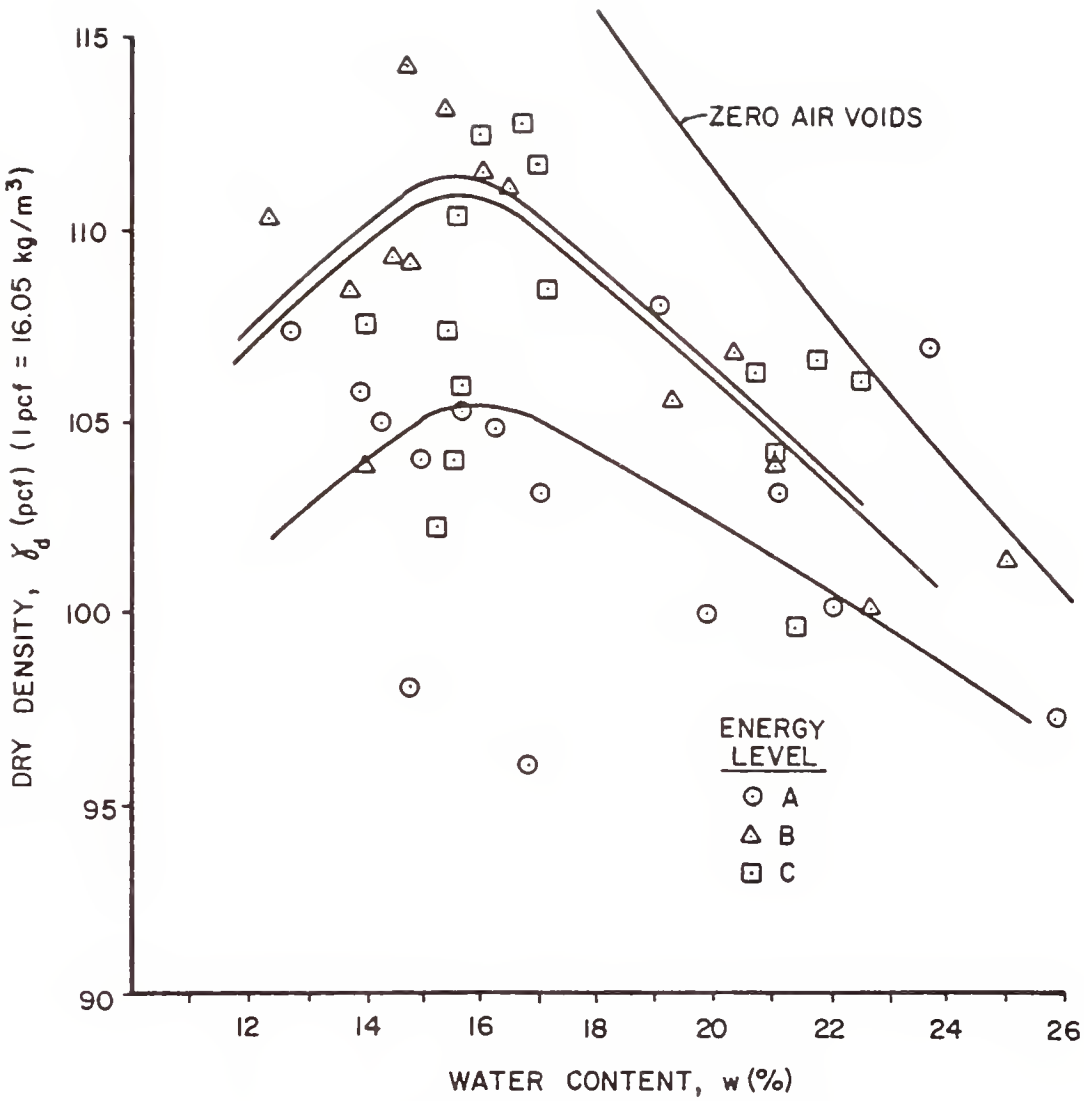

Figure 2.3 Caterpillar Compaction Curves for Field Nuclear Gage Values

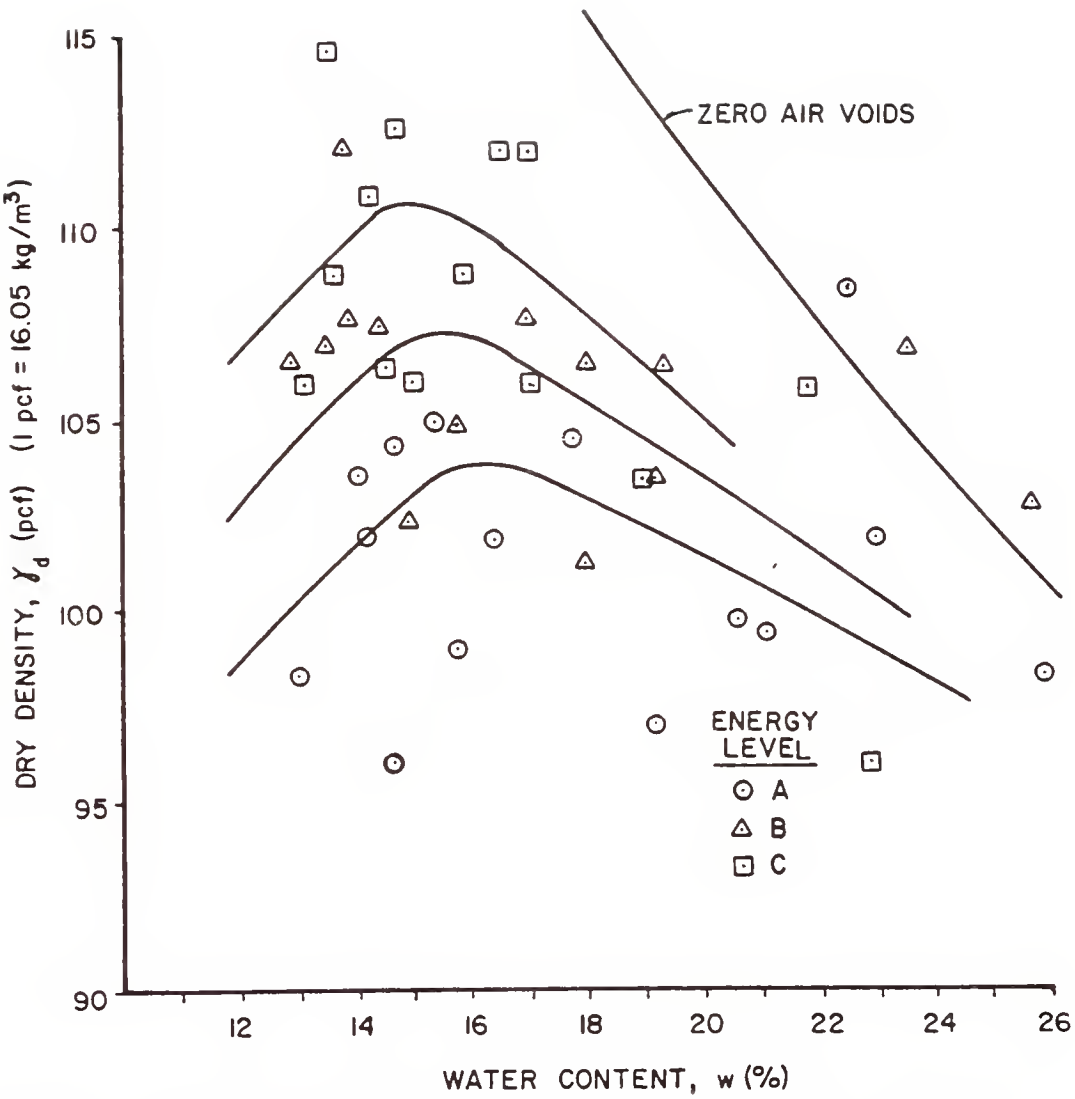

Figure 2.4 Rascal Compaction Curves for Field Nuclear Gage Values

The compactors themselves could have provided a source of variation; their configurations differed, as did the ways in which they applied energy to the soil. In a single pass, the Rascal equipment applied compactive effort through one wide drum followed by two rear rubber tires spaced 3 ft (0.9 m) apart. Higher confinement, and thus higher compaction, might have been achieved near the center of this drum, with more "squeezing-out" having occurred near its ends. Applied energy was divided almost equally between static weight and dynamic vibratory force; the effect of the rubber tires was unknown.

The Caterpillar equipment used four tamping drums to apply compactive effort. For each pass of this equipment, two drums traveled over a given area of soil which increased the probability of pad-to-soil contact for a given soil location; the Caterpillar equipment also had approximately twice as many pads as the Rascal compactor. The effect of confinement was probably not as large for the narrower Caterpillar drums, and neglecting travel speed, all compaction energy was supplied by static weight. Actual weight distributions for the two compactors were not known. In view of the above discussion, it would be suggested that the Caterpillar equipment would produce more uniform compaction, but this suggestion is not evident in the data of Table 2.3 and Figures 2.3 and 2.4. Price (1978) also provided a discussion of field compaction variability.

Field Sampling

Sampling of the test pad began immediately after the required number of passes had been completed. The test pad was laid out in a 2 ft by 2 ft (0.6 m by 0.6 m) grid pattern and marked around the

perimeter with consecutively numbered stakes. The required number of sampling tubes were lightly lubricated with silicone oil and were distributed to their proper locations along with labels and plastic bags. These locations had been determined using a random number process in an earlier phase of this project. A typical sample label, and its explanation, is shown in Figure 2.5. For this study, six samples were taken for each combination of compactor type, water content level, and energy level. A total of 840 samples were collected for the entire project, of which 180 were taken for this work on swelling tendency.

Sampling tubes were driven into the ground with a drop hammer, and all tubes were driven at the bottoms of impressions left by the segmented pads of the compactors; this was done in an attempt to reduce the variability in applied energy as well as to increase the useable sample height. After being driven, the tubes were dug out of the ground, wrapped in the plastic bags, labeled, and carefully transported to the extruding area. Extrusion and other field operations are to be explained later in this section.

Sampling tubes and drop hammers were manufactured in the Central Machine Shop at Purdue University. The swell-sample tubes were made from steel tubing with an internal diameter of 2.51 in (6.38 cm), an external diameter of 2.75 in (6.99 cm), and were 5.0 in (12.7 cm) long. One end was machined to form a cutting edge. The drop hammer consisted of: (1) a driving head with a recess and four set screws used to steady the sampling tube; (2) a pipe threaded into the driving head to guide the falling weight; (3) a disk on the end

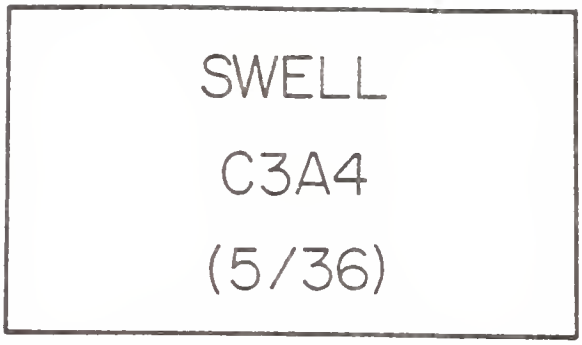

SWELL - Behavior property to be investigated

C - Compactor type

3 - Water content level

A - Energy level

4 - Sample number for the compaction conditions indicated above

5 - Grid location in the East-West direction

36 - Grid location in the North-South direction

Figure 2.5 Typical Field Sample Label With Explanation

of the pipe to use as a handle and to control the height of drop; (4) the falling weight itself; and (5) two wood cushions, one between the sampling tube and driving head, and one between the driving head and falling weight. The driving assembly, with tube, is shown in Figure 2.6. The 16.7 lb (7.6 kg) weight fell 28 in (71 cm) producing about 40 ft·lb (54 N·m) of energy per blow, with several blows (usually 10 to 25) being required to drive each tube. The complete unit weighed less than 30 lb (13.6 kg).

In place density and water content measurements were made during the sampling phase by ISHC personnel. The Troxler Model 3401 nuclear gage was used at various locations in each test pad for these measurements. Values obtained from the nuclear gage were given in Table 2.3 and the corresponding field compaction curves were plotted in Figures 2.3 and 2.4. These plots indeed showed the large variability within the soil mass. Some of the factors which contributed to this variability have previously been discussed. Those which occurred during the sampling phase were: (1) the weather during sampling was warm (90°F + daily temperatures); and (2) four to six hours elapsed from start to finish of sampling for a single test pad. Although efforts were made throughout the sampling program to mitigate moisture losses, some losses probably did occur.

Shortly after being removed from the ground, samples were extruded from the tubes using either an hydraulic jack (see Figure 2.7) or an electrically driven loading press. Samples were then wrapped in plastic, covered with cheese-cloth, and heavily coated with paraffin. Next, they were placed into plastic bags along with their

Figure 2.6 Driving Assembly with Sampling Tube

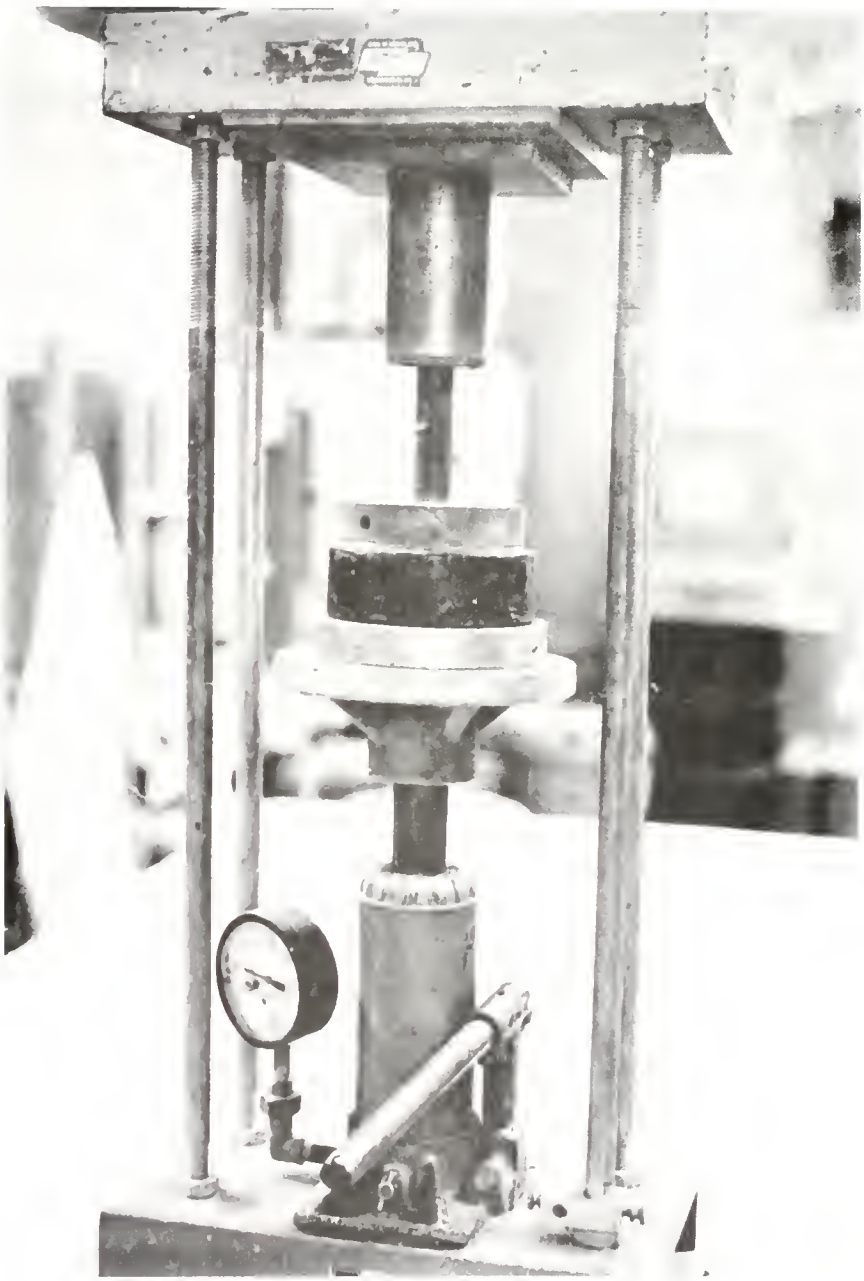

Figure 2.7 Hydraulic Jack Used for Extrusion of Tube Samples

labels, packed into 5 gallon metal cans, and padded with shredded foam. All samples of similar origin were packed together, and the cans were then transported to and stored in the Purdue Geotechnical Laboratories.

At the time of extrusion several observations were made about the samples. Rock fragments appeared in all samples and some samples were destroyed because large rocks or gravel pockets were present; other samples were scored by rocks being dragged along their periphery by the sampling tubes. Many dry-side samples were quite brittle, broke easily, and their usable height was generally shorter than the average. Some samples showed horizontal cracks while others showed distinct interfaces between individual lumps of soil which had not been intermixed by the compaction process. Samples in the low and intermediate water content ranges sometimes showed distinct zones of different water content. This was probably due to the incomplete mixing of soil lumps which were at different initial water contents. High water contents produced the longest, most uniform samples.

Preparation of Soil

Soil used for the laboratory compaction phase of this study had been obtained directly from test pads six and eight. Bag samples had been transported along with the field samples and stored in large metal cans at the Purdue Geotechnical Engineering Laboratories. While in storage, these bag samples came to an equilibrium air-dry water content of about 2.5% (± 0.3%).

In this air-dry condition the soil formed very hard lumps, with rock fragments of varying sizes also being observed. A small

jaw crusher was used to break the lumps which could not easily be broken by hand. In the preparation process the bag samples were first passed through the No. 4 sieve, and rock fragments were removed from both the retained material as well as from that which passed through the sieve. Soil retained on the sieve was then transferred to the jaw crusher. After crushing, the material was sieved and rock pieces again removed. This crushing and sieving operation was repeated for each batch of soil until the breakdown was accomplished. After sieving, the soil was stored in two large metal cans which were lined with polyethylene bags.

The object of the crushing operation was to produce a soil mixture which could be used with ASTM Standard Test Designations D 698 (Standard Proctor) and D 1557 (Modified Proctor) for compaction of soil passing the No. 4 sieve. To avoid crushing rock fragments embedded within soil lumps, the jaws on the crusher had been set wider than the No. 4 sieve opening. It is felt that the crushing process did not significantly change the grain size distribution; the process prevented crushing of most larger rocks while it removed only a small portion of those fragments passing the No. 4 sieve. This method of crushing proved helpful since 370 lb (168 kg) of soil was prepared.

Since the bulk soil remained near 2.5% water content, mixing proportions were easily and accurately determined. Soil required for compaction (about 5.3 lb or 2.4 kg) was placed in a mixing pan, and demineralized water was added with a hand-operated atomizer until the desired water content was reached. Frequent mixing prevented

the formation of large aggregations and helped to produce a relatively uniform moisture distribution.

After mixing, the soil was put into two layers of plastic bags, closed securely with twist ties, and labeled. The bags of soil were then placed in a humid plastic barrel and allowed to cure a minimum of 3 days prior to compaction. Humidity in the barrel was maintained by using a bottom layer of water and gravel and a tightly fitted cover. Previous investigators (see Weitzel, 1979) found this 3-day period to be appropriate for ensuring moisture homogeneity.

Laboratory Compaction

Laboratory compacted samples used in this study were prepared by both kneading and impact methods. Kneading compaction was used for two reasons: (1) companion studies in this project used the method; and (2) it was believed that this method produced shearing strains and loading patterns more similar to those produced by field compaction (Weitzel, 1979). Impact compaction was used to provide a standard basis for comparison. Laboratory samples were labelled in a manner similar to that used for field samples; "K" and "I" were used to designate kneading and impact samples, respectively.

Kneading Compaction

The kneading compactor was manufactured by the August Manufacturing Company of Oakland, California and is shown in Figure 2.8. It is an automatic apparatus with mold rotation and foot tamping being driven by an electric motor; a pneumatic-hydraulic system supplies the foot pressure. The mold rotates 60° between tamps that are applied

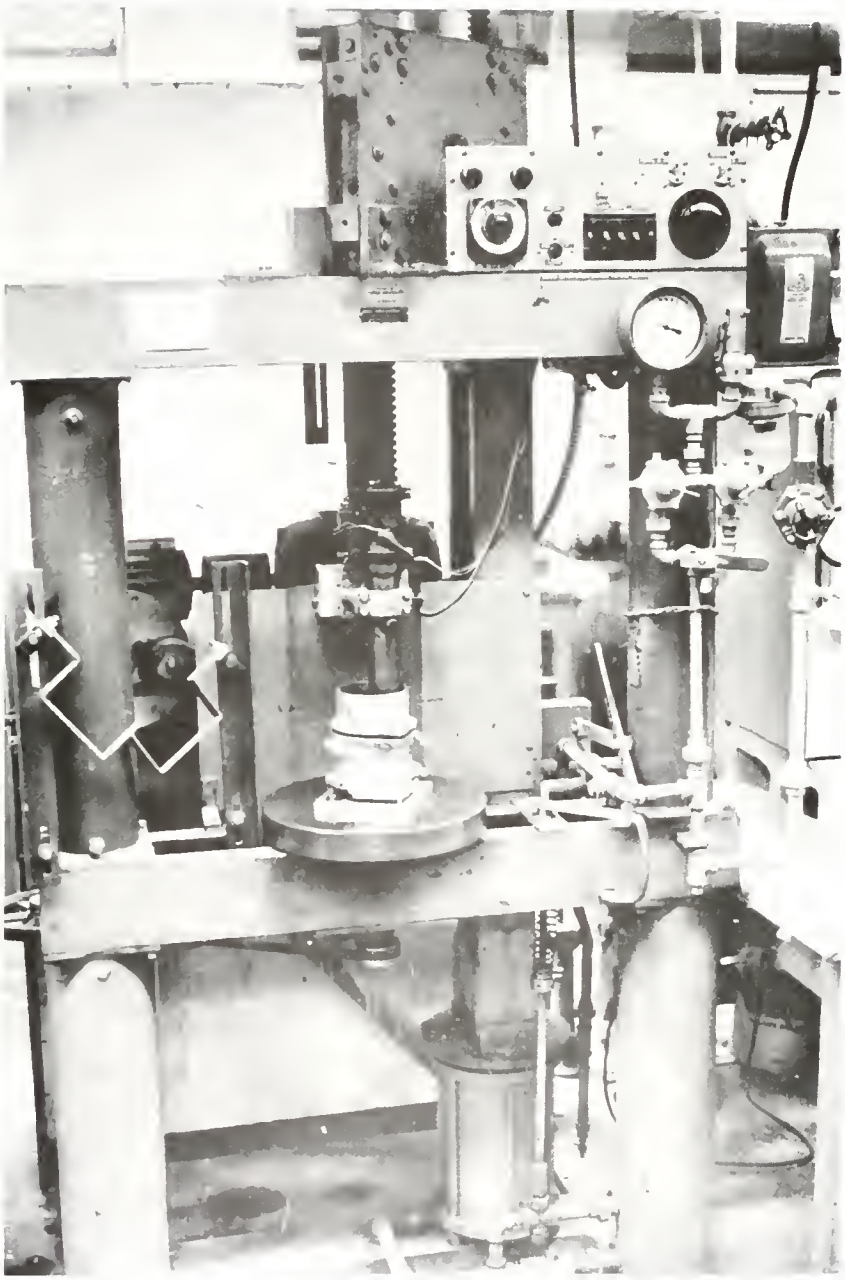

Figure 2.8 Kneading Compactor

at a rate of 30 per minute, with full face coverage of the soil layer being achieved by six tamps of the compactor foot. A more complete description of this compactor is given by Gaudette (1960).

Samples were compacted at three energy levels (foot pressures) chosen to simulate the compaction curves produced by impact compaction. Figure 2.9 shows the relationship between kneading and impact compaction obtained by DiBernardo (1979). This figure, along with preliminary compaction tests, was used to determine the appropriate foot pressures shown in Table 2.4.

Table 2.4 Energy Levels for Kneading Compaction

Energy Level	Foot Pressure (psi)	Corresponding Impact Test
A	4	Low Energy Proctor
B	7	Standard Proctor
C	26	Modified Proctor

Energy levels were labelled "A", "B", and "C" for identification purposes similar to the method used for field samples.

To compact a sample, a Standard Proctor split mold of 1/30 ft^3 (944 cm^3) with a collar (see Figure 2.10) was positioned and securely bolted to the rotating table of the compactor. The mold and collar had been lightly lubricated with silicone oil to facilitate

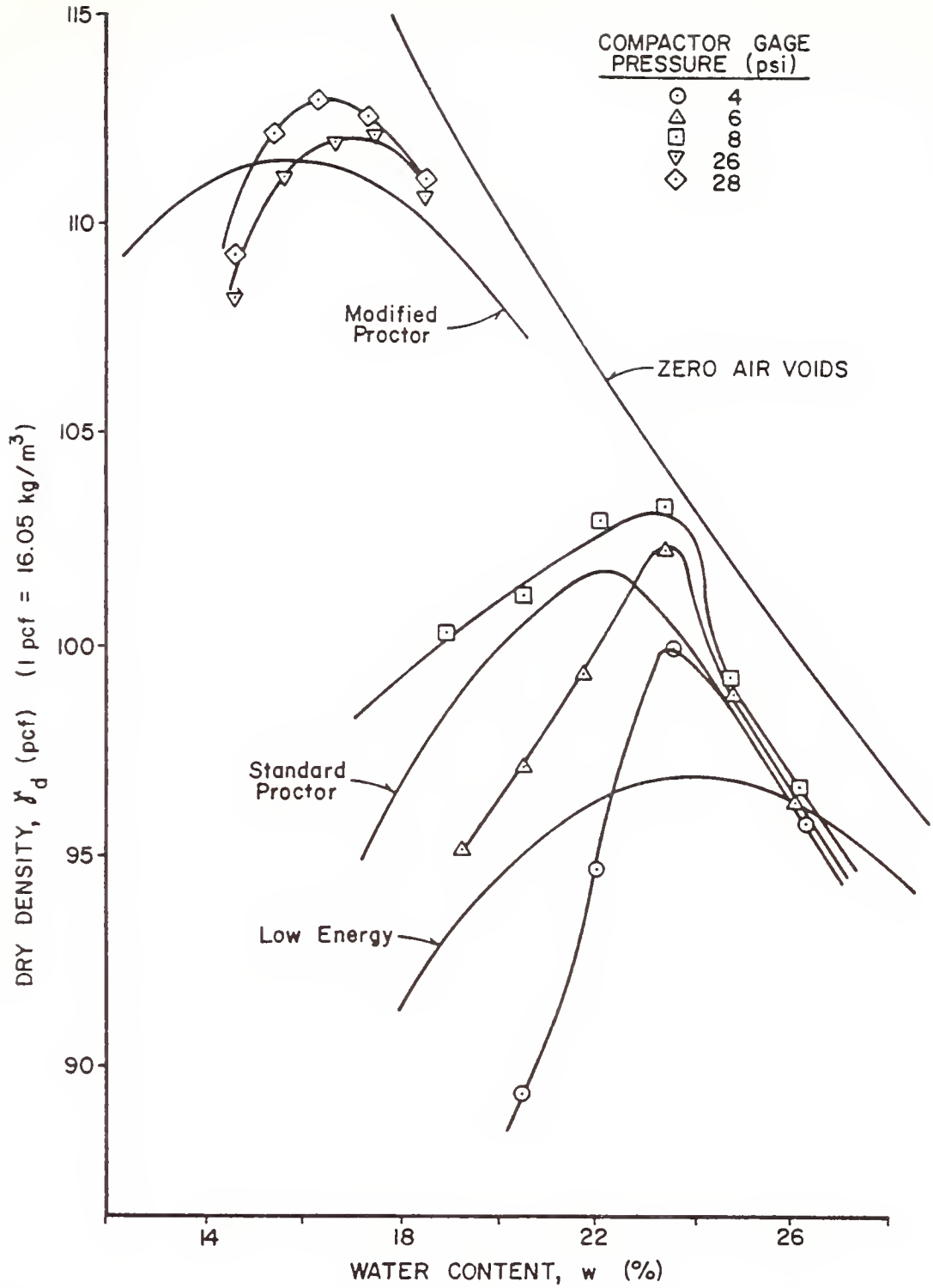

Figure 2.9 Comparison of Impact and Kneading Compaction Curves (after Di Bernardo, 1979)

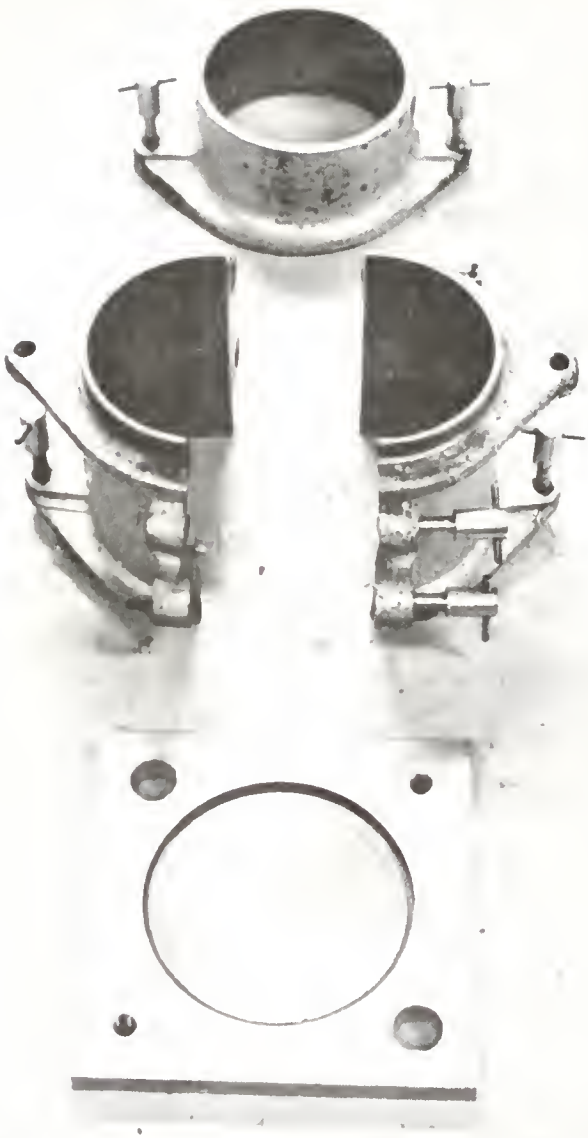

Figure 2.10 Standard Proctor Split Mold with Collar

future trimming and sampling operations. A batch of soil which had been allowed to cure was sampled for water content and spooned into the mold. The soil was compacted in five layers of approximately equal thickness and each layer received 30 tamps from the foot. The top of each layer was scarified before adding more soil to ensure sample homogeneity. This was most important for the drier samples. Upon completion of compaction the mold was unbolted from the compactor table, the collar was removed, excess soil was screeded from the top of the sample, and mold and soil were weighed for the density determination. Compaction curves resulting from these measurements are shown in Figure 2.11.

Impact Compaction

Impact compaction was also performed for three different energy levels. The Low Energy Proctor samples were prepared as specified in the U.S. Army Engineering Manual EM 1110-2-1906 (1970) and labelled "A" for identification purposes. The Standard Proctor (B) and Modified Proctor (C) were specified in ASTM D 698 and D 1557, respectively. Information regarding these procedures is given in Table 2.5. As with kneading compaction, a Standard Proctor split mold was also used. Procedures for soil handling, sampling for water content, scarifying, trimming, and weighing were the same as for kneading samples. The Impact Compaction curves are shown in Figure 2.12.

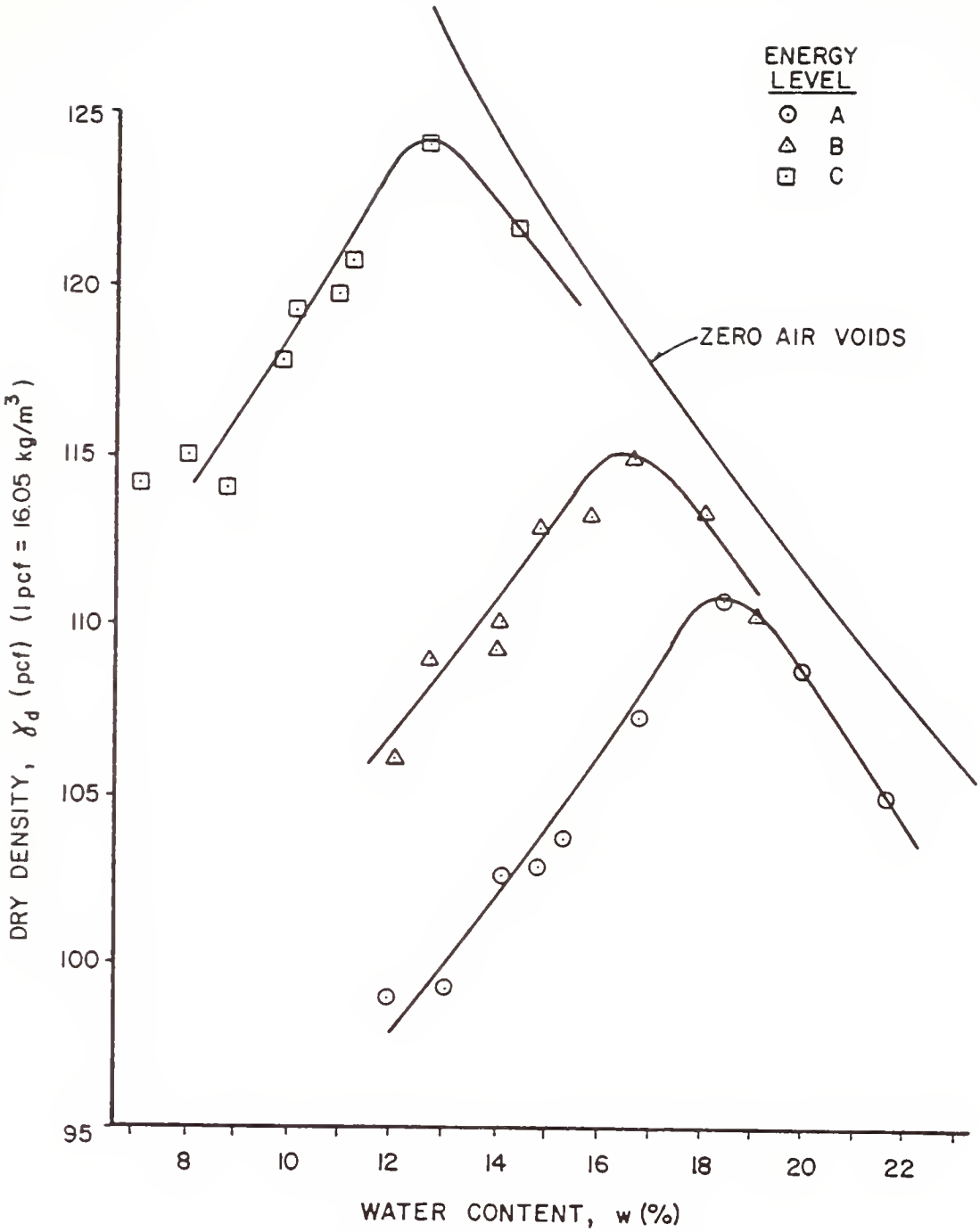

Figure 2.11 Kneading Compaction Curves for Compaction Mold Values

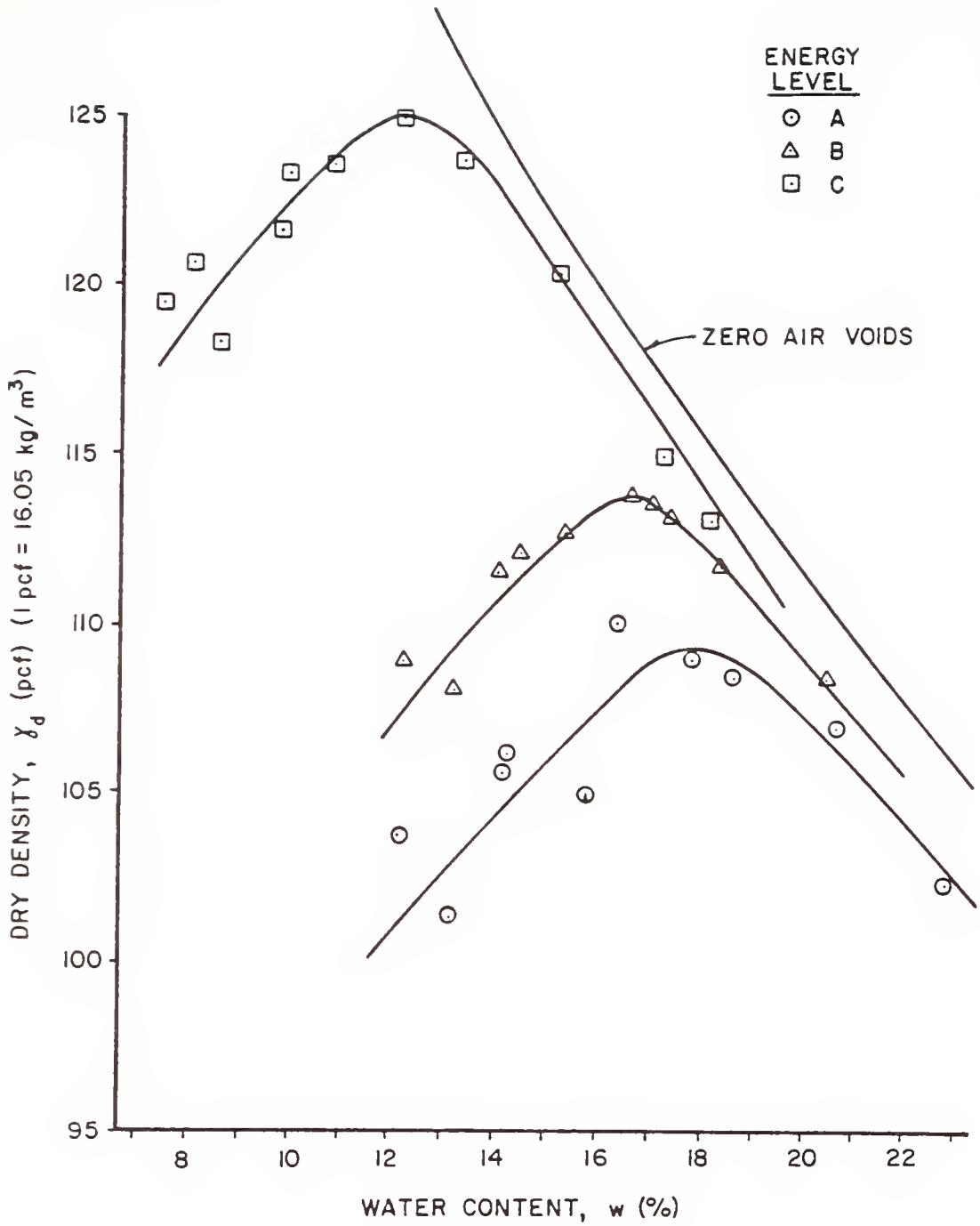

Figure 2.12 Impact Compaction Curves for Compaction Mold Values

Table 2.5 Energy Levels for Impact Compaction

Energy Level	Hammer Weight	Drop Height	Number of Layers	Blows/ Layer	Compaction Method
A	5.5 lb	12 in	3	15	Low Energy Proctor
B	5.5 lb	12 in	3	25	Standard Proctor
C	10 lb	18 in	5	25	Modified Proctor

Tube Sampling

After compaction it was desired to treat laboratory samples in a manner similar to that used for field samples. For this reason, tube sampling was performed on the compacted soil in the mold.

With the halves of the split mold securely tied together with heavy latex surgical tubing (designed for use as a tourniquet), the four screws holding the halves together were unscrewed, and the mold was removed from its base. The mold was then placed on the ram of an hydraulic jack. A sampling tube (the kind used for field sampling) was lightly lubricated with silicone oil and centered on top of the soil in the mold. The tube was then jacked in at a constant rate through the full height of soil in the mold. Figure 2.13 shows these features with the sampling tube partially inserted into the soil.

Excess soil was removed from around the sampling tube and some was used for water content determinations. The sample was then extruded from the tube with the hydraulic jack. This same operation was shown for field samples in Figure 2.7. After extrusion, each

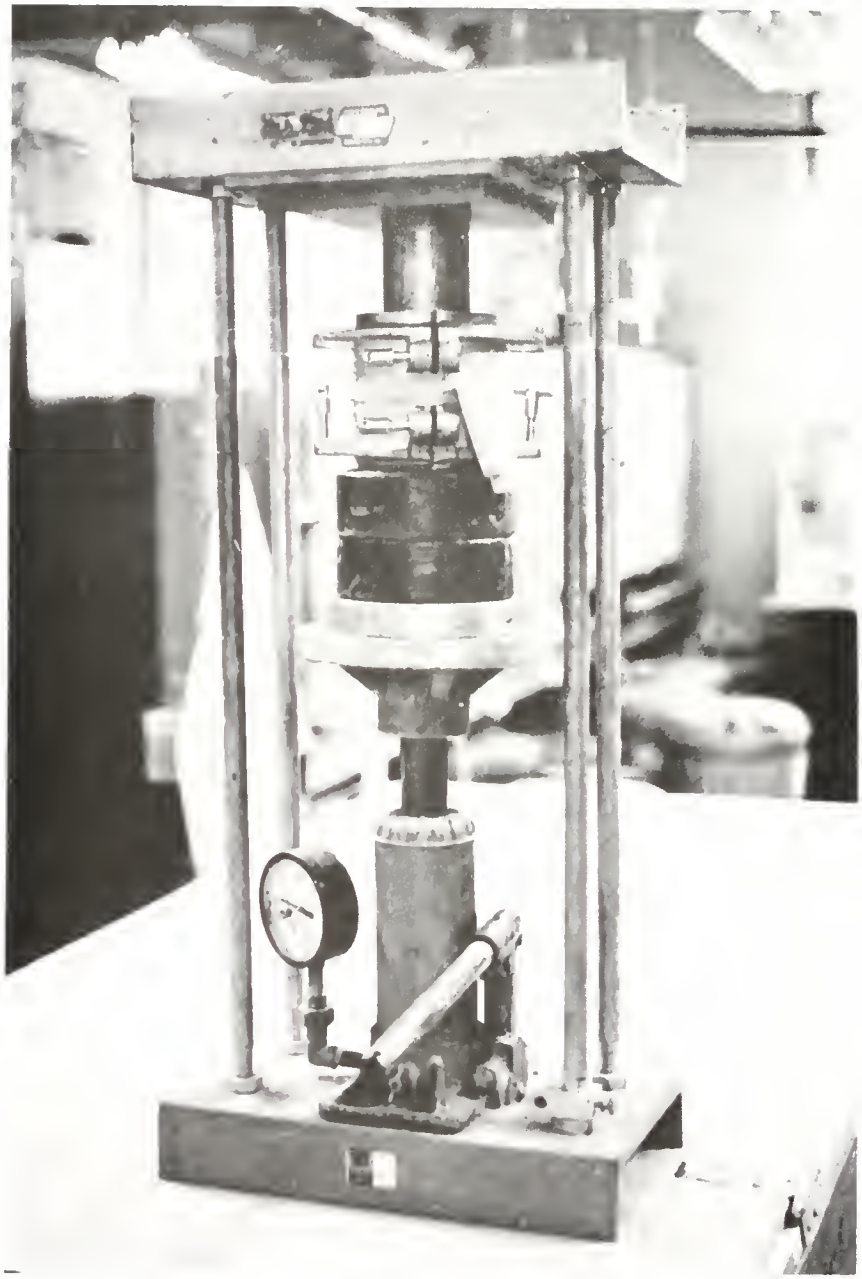

Figure 2.13 Tube Sampling of Laboratory Compacted Samples

sample was wrapped in a double thickness of polyethylene bags, cushioned with paper towels, and stored in a humid container. Storage time was set at three to four days to allow equilibration of moisture within the sample.

The tube sampling procedures were the result of several trials at obtaining quality samples. During the sampling operation, the latex tubing provided enough lateral support to prevent the soil in the mold from cracking as the tube was inserted, but allowed enough expansion to accommodate the added volume of the sampling tube. Previous investigators on this project (Di Bernardo, 1979; Johnson, 1979; Weitzel, 1979) used a somewhat different method of tube sampling. They compacted soil into a Standard Proctor mold and extruded it into a mold which was split on one side. Tube sampling was then done in this semi-split mold. Preliminary work done for this study indicated that the semi-split mold could not accommodate the volume of the sampling tube without causing excess soil disturbance.

Trimming of Soil Samples

Constant volume swell (CVS) tests were conducted in Geonor bench top consolidometers. Test specimens for this apparatus were cylindrical with a 2.44 in^3 (40.0 cm^3) volume, a 1.99 in (5.05 cm) diameter, and a 0.787 in (2.0 cm) height. This required the use of a special Geonor simulated piston sampling apparatus.

The Geonor sampling apparatus was designed for use with soft clays; its purpose was to cut a soil sample, of the correct diameter and with minimum disturbance, directly into the stainless steel confining ring used in the consolidometer. This could not be achieved

satisfactorily with the relatively stiff clay used in this study. Preliminary trials resulted in test specimens which were loose in the confining ring. This condition was undesirable for constant volume swell tests; other investigators (Dawson, 1956; Gromko, 1974) have shown that allowing even a very small amount of expansion can greatly reduce the measured swell pressure. To avoid this situation, stainless steel cutting rings were manufactured with an inside diameter 0.039 in (1.0 mm) larger than that of the confining ring. These cutting rings produced specimens which could be trimmed to fit tightly in the confining ring.

Sample number, field location, and initial sample height were recorded for each sample. Other notes were made throughout the trimming process that indicated such things as: color, homogeneity, consistency, water content, plasticity, defects, irregularities of shape, and the number, size, and location of rocks and voids.

The first step in the trimming process for field samples was to remove the wax and cheese cloth covering. This was accomplished using a sharp utility knife to cut through the covering, and care was taken to prevent damage of the soil sample inside. Laboratory samples were simply removed from their polyethylene bags.

The next step was to prepare tube samples for use in the Geonor sampling apparatus. The ends of the sample were trimmed perpendicular to the axis of the sample cylinder, leaving a maximum height of about 2.5 in (6.4 cm). The ends were trimmed with a wire saw for the wetter samples and with a sharp pen knife for the drier ones. These end trimmings were saved for the companion study of pore size distribution.

Care was taken to trim all test specimens from as close to the mid-height of tube samples as possible. This minimized the effects of systematic density variation in a compacted soil, as described by Gau and Olson (1971).

After this initial trimming, the soil sample was centered on the platen of the Geonor sampling apparatus, and the top piston was lowered into position; the piston prevented movement of the sample as the cutting ring was being advanced. This situation is illustrated in Figure 2.14. The cutting ring was advanced by rapidly pushing the top handle down, and Figure 2.14 also shows the cutting ring fully advanced into the soil sample. The cutting ring was held in the apparatus by spring clips such that when the handle was subsequently raised, the cutting ring remained in place on the newly trimmed soil cylinder. Trimmings produced by this cutting action were then used for water content determination. Figure 2.15 shows the newly formed soil cylinder and cutting ring, with trimmings removed from the perimeter. The cutting ring was then advanced completely through the sample by hand with the aid of a stainless steel tube.

This trimming procedure was slightly modified for laboratory samples compacted relatively dry at the highest (C) energy level. The cutting ring was started into the sample with the Geonor device. When further advance could not be achieved by hand, the sample was placed in an hydraulic jack. The cutting ring was then advanced through the sample with the jack, aided by the previously mentioned stainless steel tube.

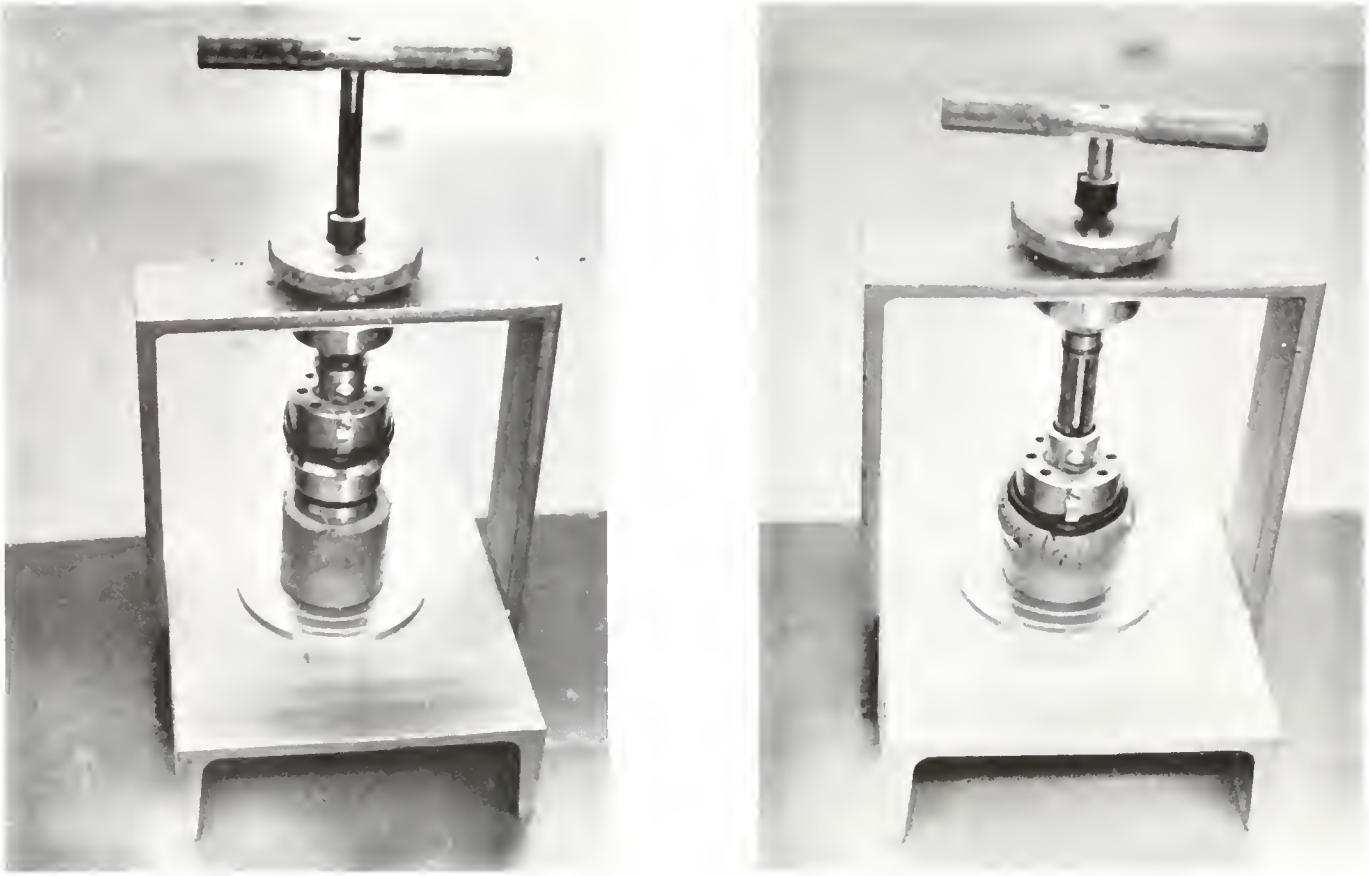

Figure 2.14 Geonor Sampling Apparatus

Left: Soil sample Positioned in apparatus
Right: Cutting ring fully advanced into soil sample

Figure 2.15 Cutting Ring on Sample with Trimmings Removed

After removing the cutting ring, any voids around the perimeter of the cylinder were filled with soil shavings. These voids were usually caused by rock fragments being dislodged from the soil by the cutting ring; the size and number of these voids were recorded in the notes for each test.

Next, the confining ring was installed by hand near the sample mid-height. This ring was advanced in the same direction as the cutting ring, and much care was taken to advance it parallel to the axis of the soil cylinder. As the confining ring was advanced, it shaved off a thin layer of soil from the circumference and thereby produced a tight (but not excessively tight) fit in the ring.

Excess soil was then removed from the ends of the test specimens. A wire saw was used for wetter specimens while drier ones required cutting and/or scarifying and scraping with a sharp pen knife. These operations were performed rather gently to minimize sample disturbance. Rock fragments which protruded beyond the ends of the specimen were removed; all surface voids were filled, and their sizes and locations were recorded. Faces of the test specimen were made flush using a straightedge, and then they were covered with glass plates to prevent drying and damage. This assembly (confining ring, soil specimen, and glass plates) was weighed for subsequent water content and density determinations, and then transported to the testing area.

It should be noted that several field samples were discarded during the trimming phase. Samples which were drier than about 15% moisture content were usually quite brittle. Some of these were of insufficient height due to defects or poor recovery from the field,

while others fractured during the trimming process. Some were discarded because a large volume of rock fragments had to be removed from the test specimen, which probably made the sample unrepresentative. This latter occurrence was independent of moisture content.

Field samples were also observed to vary in plasticity from sample to sample. For this reason, liquid limit tests were performed for each field sample tested, and results are presented in Appendix A. Plastic limit tests were performed for one sample from each series (i.e., each combination of compactor type, water content level, and energy level); the resulting average and range of Atterberg limits are presented in Table 2.1. Results of these tests showed that the soil was somewhat variable but the average values remained within the bounds of the AASHTO A-6 classification.

Constant Volume Swell Test

Constant volume swell tests (CVS) were conducted on both field and laboratory compacted samples. Field samples were randomly selected for testing with the aid of a random number table; this helped reduce the amount of bias in the testing procedure. Laboratory compacted samples were similarly chosen in a random fashion. A total of 149 samples were tested, with 93 of these compacted in the field and 56 compacted by laboratory methods.

Two Geonor bench top consolidometers were located in a controlled temperature room and used for the CVS tests. These devices applied load to the soil specimen through a system of levers and weights, which was slightly modified for the CVS tests. The original weight hanger was replaced with a plastic bucket, and small glass

beads were used to apply load instead of the conventional metal weights. The glass beads were chosen for the following reasons: (1) they easily provided the range of weights (very small to very large) which were required in this application; (2) they applied load in a more continuous manner than the metal weights as swell pressure developed; (3) they permitted more precise control of the amount of weight applied, and thus the measured swell pressure.

The consolidometers were calibrated before any CVS tests were conducted, as Fredlund (1969) concluded that the compressibility of the consolidometer can have a significant effect on the interpretation of swell test data. A stainless steel cylinder was used to replace the soil specimen for these tests. Loads were applied, deflections were measured, and calibration curves were drawn. Results of these tests were used during CVS tests to ensure that the soil specimen remained nearly constant in volume. As a check, calibrations were performed periodically during the testing phase.

Preliminary calibrations were conducted with cellulose fiber filter paper placed between the porous stones and steel cylinder. This paper produced large defelections, portions of which were time-dependent. The filter paper was replaced with thin polycarbonate filter membranes (manufactured by the Nuclepore Corp., California) and the undersirable effects were eliminated.

After the trimming process was completed, the soil specimen and confining ring were placed in the consolidation chamber. Porous stones in a saturated surface dry condition and dry filter membranes were placed over the ends of the specimen. A collar with bolts was installed to hold the confining ring in position, and a loading platen

was placed over the top stone. Figure 2.16 shows the consolidation chamber both before and after assembly.

The chamber was then placed on the loading frame of the consolidometer. In this condition, the apparatus was balanced to apply no load to the specimen. A seating load of 1.3 psi (9.0 kPa) was applied in order to get a reliable initial reading of vertical deflection. While this load was sufficient to seat the soil, porous stones, and other parts of the consolidometer, its magnitude and duration were not large enough to cause any appreciable sample disturbance. It was essential to get a reliable initial reading because all subsequent measurements of volume change were based upon this value.

Next, 380 ml of demineralized water was added to the chamber, which reduced the seating load to 1.0 psi (6.9 kPa). The water was permitted to reach the soil through both porous stones, and swelling commenced immediately upon inundation. Loads were applied as swell pressures developed, and values were tabulated. Deflections were measured after each load application with a dial gage that read to 0.0001 in (0.0025 mm). These measured values were then compared with the deflections required to maintain a constant volume. Time and temperature were also recorded. The consolidometer with chamber in place is shown in Figure 2.17.

During the test, loads were added only if the deflection measurements indicated that the specimen was still expanding; maximum swell pressure was achieved when the soil specimen produced no further expansion under the sustained load. Laboratory samples compacted very dry of OMC exhibited a sudden reduction in volume after reaching maximum swell pressure. When this occurred, weights were removed

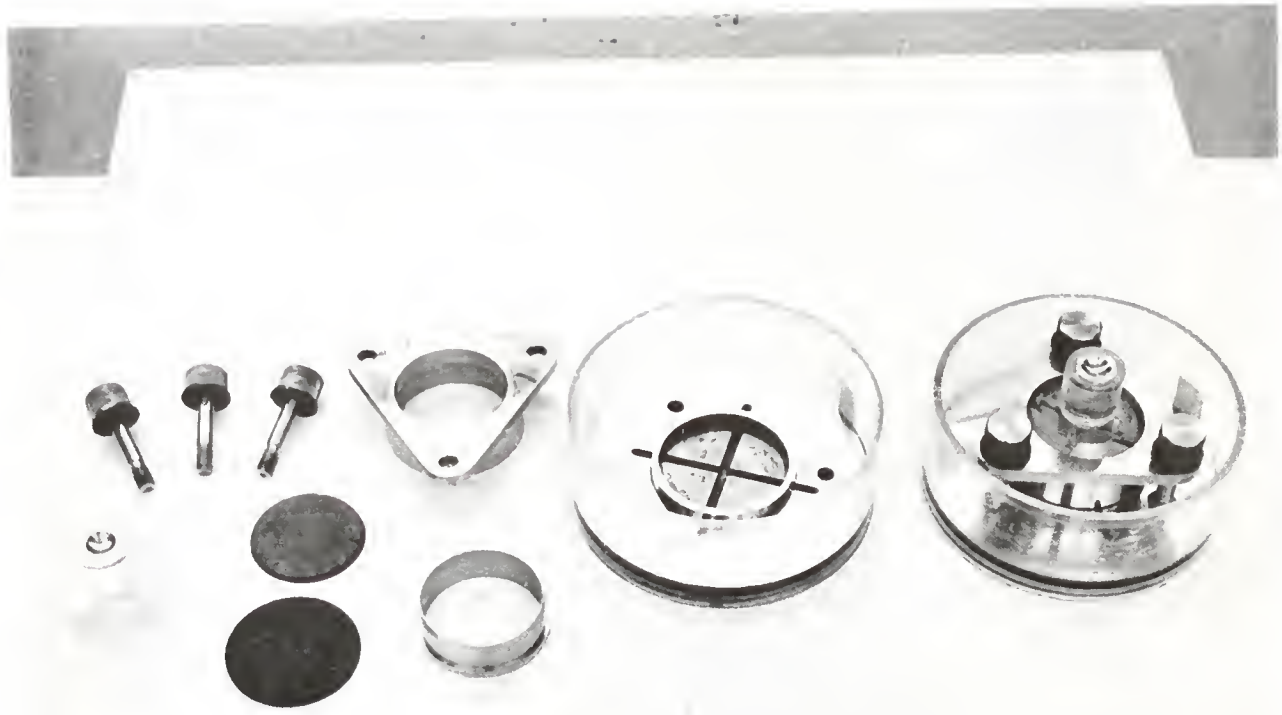

Figure 2.16 Consolidation Chamber Before and After Assembly

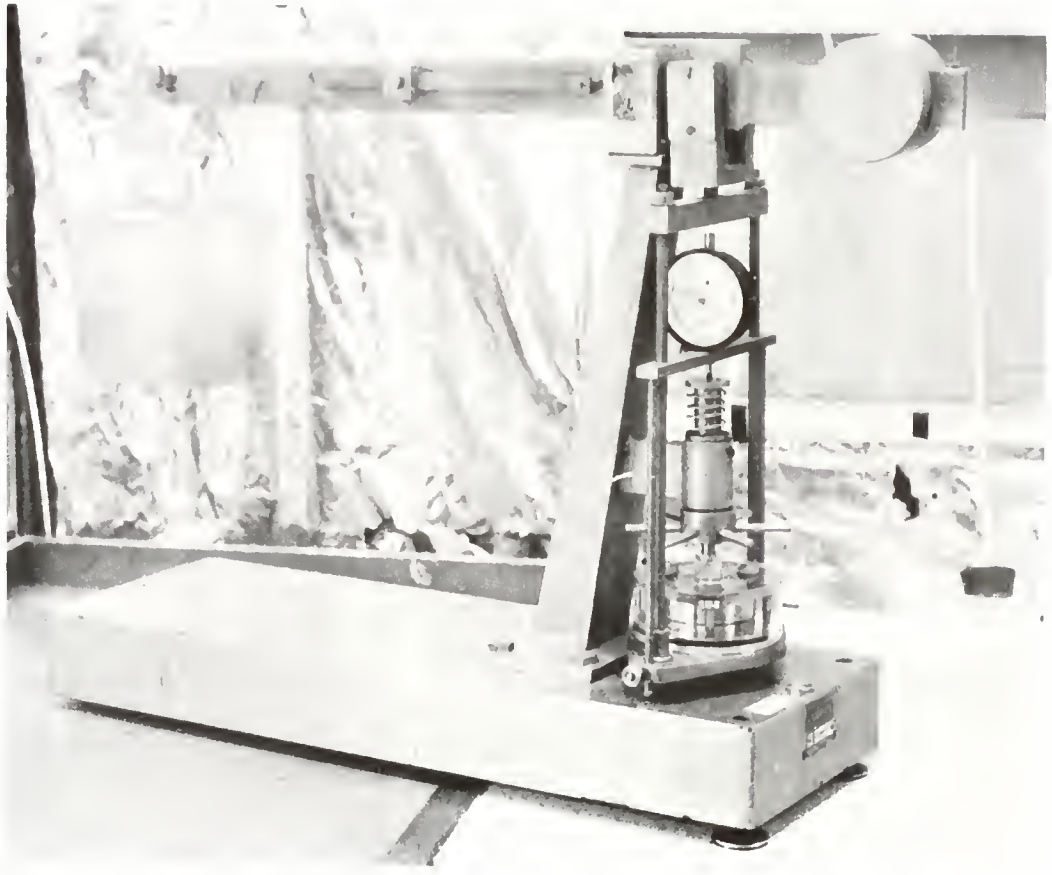

Figure 2.17 Geonor Benchtop Consolidometer

until no further volume change took plase, and thus an equilibrium swell pressure was achieved. The maximum or equilibrium load was then maintained for a minimum of 18 hours.

After completion of the CVS test, the chamber was removed from the consolidometer frame and the water was drained. The soil sample was then extruded from the confining ring, weighed for water content and density determinations, oven-dried for a minimum of 24 hours, and weighed again. Compaction curves resulting from these oven-dry test specimen values are presented in Figures 2.18 through 2.21 inclusively.

For laboratory compacted samples, these curves are very similar to the ones produced from compaction mold values. This indicates that the trimming and testing procedures cause little change in these measured quantities. For the field compacted samples, however, large differences exist between field nuclear gage and test specimen values. This is evident by comparing Figures 2.3 and 2.4 with Figures 2.18 and 2.19, respectively. The figures show that higher densities, less data scatter, and more well-defined curves appear for the specimen values. These discrepancies can be attributed to several factors. Some drying may have occurred during storage, thus causing increases in dry densities. As with the laboratory compacted samples, the trimming and testing procedures probably had some effect on w and γ_d. All field samples were taken from the bottoms of impressions left by the compactor. Nuclear gage measurements were made at random points in the fill and represented a volume somewhat different from that of the field test specimens. As a result there is a large probability that test specimens soil received a larger applied energy than did the

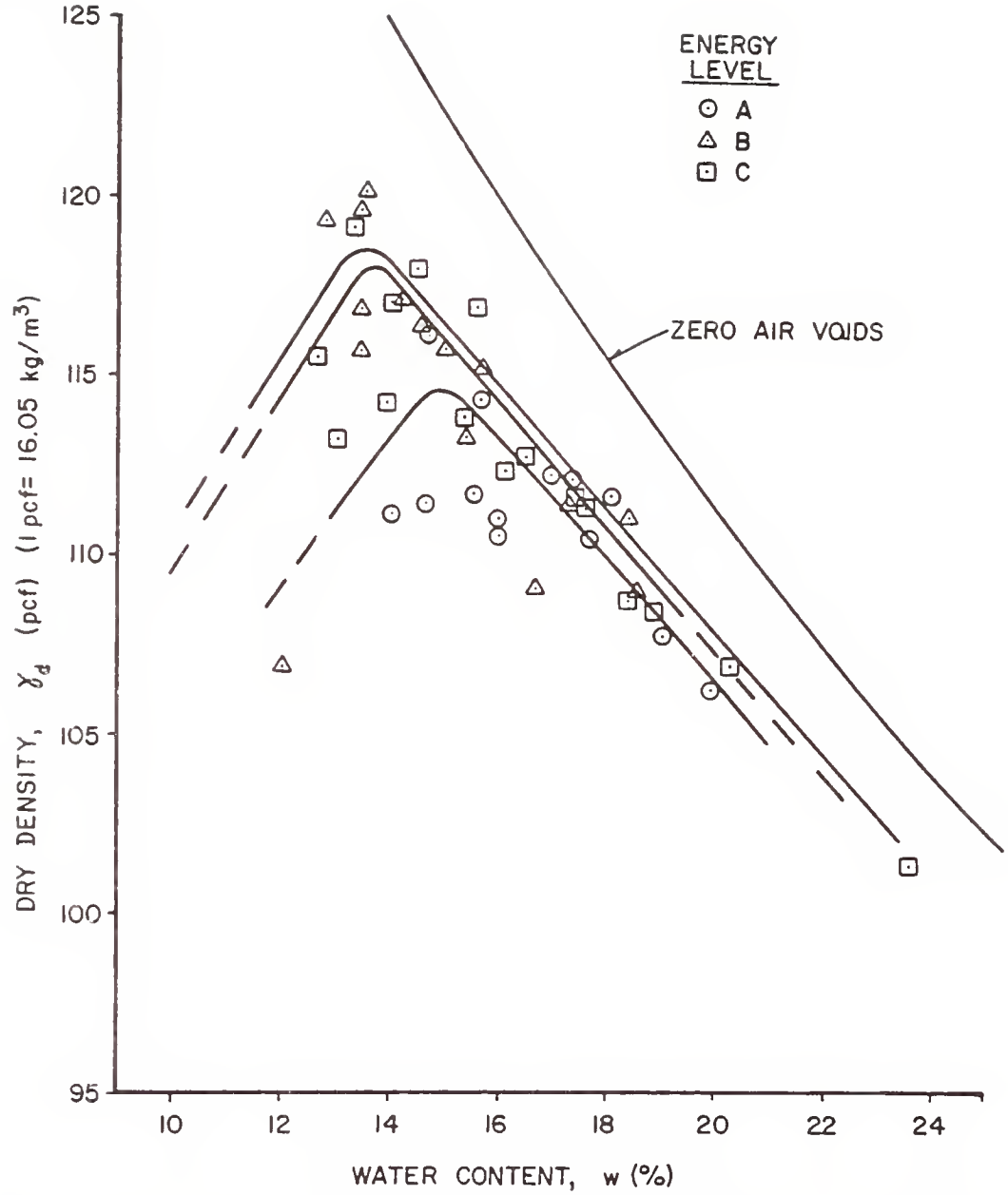

Figure 2.18 Caterpillar Compaction Curves for Test Specimen Values

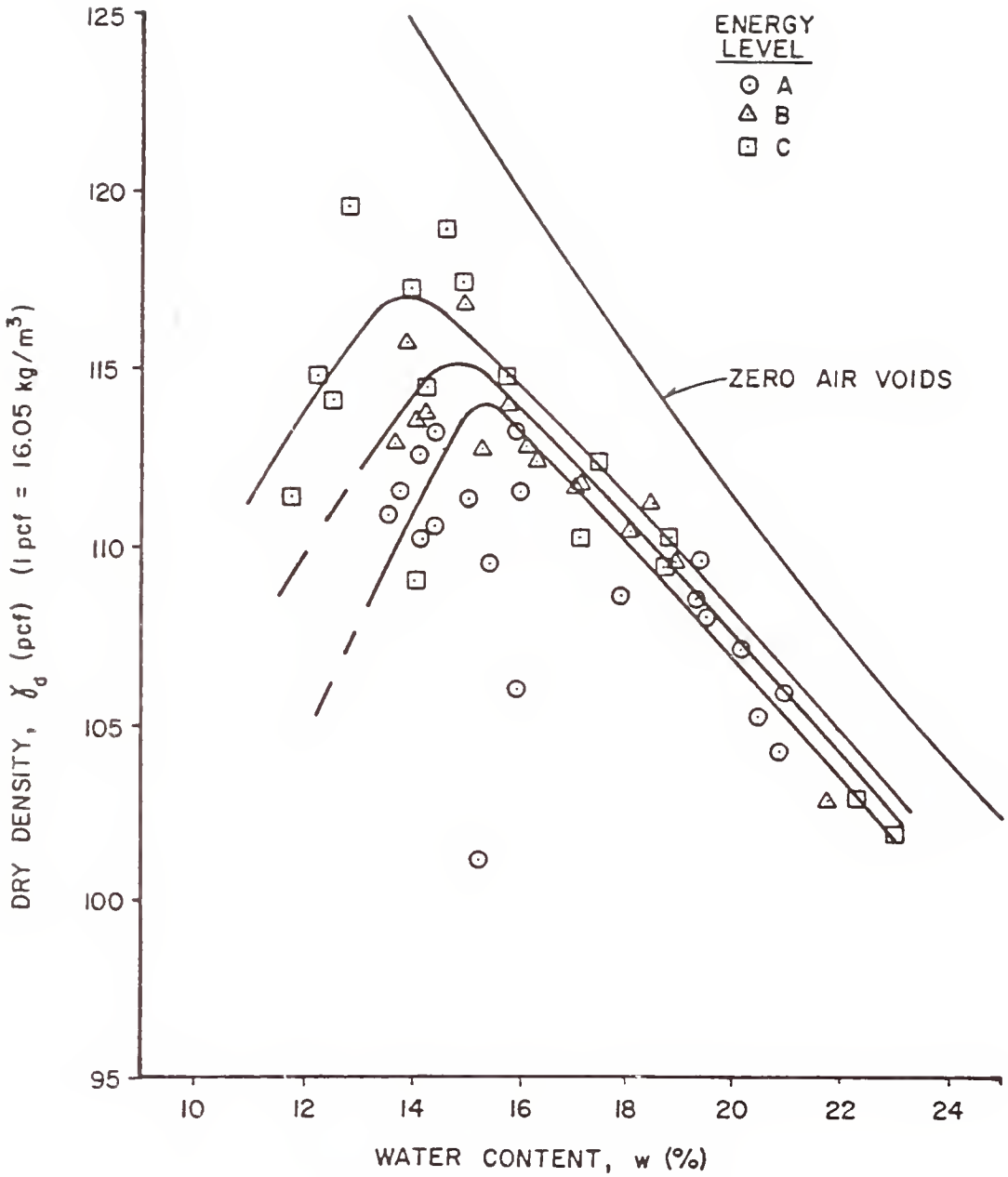

Figure 2.19 Rascal Compaction Curves for Test Specimen Values

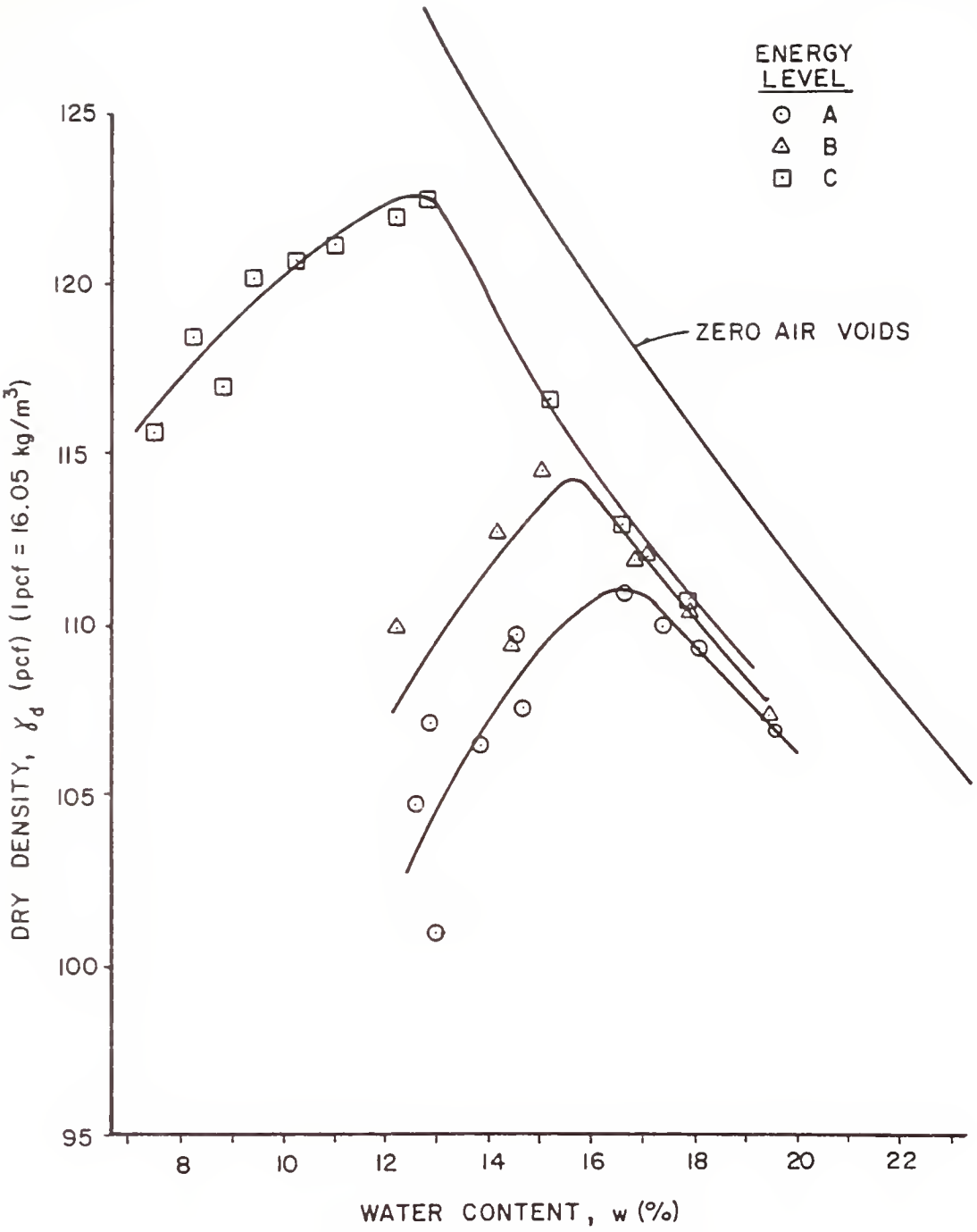

Figure 2.20 Impact Compaction Curves for Test Specimen Values

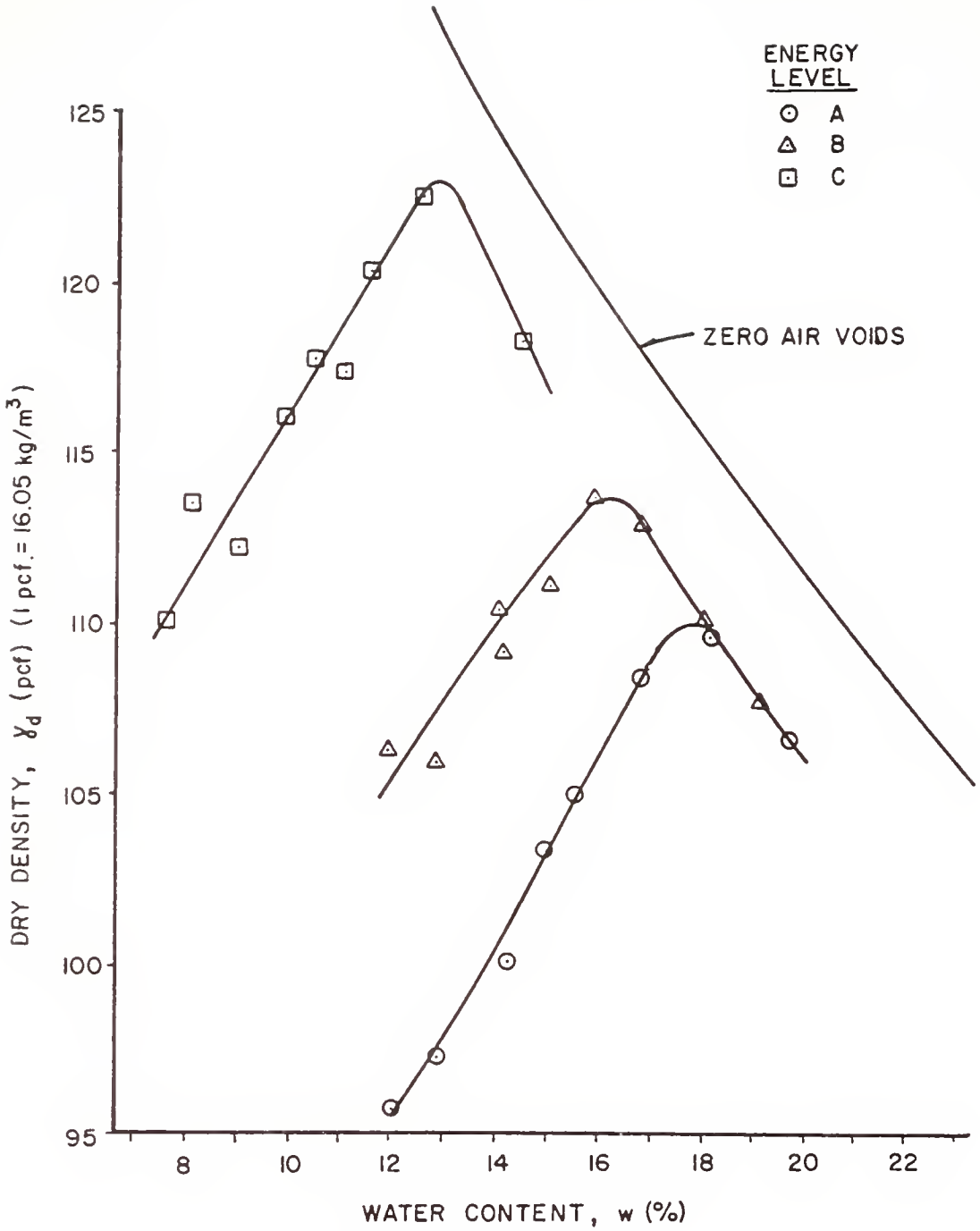

Figure 2.21 Kneading Compaction Curves for Test Specimen Values

volume surveyed by the nuclear gage. In addition, because the two sets of data were taken by different groups of people, there is a strong possibility that the nuclear gage data reported herein have not had applied to them the usually routine corrections based upon sand-cone density data.

Figure 2.22 shows how swell pressure increases with time for typical samples. The pressure builds rapidly upon inundation, and most samples achieve maximum values in from two to six hours. Other investigators (Seed et al., 1961; Parcher and Liu, 1965) have found swell pressure as well as expansion to continue increasing for several days, which was not observed in this study. This contradiction probably occurs for the following reasons: (1) the samples in this study are smaller in size than those used by others; (2) this study permits water to enter the test specimen through both ends, while others may not; (3) the soils studied may have idfferent tendencies to swell.

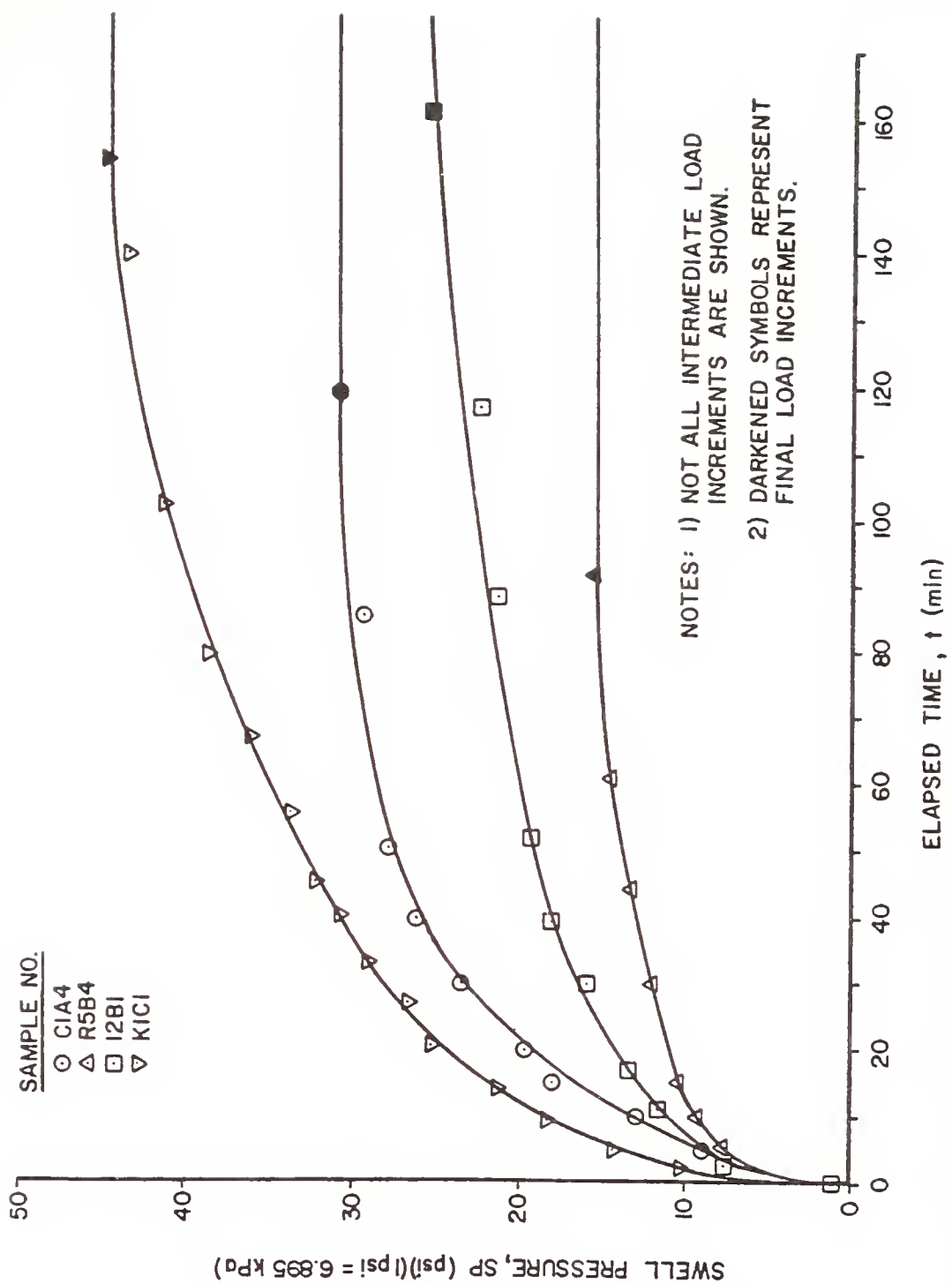

Figure 2.22 Swell Pressure Vs. Time for Typical Samples

3 - ANALYSIS OF DATA

Introduction

The purpose of this study was to find the best prediction model for the tendency to swell induced by compaction, i.e., the swell pressure. As the data were gathered, it became apparent that variation existed in all the measured parameters. This precluded the use of a functional model, i.e., one in which all data points lie on the locus of the function. Rather, a statistical relation was derived by linear regression analysis. As Neter and Wasserman (1974) stated,

> A regression model is a formal means of expressing the two essential ingredients of a statistical relation:
>
> (1) A tendency of the dependent variable Y to vary with the independent variable or variables in a systematic fashion;
>
> (2) A scattering of observations around the curve of statistical relationship.

The regression equation produces a curve or surface of "best fit" through the data points. These "fitted values" are not adequate for predictive purposes, as the analysis must also assess the variability of the data set. In some cases the variability can be quite high with respect to the expected value. As the amount of data scatter increases, the usefulness of a fitted value model decreases. The predictive models for swell pressure are based upon a regression equation to which is added the appropriate amount of variability (the way in which this variability was assessed will be explained in a later

section). The resulting model is then expressed as a fitted or expected value plus a variability term. This then creates a "ceiling value" for prediction purposes. This ceiling value represents the predicted maximum swell pressure that should be observed in the embankment. The engineer can use this to guide his design and/or compaction specification with assurance that he has control over the tendency to swell which is induced by compaction.

This analysis paralleled that done by Price (1978) but contained the following differences.

(1) This analysis was extended to include the prediction of field swell behavior from laboratory compaction variables.

(2) Some of the independent variables were represented in a different manner (see "Selection of Variables" section).

(3) Both sides of optimum moisture content were achieved in the field and were accounted for in this analysis.

(4) The Ridge Regression computer program was not used; instead, variables were selected using hypothesis testing.

Selection of Variables

The basic independent variables chosen for the analysis were water content as a deviation from the optimum moisture content (Δw) and energy ratio (E_R) based on the lowest gross input energy for each compactor type; dry density (γ_d) was also used for swell pressure prediction. Δw was chosen because some investigators say it is the controlling variable for behavior (Price, 1978). Weitzel (1979) showed that it was difficult at best to determine the amount of input energy

which was actually used to compact the soil in a laboratory kneading compactor. The largest problem came from the inability to measure the soil rebound as the tamping foot was raised. Similar problems occur with laboratory impact compaction. In addition, the applied field energy also escapes exact measurement. Therefore, energy ratio was chosen because it could easily be quantified for each type of compactor and used for comparisons (Table 3.1). It must be remembered, however, that energy ratios were not exactly comparable as each set (lab and field) was based on a different datum.

Table 3.1 Energy Ratios

Compactor Type	Quantity Measured	E_R	Energy Level
Caterpillar	No. of Passes		
&	4	1.0	A
Rascal	8	2.0	B
	16	4.0	C
Impact	Applied Energy (ft · lbs)		
	247.5	1.00	A
	412.5	1.67	B
	1875.0	7.58	C
Kneading	Gage Pressure (psi)		
	4	1.00	A
	7	1.75	B
	26	6.50	C

Analytic Procedures

The first step in the analysis was to plot dry density against absolute water content for each energy level and type of compactor to obtain the corresponding compaction curves. Maximum dry density and optimum moisture contents (OMC) were selected for each curve. Dry density was then plotted against water content from optimum (Δw) and energy ratio (E_R). Swell pressure (SP) was plotted against water content from optimum (Δw), dry density (γ_d), and energy ratio (E_R).

The curvilinear nature of these scatterplots was clearly evident. Therefore, second order terms of the basic independent variables were also included in the regression analysis. In order to account for possible interactions between independent variables, they were combined two at a time to a maximum power of two for each independent variable (e.g., $\Delta w^2 \times \gamma_d^2$ represents the highest order used).

After selecting the appropriate set of independent variables, the Purdue computer program DRRSQU was employed. This gave values of the coefficient of multiple determination (R^2) in ranking order for all possible combinations of independent variables. R^2 measured the proportion of total variation that was "explained" or "accounted for" by the set of variables used in that regression model. While R^2 was the only statistical descriptor used in this phase of the analysis, it was not the only criterion used for selecting the final prediction model. Other selection criteria which were used will be explained later in this section.

Equations which showed a reasonably high R^2 value were subjected to additional analysis using the REGRESSION computer program

(an SPSS program developed by Nie, et al., 1975). Only those equations with three or fewer independent variables were considered. Increasing the number of independent variables beyond three did not appreciably affect the R^2 values, but it did serve to complicate the model. Plots of the residuals were made and studied, and no trends were observed. This indicated that the residuals behaved in a random, independent manner and that the error variance was constant; meeting these conditions were basic requirements of least squares regression analysis. For each of the models selected, the analysis then determined if the entire equation, as well as each term contained therein, significantly contributed toward the description of the true relationship. All such hypothesis testing used a 95% confidence coefficient, which implies that the risk of making a Type I statistical error was controlled at 5%. A Type I error in this context would be to claim that a regression equation, or variable(s) in an equation, did not contribute toward the true description when in fact it did contribute.

It was mentioned earlier that a high value of R^2 alone did not provide an adequate criterion for selecting the final prediction model. The analysis described in the preceding paragraph, along with the criteria in Table 3.2 were used to select the final prediction model. Each category of data required somewhat different treatment. Therefore, more detailed descriptions follow.

Dry Density and Swell Pressure Magnitude

Swell pressure magnitude was analyzed first. Data were first separated by compactor type and whether compaction was performed in the lab or in the field. Water content and dry density had been

Table 3.2 Criteria Used for Selecting Prediction Models

1. The Model must be relatively simple in order to encourage use (this includes using the minimum number of independent variables and equations).
2. The model must provide a good statistical fit (this refers to R^2, residual analysis, and hypothesis testing).
3. The shape of the regression surface should reflect the trends shown by the data points.
4. The model must describe the variability associated with the data.
5. The model must be able to predict field response from laboratory data.

measured in two ways for each compactor type, but only one set of measurements could be used for the analysis. The set of measurements chosen for each case was based on the ability to describe the statistical relationship as well as the ease of gathering data for future application of this research.

For laboratory compaction, water content and dry density were measured for both the compaction mold and the test specimen. These compaction curves are shown in Figures 2.11 and 2.12, and Figures 2.20 and 2.21, respectively. From these curves it can be seen that the place of measurement caused little difference in the measured values. Since the measurements were nearly equal compaction mold values were used for the analysis. It was felt that little, if any, accuracy was lost by choosing these instead of test specimen values.

Plots of swell pressure versus water content deviation from optimum (Δw) for impact and kneading compaction are given in Figures 3.1 and 3.2 respectively. The data suggest that swell pressure is a continuous function of Δw for each energy level. As a result, the data sets for laboratory compaction did not require further breakdown into subsets. Resulting regression equations are presented in Table 3.3. It is interesting to note that the same variables appear in the equations for both types of laboratory compaction, but with different regression coefficients.

For field compaction, water content and dry density measurements were taken in the field by nuclear devices and also from test specimens in the laboratory. Initial analyses were performed using the field measurements. As Figures 2.3, 2.4, 2.18 and 2.19 showed,

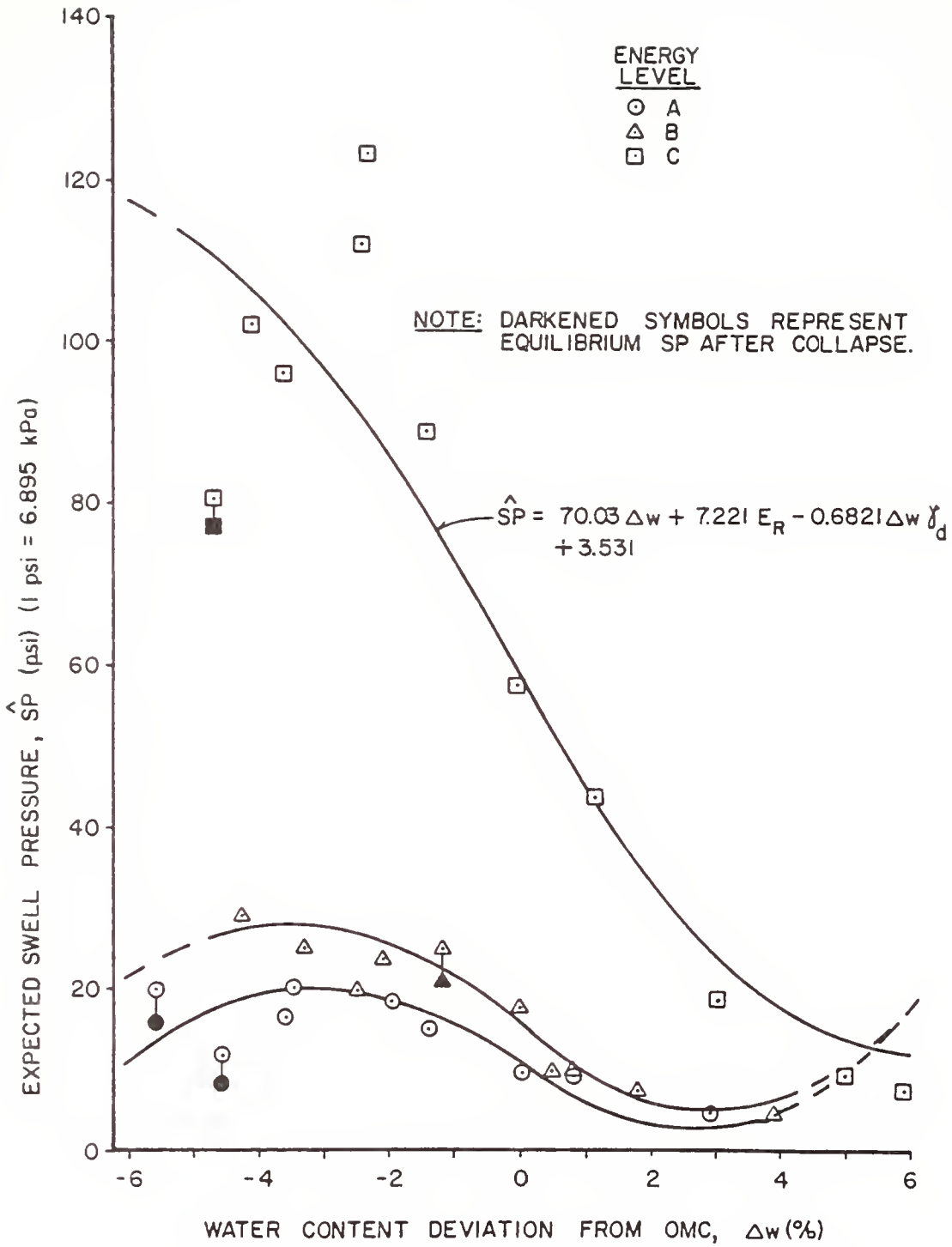

Figure 3.1 Impact Swell Pressure Relationships for Compaction Mold Values

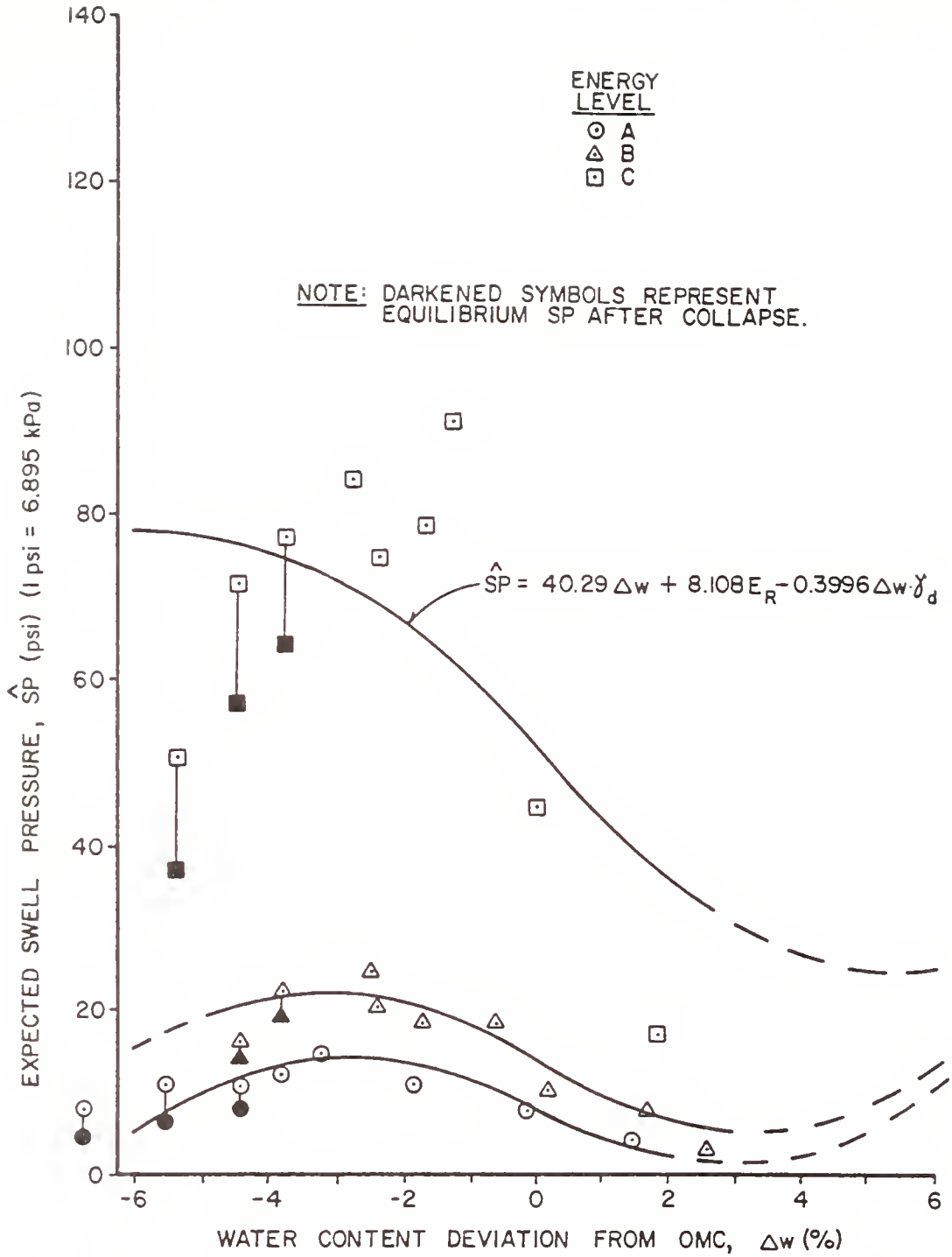

Figure 3.2 Kneading Swell Pressure Relationships for Compaction Mold Values

Table 3.3 Regression Results

Compactor Type	Conditions for Application	Regression Model	R^2
Caterpillar	Dry of OMC	$\hat{\gamma}_d = 5.863\ \Delta w + 118.3$	0.458
	Wet of OMC	$\hat{\gamma}_d = -1.609\ \Delta w + 1.006\ E_R + 114.3$	0.828
	Dry of OMC	$\hat{SP} = 21.72\ \Delta w + 44.12$	0.461
	Wet of OMC	$\hat{SP} = -10.87\ \Delta w + 0.7998\ \Delta w^2 + 43.08$	0.695
Rascal	Dry of OMC	$\hat{\gamma}_d = 1.906\ \Delta w + 1.390\ E_R + 112.5$	0.609
	Wet of OMC	$\hat{\gamma}_d = -1.378\ \Delta w + 1.044\ E_R + 112.0$	0.723
	A & B Energy Levels	$\hat{SP} = 0.2919\ \Delta w^{2*} + 4.593\ E_R^{*} - 0.02357\ \Delta w\gamma_d + 9.908$	0.260
	C Energy Level	$\hat{SP}^{**} = -16.08\ \Delta w^{*} + 0.1501\ \Delta w\gamma_d^{*} + 14.50$	0.269
Impact	Dry of OMC	$\hat{\gamma}_d = 1.428\ \Delta w + 2.194\ E_R + 109.1$	0.943
	Wet of OMC	$\hat{\gamma}_d = -1.849\ \Delta w + 1.976\ E_R + 110.2$	0.928
	All Δw and E_R	$\hat{SP} = 70.03\ \Delta w + 7.221\ E_R - 0.6821\ \Delta w\gamma_d + 3.531^{*}$	0.917
Kneading	Dry of OMC	$\hat{\gamma}_d = 2.034\ \Delta w + 2.126\ E_R + 109.9$	0.960
	Wet of OMC	$\hat{\gamma}_d = -2.190\ \Delta w + 2.164\ E_R + 111.0$	0.960
	All Δw and E_R	$\hat{SP} = 40.29\ \Delta w + 8.018\ E_R - 0.3996\ \Delta w\gamma_d + 0.04564^{*}$	0.867

*Independent variable is not significant at 0.05 α-level

**Entire equation is not significant at 0.05 α-level

large differences existed between laboratory and field measurements for each field compactor type. Probable causes for these discrepancies were previously discussed. Variations in water content and dry density existed within each combination of water content level, energy level, and compactor type.* This was evidenced for both field and test specimen values in Table 2.3 and Appendix A, respectively. These variations, in turn, produced variability in swell pressure measurements within a series. It was impossible to directly relate a specific field measurement with any given test specimen, and therefore average values of field water content and dry density had to be used for each sample series. These averages limited the analysis to only five discreet combinations of water content and dry density per energy level when, in fact, the test specimens produced a minimum of 14 such combinations. At each average field water content the swell pressure varied greatly (see Figures 3.3 and 3.4), the statistical relationship was obscured and poor R^2 values resulted. Because of this, it was decided to investigate swell pressure as a function of test specimen water content and dry density.

Figure 3.5 shows swell pressure plotted against test specimen water content deviation from OMC for the Caterpillar compactor. A distinct cusp is evident near the OMC with different trends in the data points on each side of it. Polynomial regression equations do not adequately describe these features over all water contents; therefore the data are broken into two subsets. All data points dry of OMC are grouped together for analysis. The resulting equation, shown in

---

*A combination of water content level, energy level, and compactor type will also be referred to as a series or sample series.

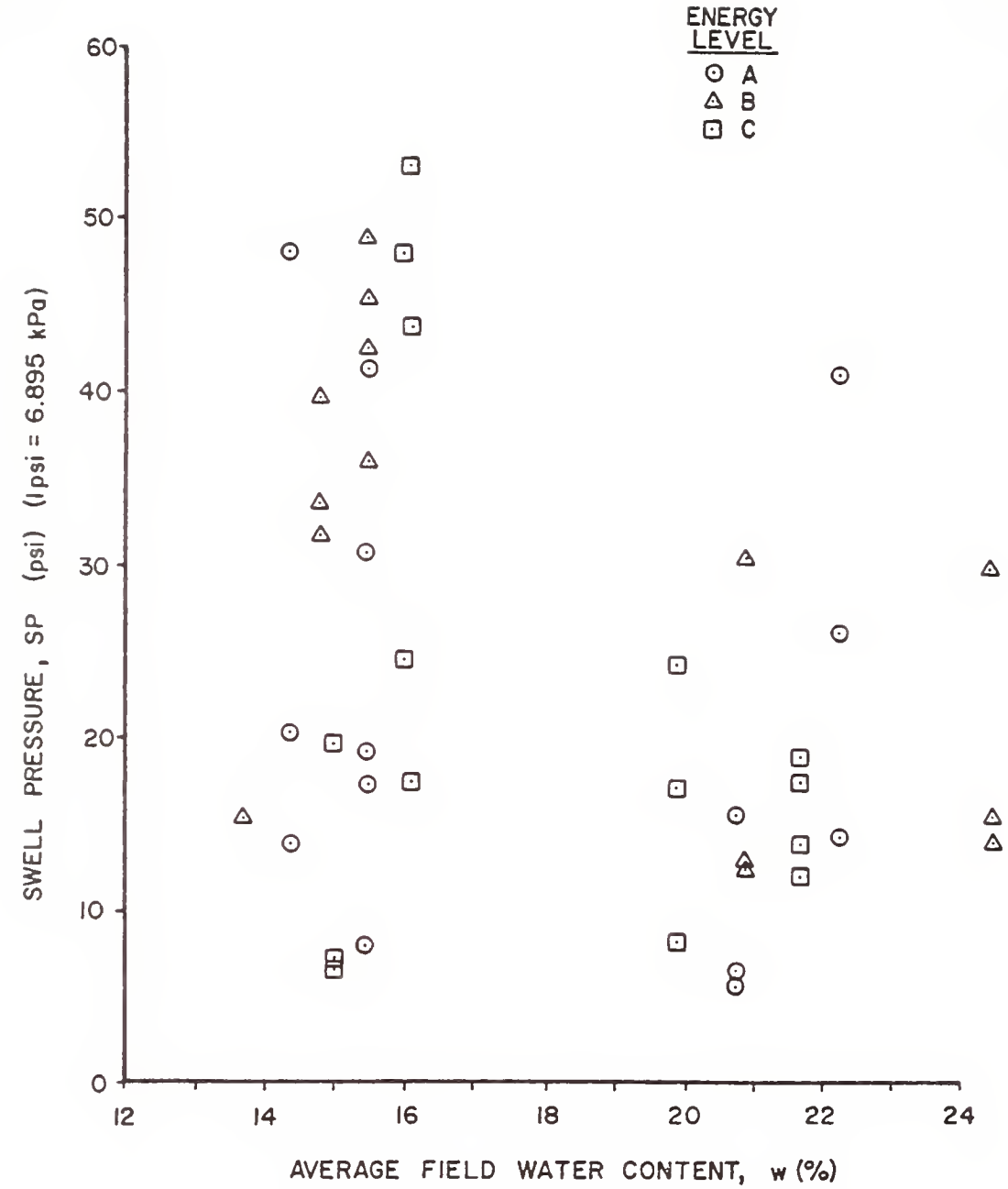

Figure 3.3 Caterpillar Swell Pressure Data for Field Nuclear Gage Values

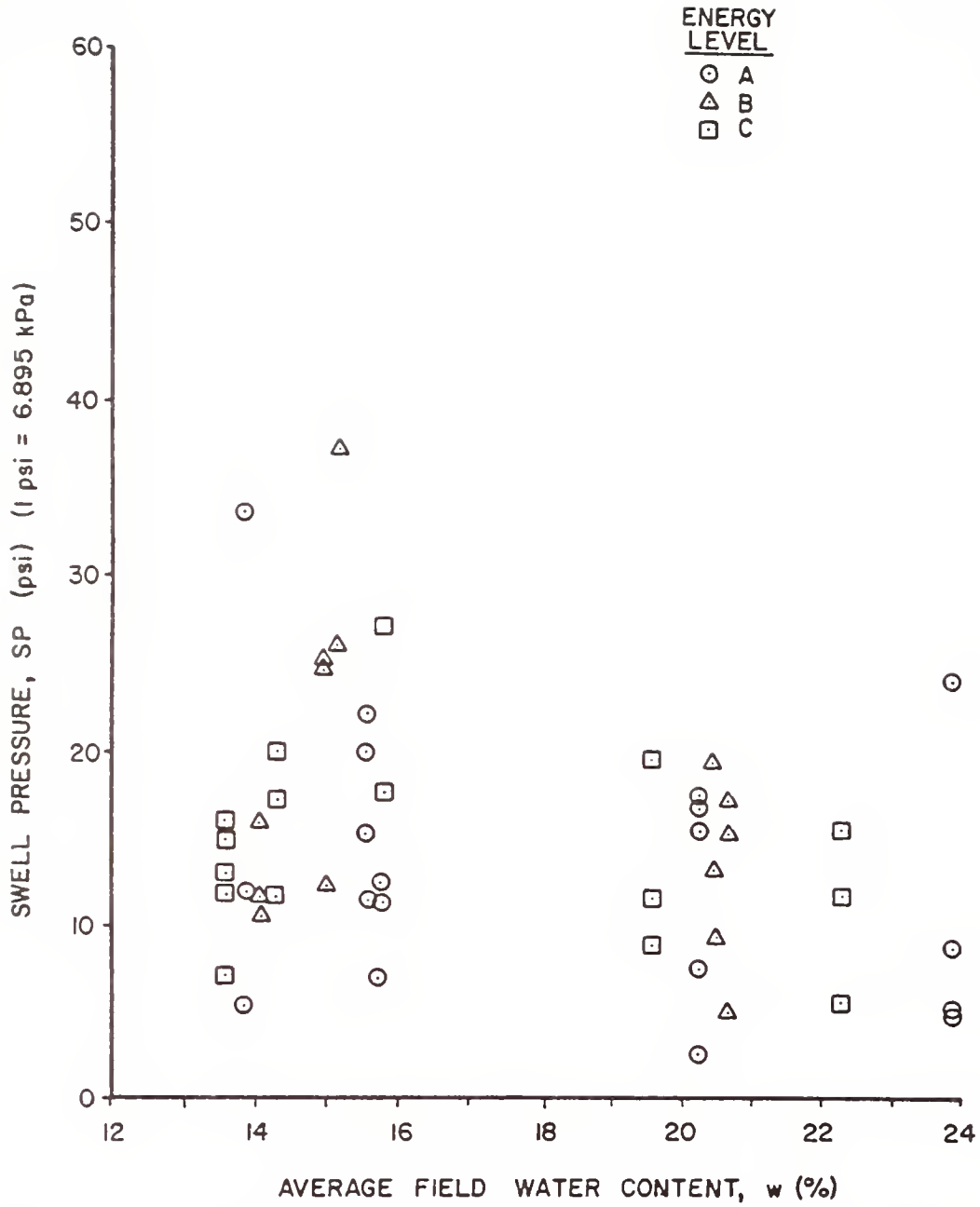

Figure 3.4 Rascal Swell Pressure Data for Field Nuclear Gage Values

Table 3.3, reflects the linear trend in these data. For points wet of OMC, similar analysis results in a quadratic regression equation. Peak values of swell pressure occur slightly dry of OMC, and are also included in the analysis of wet side data. They serve to raise this regression line such that it intersects the dry side regression line closer to OMC and at a higher swell pressure. This is believed to be appropriate and desirable for the given data set. It does not appreciably change any statistical parameters. It should be noted that water content from optimum (Δw) is the only significant descriptor of swell pressure induced by the Caterpillar compactor.

Swell pressure data for the Rascal compactor are shown in Figures 3.6 and 3.7. More data scatter is apparent here than for the Caterpillar data which resulted in consistently lower R^2 values. Similar trends in the data occur for the A and B energy levels. To adequately describe them, they had to be separated from the C energy level. The data from the C energy level show a flat response with much scatter and, as a result, a significant regression equation could not be found for this energy level. The regression equations are again given in Table 3.3.

Dry density was a significant variable in many of the regression relations for swell pressure. Because of this it was also subjected to regression analysis. Water content and dry density measurements were taken from the compaction mold for laboratory compacted samples and from test specimens for field compaction. Data from each compactor type were again analyzed separately.

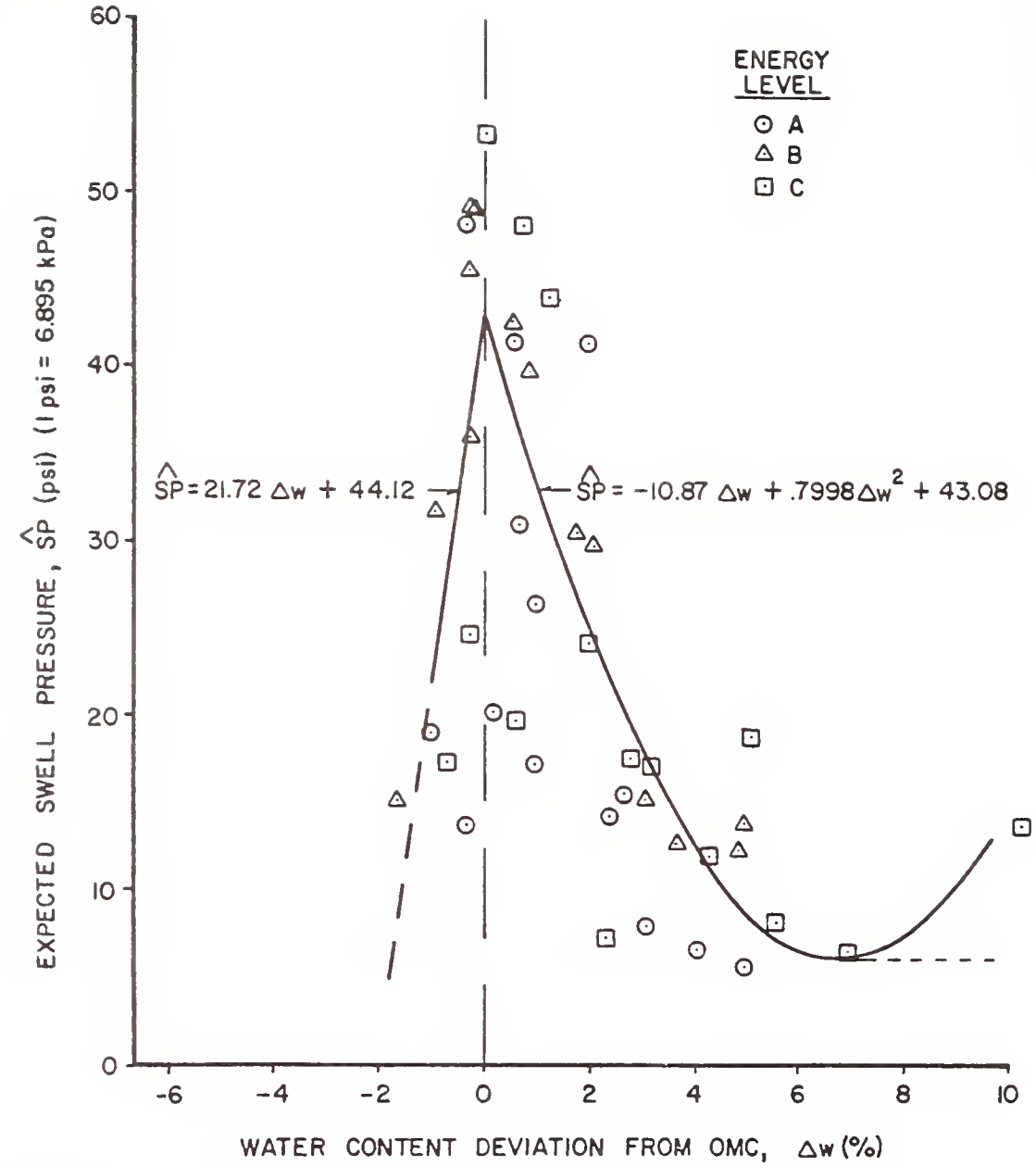

Figure 3.5 Caterpillar Swell Pressure Relationships for Test Specimen Values

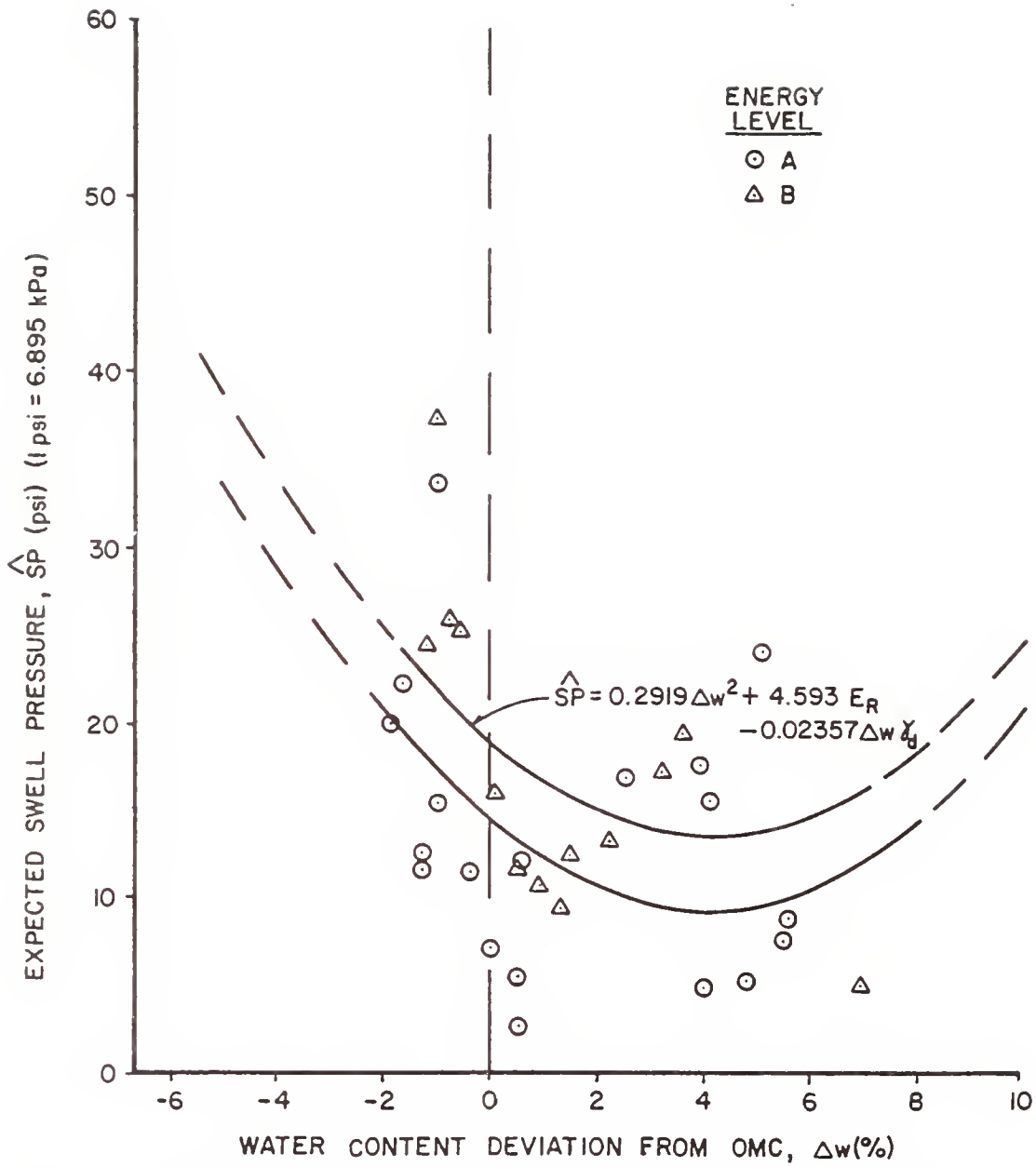

Figure 3.6 Rascal Swell Pressure Relationships for Test Specimen Values, A and B Energy Levels

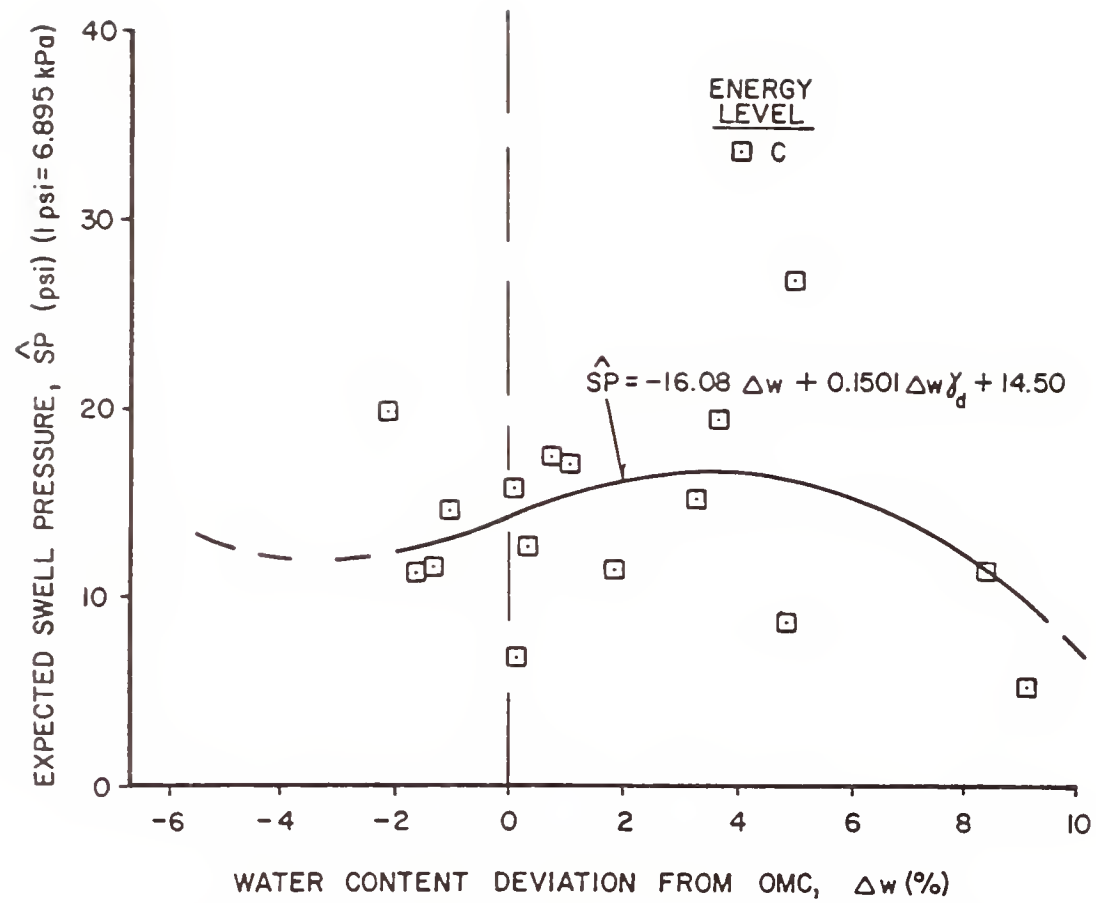

Figure 3.7 Rascal Swell Pressure Relationship for Test Specimen Values, C Energy Level

After compaction curves were drawn and optimum moisture contents selected, each data set was analyzed. Initial analyses showed that quadratic models poorly described the data over all water contents, but still produced a high value of R^2. For this reason the data sets were subdivided into dry of OMC and wet of OMC subsets. The results of the regression analysis are shown in Table 3.3. It should be noted that both the impact and kneading compaction data sets contained one point wet of OMC which was not tested for swell pressure. These data points were needed to help define the compaction curves but not the swell pressure curves.

Variability of Dry Density and Swell Pressure

The statistical analysis for variabilities associated with dry density and swell pressure also paralleled that of Price (1978). The variability in water content and dry density for all of the compaction conditions studied influenced other soil properties such as strength and, in this case, swell pressure. Therefore, swell pressure variability was not determined for specific values of water content and dry density, but rather for a range of these values at a particular compactive effort.

Two ways of measuring the variability of a data set are of interest in this report. The variance of n observations (a data set) essentially measures the average deviation from their mean, $\bar{Y}$. The standard deviation is the square root of this variance. Another measure, the error mean square (MSE), assesses the deviation of observed values (Y_i) around the fitted regression line. The difference between these two measures is illustrated in Figure 3.8. The first approach

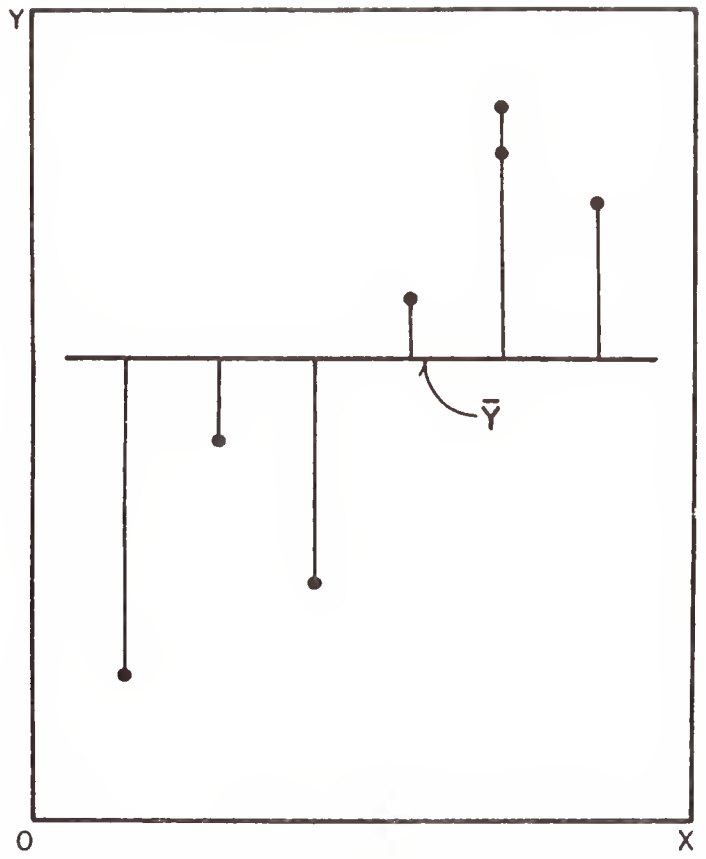

DEVIATION OF OBSERVED VALUES AROUND THEIR MEAN.
(STANDARD DEVIATION CONCEPT)

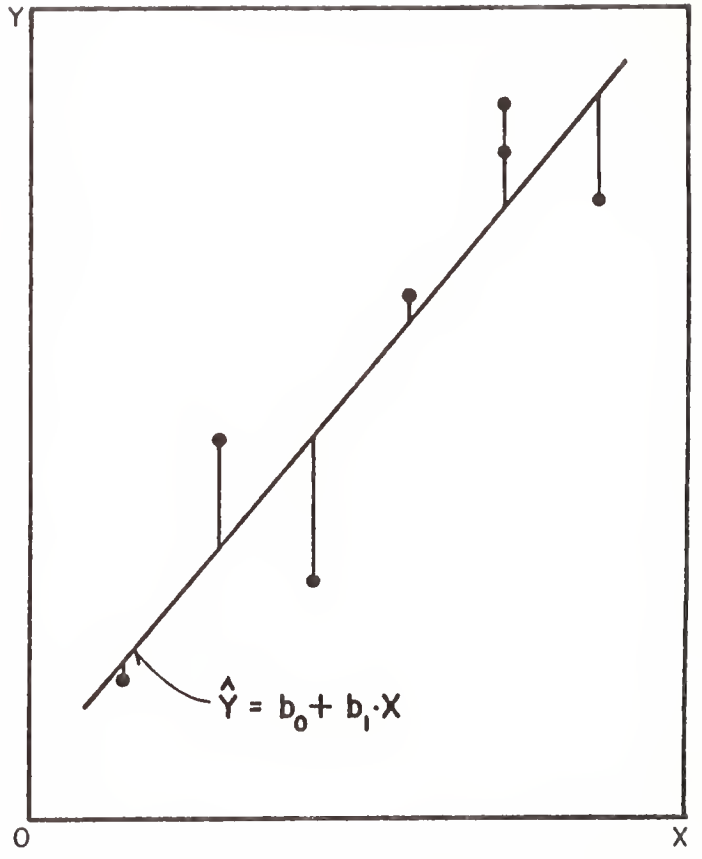

DEVIATION OF OBSERVED VALUES AROUND THE FITTED REGRESSION LINE.
(ERROR-MEAN-SQUARE CONCEPT)

Figure 3.8 Two Ways of Assessing the Variability of a Data Set

measures the scatter around a single value. This study, however, indicates that dry density and swell pressure vary in a systematic fashion with other variables. This makes it necessary to determine the variability at several response levels. Therefore, the error mean square method is appropriate for application in this analysis.

All regression models estimate the true relationship among the variables in a data population; this produces an inherent uncertainty in the accuracy of the model. As a result, these estimates are most accurate near the average values of the dependent variable and all independent variables. Accuracy of estimation decreases with distance from these mean values. Therefore, for a given degree of confidence, the confidence interval must increase in size with distance from these means.

For a general linear regression model, the following formula is used to give an interval estimation (confidence interval) of the mean response $E(Y_h)$ at one point:

$$\hat{Y}_h - t(1 - \alpha/2;\ n - p) \cdot S(\hat{Y}_h) \leq E(Y_h) \leq \hat{Y}_h + t(1 - \alpha/2;\ n - p) \cdot S(\hat{Y}_h)$$

Where:

$E(Y_h)$ = the expected mean response for the given levels of the independent variables $[X_h]$

$\hat{Y}_h$ = the fitted regression value for the given values of $[X_h]$

n = the number of observations in the data set

$p - 1$ = the number of independent variables in the regression equation

α = probability of committing a Type I error

$t(1 - \alpha/2;\ n - p)$ = appropriate t-statistic

$S(\hat{Y}_h)$ = square root of $S^2(\hat{Y}_h)$

$S^2(\hat{Y}_h) = MSE[X_h'(X'X)^{-1}X_h]$ = estimated variance of $\hat{Y}_h$

MSE = error mean square. This value was obtained from the REGRESSION computer program output

[X] = matrix of observed values of the independent variables in the regression model

[X]' = [X] transposed

$[X_h]$ = column vector containing values of the independent variables for the response level under investigation

$[X_h]'$ = $[X_h]$ transposed.

This formula for variability is usually evaluated for $E(Y_h)$ by using a fixed set of independent variables, $[X_h]$. This produces a point on the response surface, $\hat{Y}_h$, and also the confidence interval at that response level. Although this is sufficient for most applications of this formula, it does not suffice for studies of soil compaction.

The state-of-the-art of compaction cannot guarantee precise values of $[X_h]$ (i.e., w, γ_d, E_R). Rather, these quantities must be viewed as expected values, at each response level, with some inherent variability. These additional deviations must also be included in the total variability of the dependent variable.

In this study, although each test pad was constructed to have a nearly constant water content, a relatively large variation did occur. The range in water content was calculated for each level of compactive effort and compactor type. The average range for both compactors was

approximately 2.8% for the test specimens and 3.5% for field nuclear gauge measurements. Since these values will not apply to all compaction projects, dry density and swell pressure variabilities were calculated for several different water content ranges. For illustrative purposes herein an expected range of 2.8% was used.

The amount of variability associated with compactive effort could not be quantified and, therefore, was assumed to be zero for this analysis. The regression equations presented in the previous section were used to determine the expected dry density for each level of Δw and E_R. A 95% confidence criterion was arbitrarily chosen for determining dry density variability. For each value of Δw chosen, the 95% confidence interval of dry density was calculated for Δw plus and Δw minus the half-range variation in water content (equal to 1.4% here). The larger of these two values was then chosen as the expected dry density variability, $V(\hat{\gamma}_d)$. This method was also used to determine the swell pressure variability for the Caterpillar compactor, since Δw was the only significant variable in the regression model.

The following method was used to estimate swell pressure variability for the other compactor types. Since Δw and dry density appear in these models, the variability of both was included in the analysis. It was assumed that Δw and dry density varied independently at each response level. Therefore, swell pressure variability, $V(\hat{SP})$, was calculated for the four conditions shown below:

Δw	γ_d	$V(\hat{SP})$
$\Delta w + 1.4$	$\hat{\gamma}_d + V(\hat{\gamma}_d)$	$V(\hat{SP})_1$
$\Delta w + 1.4$	$\hat{\gamma}_d - V(\hat{\gamma}_d)$	$V(\hat{SP})_2$
$\Delta w - 1.4$	$\hat{\gamma}_d + V(\hat{\gamma}_d)$	$V(\hat{SP})_3$
$\Delta w - 1.4$	$\hat{\gamma}_d - V(\hat{\gamma}_d)$	$V(\hat{SP})_4$

The largest value of $V(\hat{SP})$ obtained from the four combinations was chosen as the expected swell pressure variability for that response level. This analysis was also done for a 95% confidence criterion.

A two-sided confidence interval was used for calculation of dry density variability. The appropriate t-statistic was $t(1 - \alpha/2; n - p)$ or $t(0.975; n - p)$. The purpose of the swell pressure variability was to create a "ceiling value" for swell pressure, which required the use of a one-sided confidence interval. In this case however, four values of variability were calculated at each response level. In order to maintain an overall α-level of 0.05, each variability was evaluated at a level of $\alpha/4$. The appropriate t-statistic was $t(1 - \alpha/4; n - p)$ or $t(0.9875; n - p)$. This was analogous to using $\alpha/2$ in a two-sided test at a single point. As previously mentioned, swell pressure variability for the Caterpillar compactor needed to be evaluated at only two points. The appropriate t-statistic therefore was $t(0.975; n - p)$.

The analysis presented here was evaluated for one water content range (2.8%) and confidence coefficient (95%). The computer programs presented in Appendix B can be adjusted to accomodate the expected conditions of future projects.

4-DISCUSSION OF RESULTS

Dry Density and Swell Pressure Magnitude

Dry density is a significant prediction variable in swell pressure equations for three of the four compactor types used in this study; thus, prediction models for dry density are also developed and presented. For these three compactors, models for dry density are needed to predict both the magnitude and the variability of swell pressure. These models also enable the prediction of field dry density for inspection testing, as outlined in the "Application of Results". The dry density models can be directly substituted into those for swell pressure, but this does not simplify the calculation of $\hat{SP}$. Such a substitution requires the use of two swell pressure models (one for dry of OMC and one for wet of OMC) where one had previously sufficed.

Caterpillar Compactor

Regression results show that dry density is not a function of energy ratio for points dry of OMC. The slope of this regression line (the regression coefficient of Δw) is shown in Table 3.3 and Figure 4.1, and is approximately three times steeper than those for the other compaction types. These features could be a result of: (1) a relatively small number of data points dry of OMC for this compactor (only 12 points); (2) the narrow range of water contents

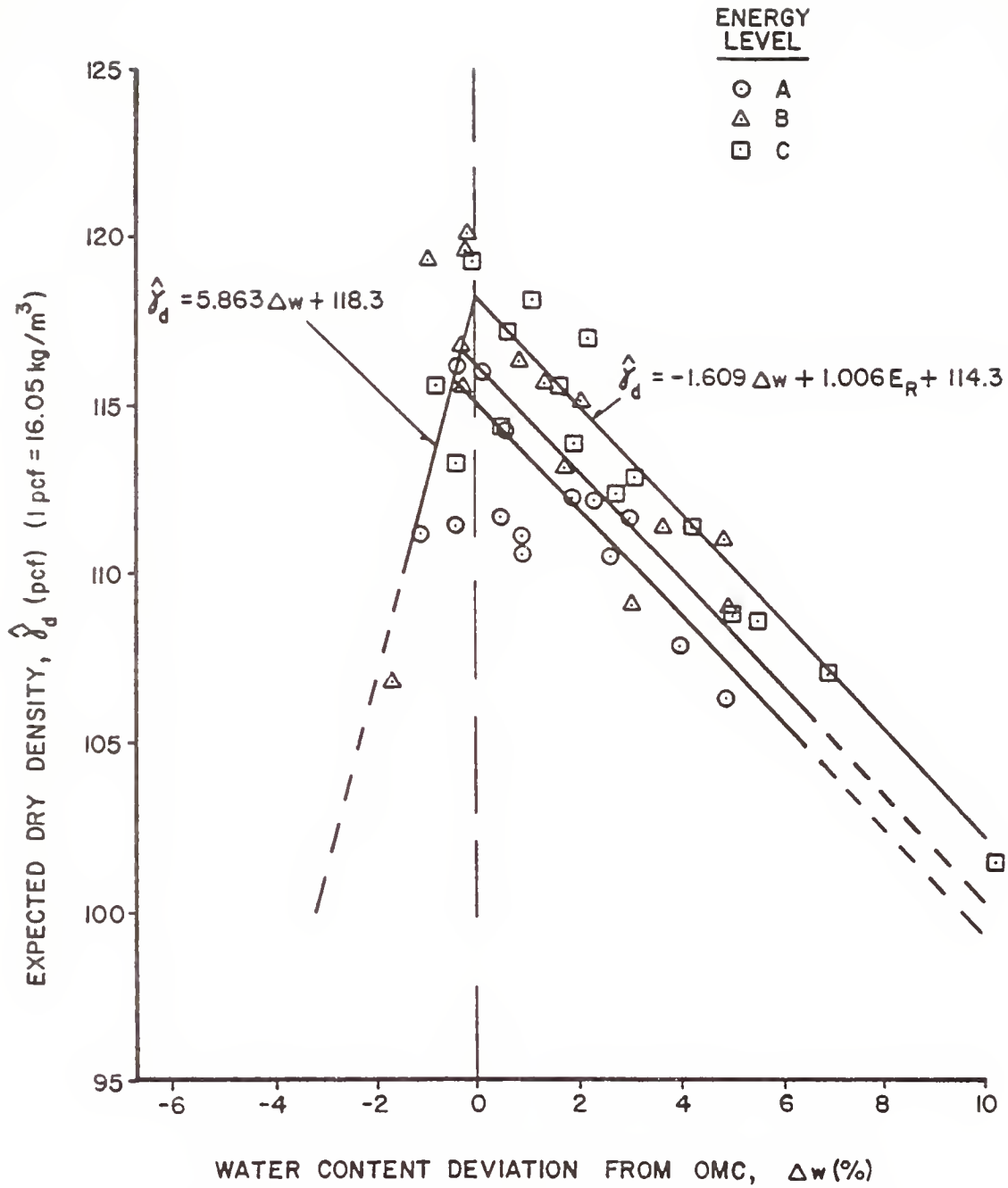

Figure 4.1 Caterpillar Dry Density Relationships for Test Specimen Values

achieved dry of OMC in the field (all Δw wetter than -2%); (3) an exceptionally large amount of variability in the data; (4) the inability of this compactor to achieve consistent densities in this soil when compacted dry. Wet of OMC, dry density is a function of both Δw and E_R, and regression results are comparable to those for the other compactor types. Regression relations for the Caterpillar compactor dry density are shown in Figure 4.1.

Dry of OMC, swell pressure is a function of Δw only and reaches a maximum near OMC. This trend is contrary to results obtained for the other compactor types. In general, swell pressure has been observed to increase to a plateau as water content decreases. This discrepancy could be a result of the same four factors mentioned in the preceding paragraph, especially item (4). Nalezny and Li (1967) postulated that if dry density becomes quite low at low molding water contents, many large pores exist. As water is imbided, the aggregates expand into the pore space, which reduces the measured swell pressure.

Wet of OMC, swell pressure is a curvilinear function of Δw. Again, dry density and energy ratio are not significant variables. The swell pressure decreases as water content increases, which is consistent with other compactor types used in this study, as well as with results presented by other investigators. However, the regression relation increases in magnitude beyond approximately Δw = 7%. This is believed to be a consequence of the parabolic equation rather than of the actual data points, and the equation should not be used beyond this value of Δw. The horizontal asymptote shown in Figure 3.5 is believed to be more appropriate in this range.

Rascal Compactor

Regression analyses for dry density reveal that Δw and E_R are significant prediction variables both wet and dry of OMC. Table 3.3 and Figure 4.2 present these results. The figure reveals that more data scatter exists for points dry of OMC than for those wet of OMC.

Swell pressure is broken into two data sets for analysis; the A and B energy levels form one set while the C level comprises the other. Figure 3.6 shows that the A and B energy levels exhibit similar trends, with generally higher swell pressures being displayed for the B level. This swell pressure regression relation decreases as Δw increases, reaching a minimum value slightly wet of OMC; at larger values of Δw, swell pressure again increases. The increase in swell pressure wet of OMC is contrary to results of studies on lab compacted soils found in the literature (Seed and Chan, 1961; Nalezny and Li, 1967). This phenomenon could be the result of: (1) the large amount of data scatter produced by this compactor, as discussed in the "Analysis of Data" chapter and evidenced by the low R^2 values; (2) changes in soil fabric that may occur at certain water contents for this vibratory compactor. It should be noted that White (1980) found no significant differences in pore size distribution for samples compacted wet of OMC by this roller. Table 3.3 indicates that Δw^2 and E_R are not significant variables in the equation presented, but these variables are retained in the model for the following reasons: (1) Δw^2 provides the curvature of the model and this is believed to be appropriate; (2) E_R produces two distinct curves, and the data trends suggest this.

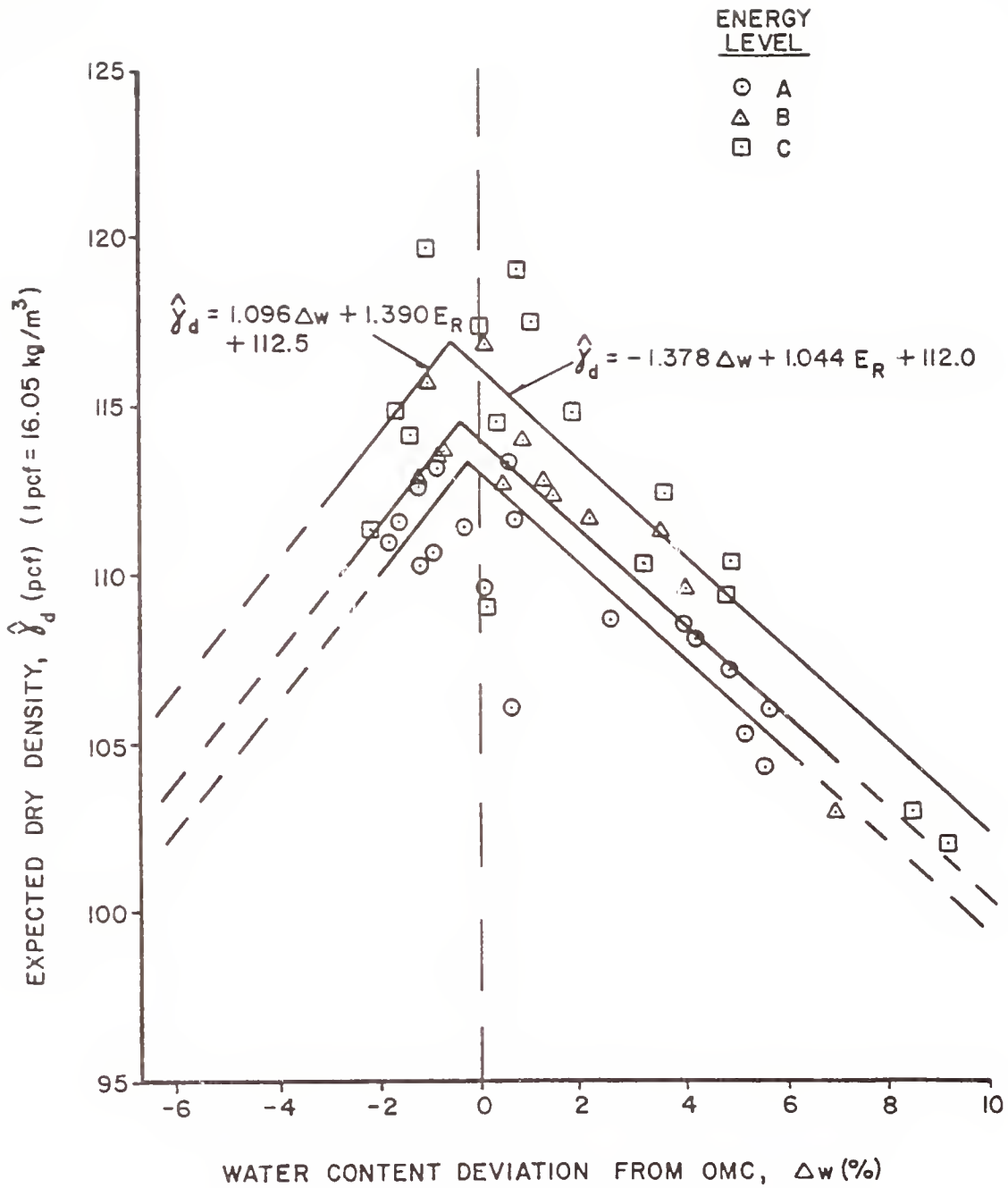

Figure 4.2 Rascal Dry Density Relationships for Test Specimen Values

For the C energy level, a significant regression equation for swell pressure could not be found. This is due to the large amount of data scatter and the relatively flat (horizontal) trend shown in Figure 3.7. Possible causes for the data scatter are discussed in preceding sections. The flat trend in swell pressure is an interesting occurrence, but attempts at explanation only produced speculations.

It should be reiterated that a significant regression equation for swell pressure could not be found for the Rascal C energy level. Thus, the equation presented herein should be used with caution. It is believed, however, that this equation, when used with its associated variability, provides a realistic model for the swell pressure.

Laboratory Compactors

Laboratory impact and kneading compaction methods produced similar results. The comapction curves, shown in Figures 2.11 and 2.12, are nearly identical, as are their maximum dry densities and optimum moisture contents for corresponding energy levels (see Table 4.1). In general, the slopes of the kneading compaction curves are somewhat steeper than those of the impact compaction curves. All of these features also occur for the regression results presented in Figures 4.3 and 4.4, and Table 3.3.

Swell pressure responses are also very similar for the two compactor types and are shown in Figures 3.1 and 3.2. The regression equations presented in Table 3.3 include the same independent variables, but with different coefficients. These similarities are not surprising, as White (1980) found no significant differences in pore size distributions of the fabric produced by the two methods of

Table 4.1 Summary of Optimum Moisture Contents and Maximum Dry Densities Obtained from Compaction Curves

Compactor Type	Location of Measurement	Energy Level	OMC (%)	Maximum Dry Density (pcf)
Caterpillar	Test Specimen	A	15.0	114.5
		B	13.6	118.0
		C	13.4	118.5
	Field Nuclear Gage	A	15.7	105.5
		B	15.6	110.9
		C	15.5	111.5
Rascal	Test Specimen	A	15.3	114.0
		B	14.8	115.0
		C	14.0	117.0
	Field Nuclear Gage	A	16.2	103.7
		B	15.4	107.2
		C	15.0	110.6
Impact	Compaction Mold	A	17.8	109.5
		B	16.6	113.8
		C	12.3	125.0
	Test Specimen	A	16.6	111.1
		B	15.6	114.2
		C	12.5	122.7
Kneading	Compaction Mold	A	18.6	110.7
		B	16.5	114.9
		C	12.6	124.1
	Test Specimen	A	17.7	109.8
		B	16.2	113.9
		C	12.8	122.9

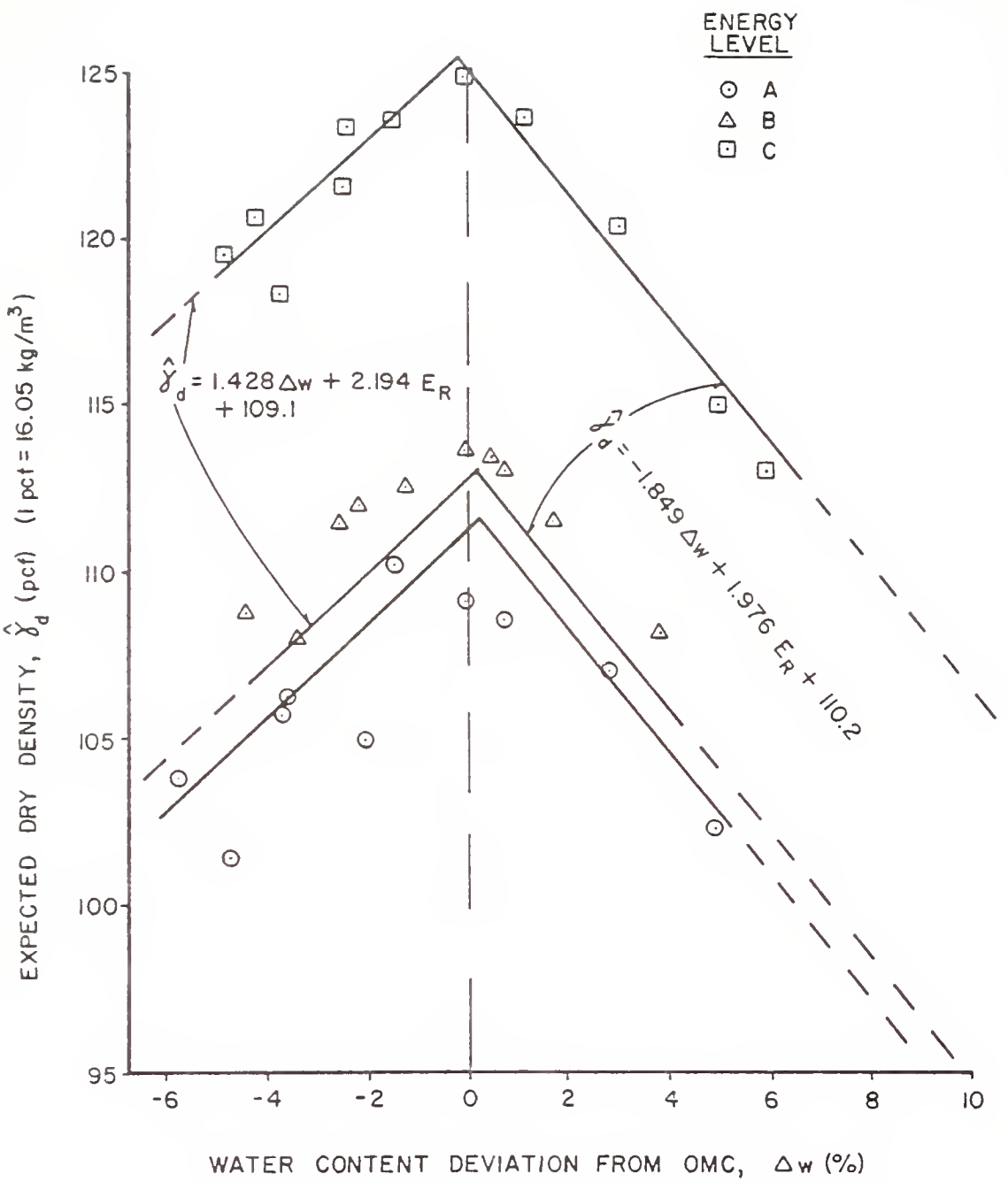

Figure 4.3 Impact Dry Density Relationships for Compaction Mold Values

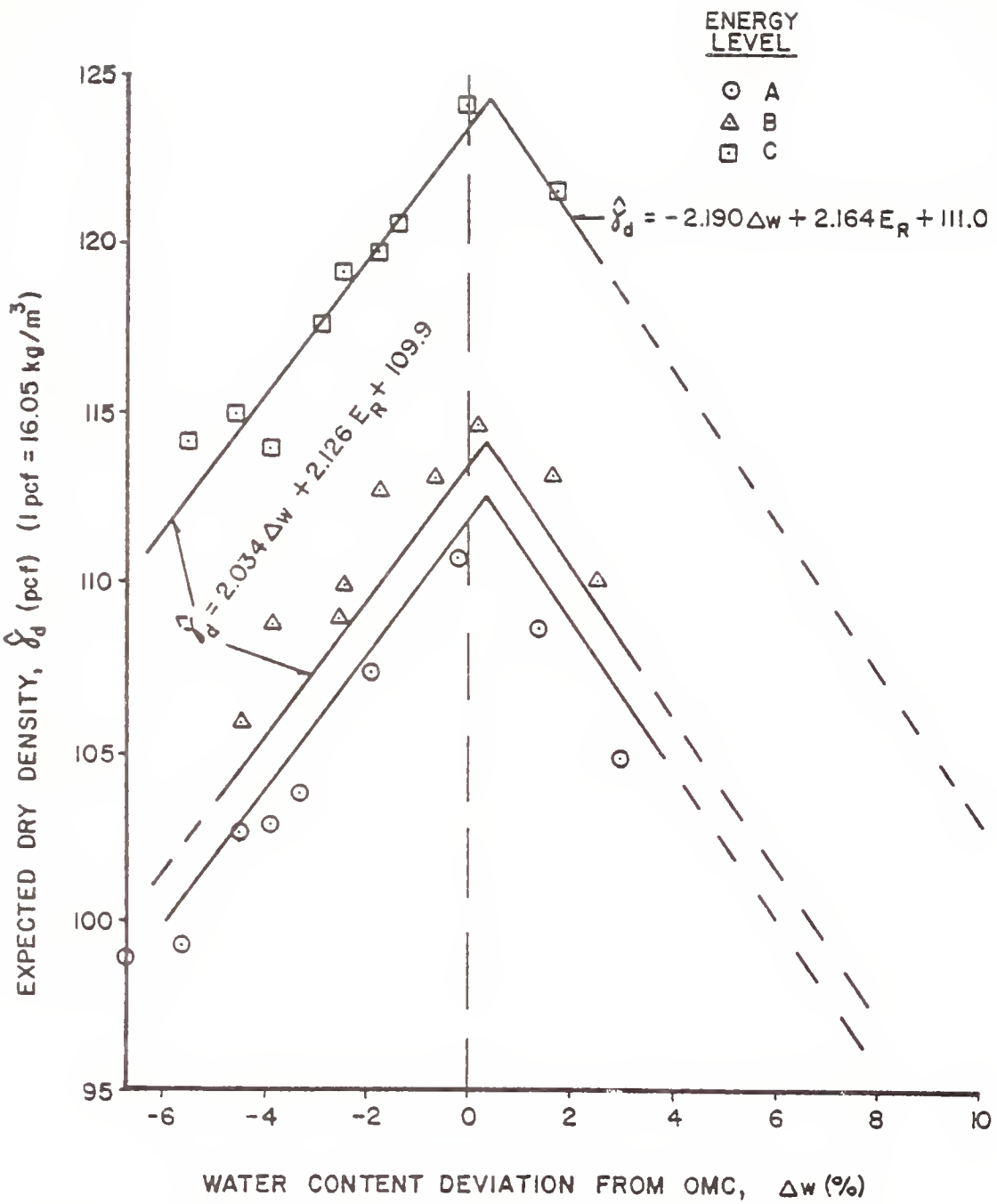

Figure 4.4 Kneading Dry Density Relationships for Compaction Mold Values

compaction. Seed and Chan (1961) also found that differences in structure, strength, shrinkage, and swell resulting from impact and kneading methods are small.

The data trends and regression curves are nearly identical for the A and B energy levels for the two compactors. These relationships are of the same general shape as those found in the literature (Nalezny and Li, 1967). For the C energy level, however, some discrepancies appear. The data points suggest a sharp peak near a water content 2% dry of OMC; swell pressure drops rapidly with distance from this peak, especially on the wet side. These peaks resemble that found near OMC for the Caterpillar compactor data, but the polynomial regression equations found for laboratory compacted samples could not simulate these sharp peaks. Another discrepancy arises from the swell pressure values near this peak. Dry of this peak, impact compaction produces swell pressures which are 10 psi to 35 psi (69 kPa to 240 kPa) higher than those for kneading compaction.

Samples compacted very dry of OMC exhibit a tendency to collapse in the CVS test. For these samples the swell pressure increases with time in a normal fashion, reaches some maximum value, then begins to rapidly reduce in volume under this sustained load. At this time, the load on the sample is decreased until no further value change occurs, and thus an equilibrium swell pressure is achieved. In Figures 3.1 and 3.2, collapsed samples are indicated by two symbols connected by a line. The open symbol shows the maximum swell pressure

prior to collapse, while the darkened symbol represents the equilibrium value after collapse. These figures also show that the onset of collapse occurs slightly wetter for kneading samples than for impact samples. This difference is also probably due to small differences in dry density and soil structure produced by the two methods of compaction. An explanation of this collapse phenomenon is given below.

Barden and Sides (1969) suggested that the collapse phenomenon occurs primarily on a macroscopic level, and is not due to microscopic changes from a floculated to a dispersed soil structure. Compaction on the dry side produces an open structure for the macroscopic particles (macropeds). These macropeds resist distortion during compaction because of their high shear strength, thus resulting in large air-filled interpedal channels. On the wet side, however, the macropeds have a lower shear strength and easily deform into a more homogeneous mass with few large voids. Observations made during this study also revealed the presence of individually visible macropeds for dry-side laboratory compaction, while wet-side samples were of a much more homogeneous nature. White (1980) also confirmed the higher frequency of large-size pores for dry-side compaction of this soil.

As water enters the relatively dry macropeds, it breaks down the surface tension menisci which results in a higher (less negative) pore water pressure and a lower effective stress. As the swell pressure develops, the higher applied load eventually causes the now softer macropeds to displace into the available pore space, thus causing collapse. Mishu (1963) concludes that collapse occurs when the combination of internal and applied stresses are such that slippage between

particles occurs. As the effective stress decreases upon wetting a reduced resistance to particle slippage results. When the applied load is large enough, slippage occurs; at lower applied loads no particle slippage takes place and swell can result. For samples compacted very dry of OMC, the combination of internal and applied stresses in the CVS test eventually reaches the onset of particle slippage, and collapse occurs.

Variability of Dry Density and Swell Pressure

Variations in the results of compaction are expected due to inherent variations in soil charcteristics, compaction processes, and testing procedures. Possible causes of these variations have been discussed in preceding sections of this work. These variations in turn, produce variability in the mechanical properties of the soil, such as swell pressure and strength.

Before the amount of variability in swell pressure was determined for the field compacted soil, the variations in the compaction variables were assessed. The compaction variables used were water content deviation from OMC, input energy ratio, and dry density where applicable. The amount of swell pressure variability caused by input energy variations could not be quantified. The variations in Δw were expressed as half-ranges, with average values found for field nuclear gage and test specimen measurements. These half-ranges were then used to determine the amount of variability associated with dry density. Finally, swell pressure variability was assessed using the computer programs given in Appendix B. A more thorough discussion of these procedures is given in the "Analysis of Data" chapter.

Other Associated Relationships

Figures 4.5 through 4.14 show some interesting relationships derived from the data. Such relationships may help to predict compaction characteristics and swell pressure behavior with a minimal amount of physical testing. Figure 4.5 shows swell pressure plotted against dry density for impact compaction. It can be seen that a "loop" function appears; dry of OMC swell pressure increases with increasing density to a point near γ_{dmax}, and then decreases as γ_d also decreases wet of OMC. This relationship shows the interdependence between water content and dry density, and its effect on swell pressure. This interdependence gives insight as to why Δw and γ_d appear in an interaction term in several of the regression equations for swell pressure. Similar trends in data are found for all compactor types used in this study, but they are most clearly illustrated by the impact compaction results.

Figure 4.6 shows that maximum swell pressure decreases as OMC increases. For a given soil, OMC can increase only if input energy decreases, which also results in lower dry densities. This combination of lower densities and higher water contents can only reduce the tendency to swell. This is consistent with evidence presented in the literature (Seed et al., 1961).

Figure 4.7 presents the relationship between the maximum swell pressure and that which develops at OMC. The Caterpillar compactor produces maximum swell pressures nearly equal to those at OMC. The other three compactor types develop maximum swell pressures which are approximately twice the magnitude produced at OMC.

Figures 4.8 and 4.9 show the relationship between OMC and the water content at which the maximum swell pressure occurs. Two distinct relationships can be seen - one for laboratory samples and one for field samples. Figure 4.9 indicates that maximum swell pressures develop dry of OMC, but nearer to it for field compacted samples than for laboratory compacted samples. In combination with Figure 4.10, these graphs also indicate that maximum swell pressure develops nearer to OMC as input energy increases.

Figure 4.11 reveals four distinct relationships for dry density as functions of water content at maximum swell pressure; these relationships roughly parallel the zero air voids curve (100% S_r curve). However, when dry density at maximum swell pressure is replotted versus its respective OMC, the points form a single relationship which also parallels the zero air voids curve (see Figure 4.12).

Figure 4.13 shows the relationship between swell pressure at OMC and energy ratio, while Figure 4.14 relates OMC to energy ratio. It is interesting to note that these relationships are nearly linear for each compactor type when plotted on semi-logarithmic axes.

It would be of interest to determine which of these ten relationships are similar (or identical) for other compaction equipment and soil types. If similarities exist, they could provide a simple basis for forecasting certain compaction characteristics and swell tendencies. Future investigations might also disclose the mechanisms which produce the relationships shown in Figures 4.5 through 4.14.

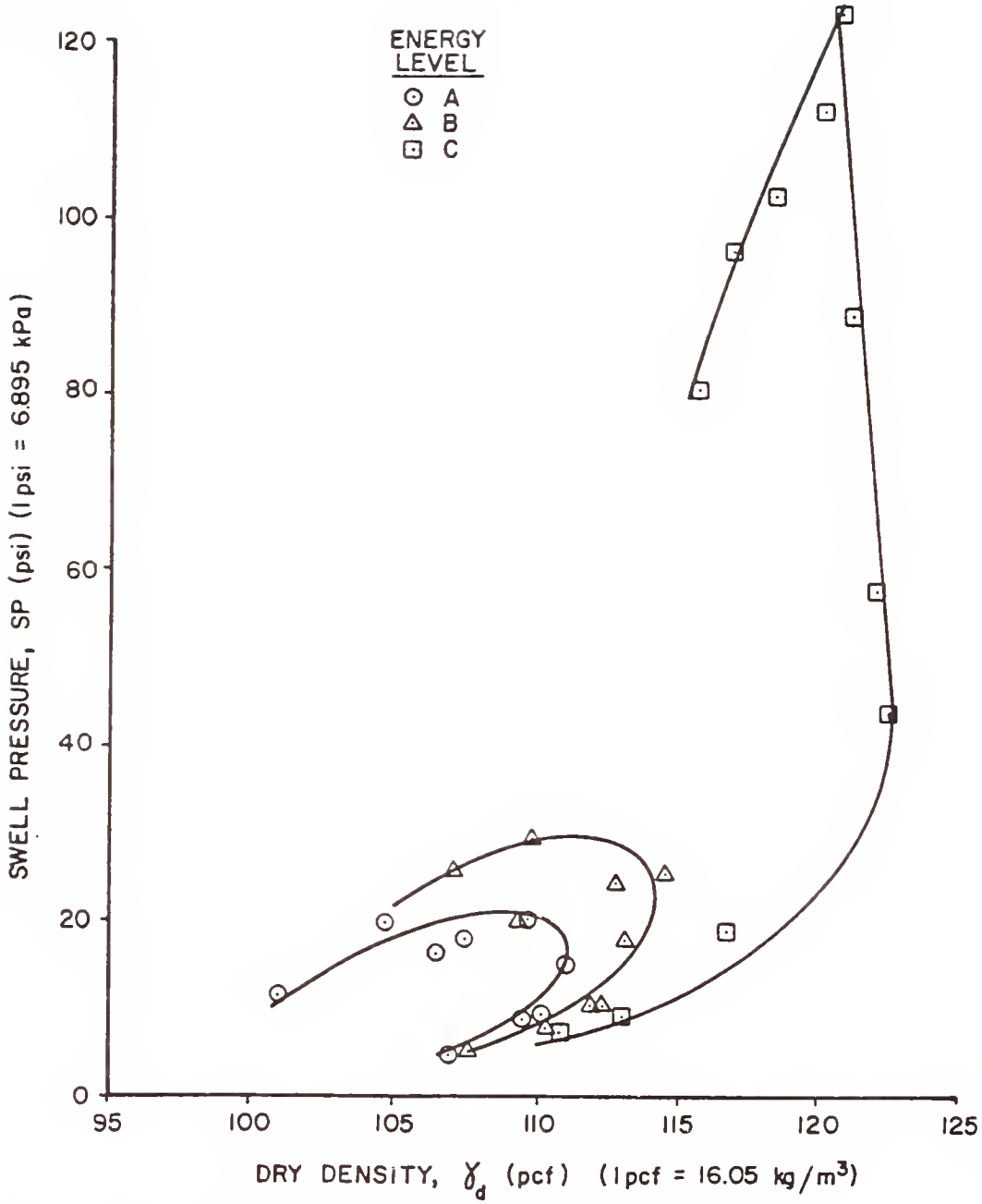

Figure 4.5 Impact Swell Pressure Vs. Dry Density

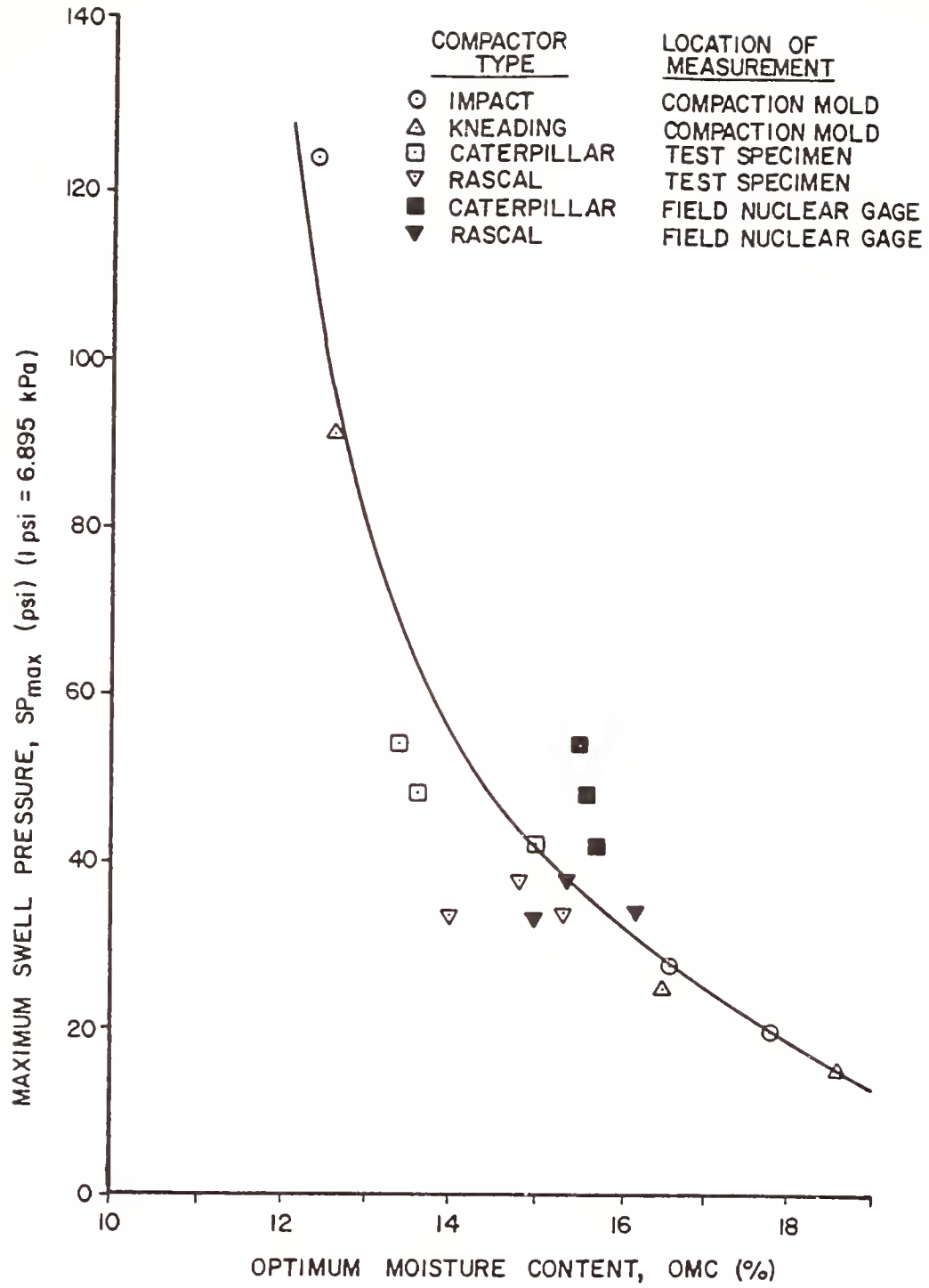

Figure 4.6 Maximum Swell Pressure Vs. Optimum Moisture Content

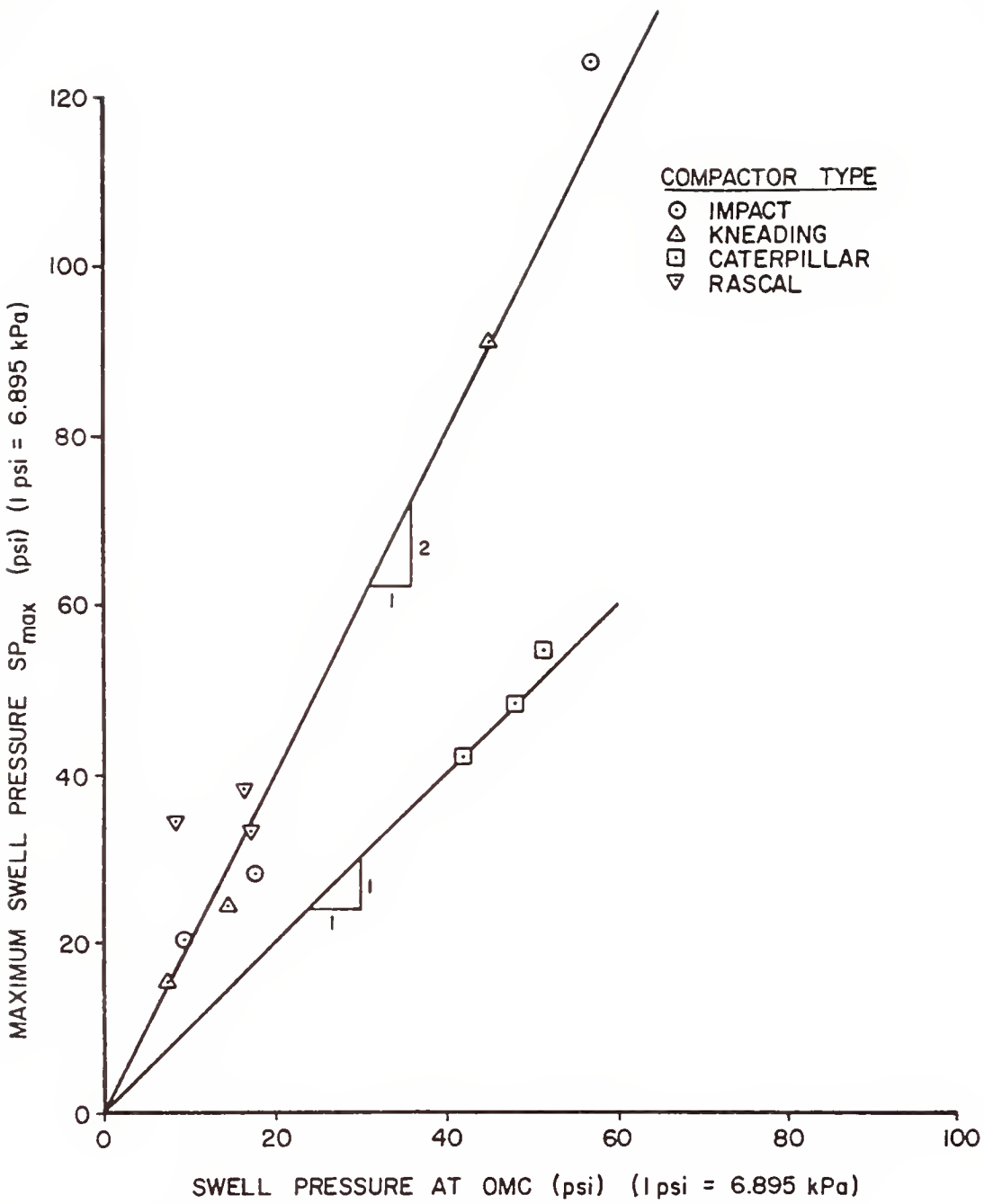

Figure 4.7 Maximum Swell Pressure Vs. Swell Pressure at OMC

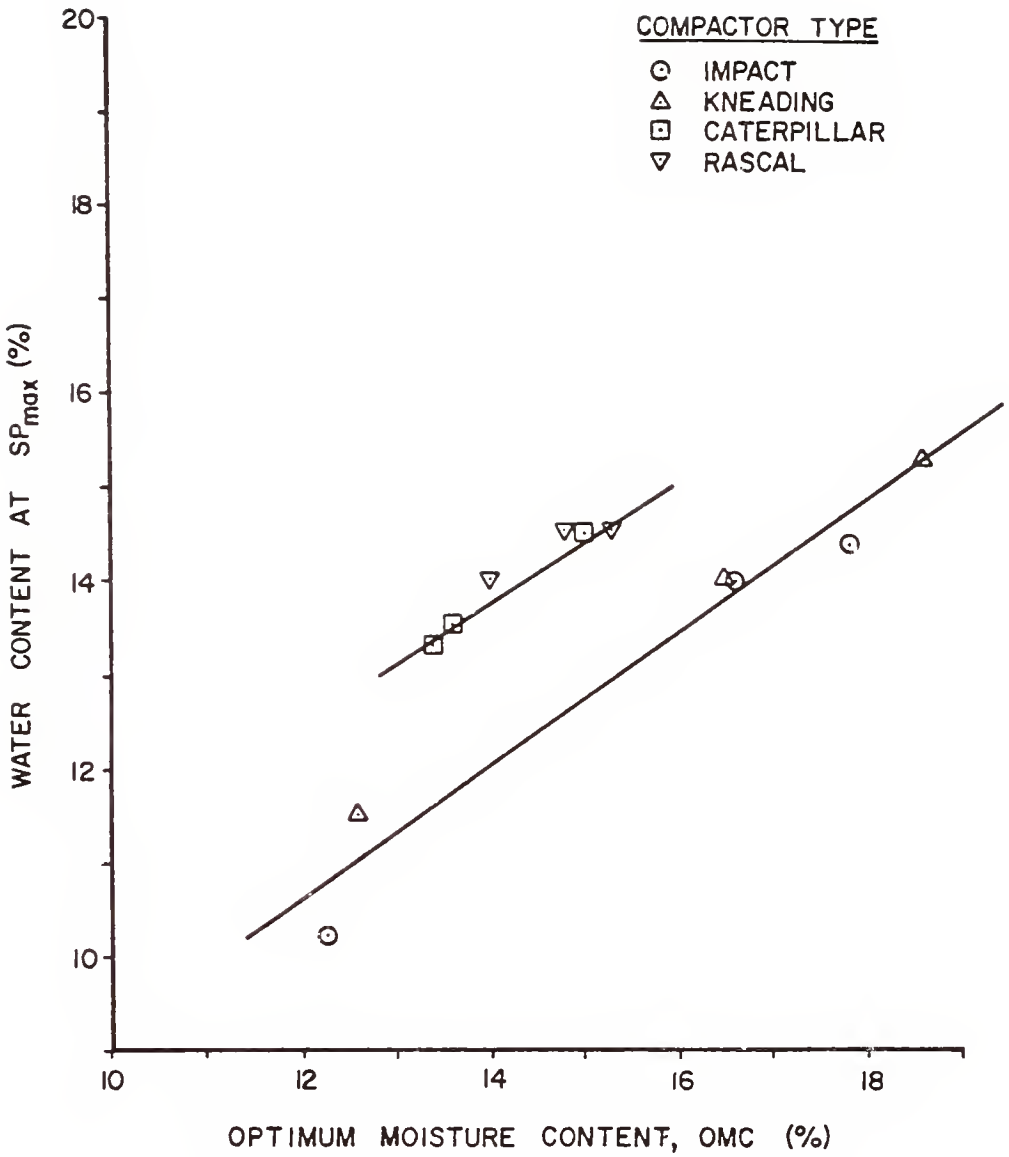

Figure 4.8 Water Content at SP_{max} Vs. Optimum Moisture Content

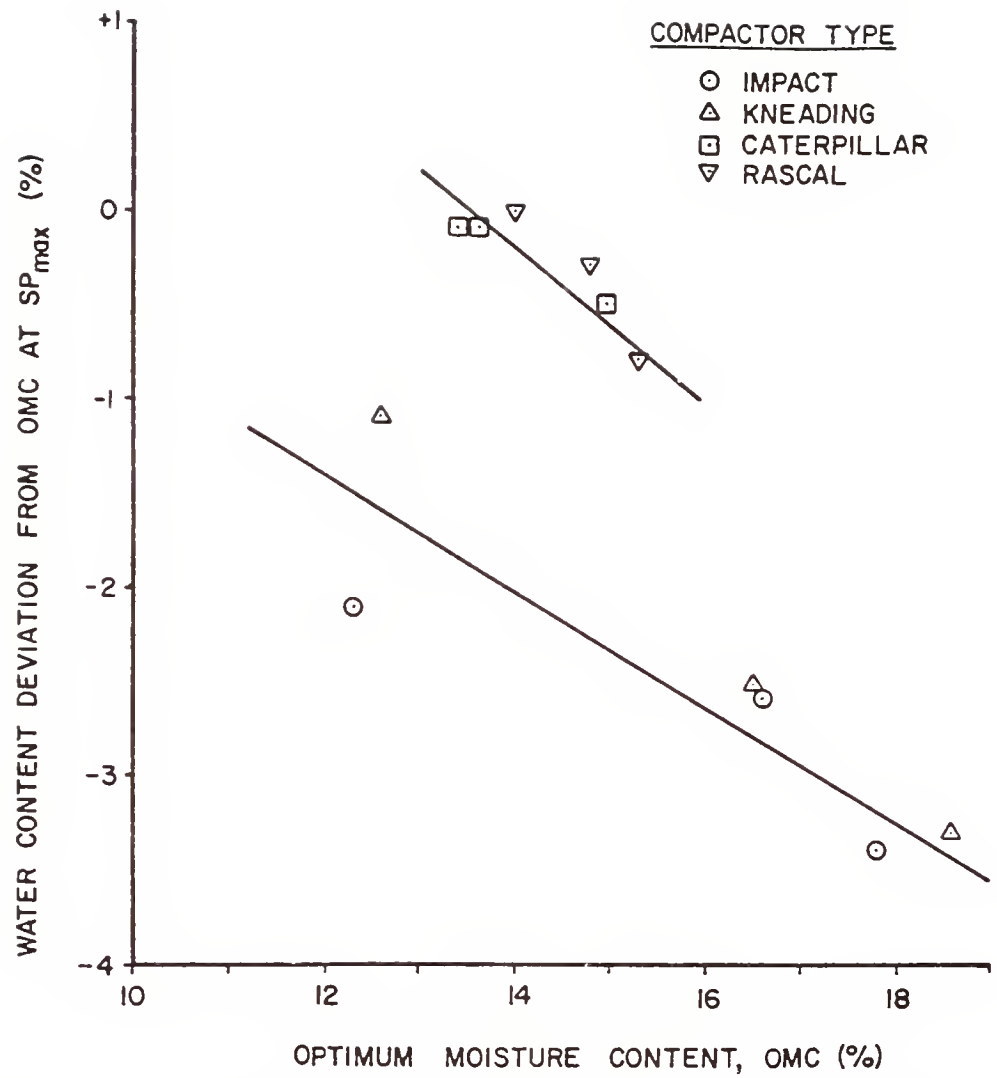

Figure 4.9 Water Content Deviation from OMC at SP_{max} Vs. Optimum Moisture Content

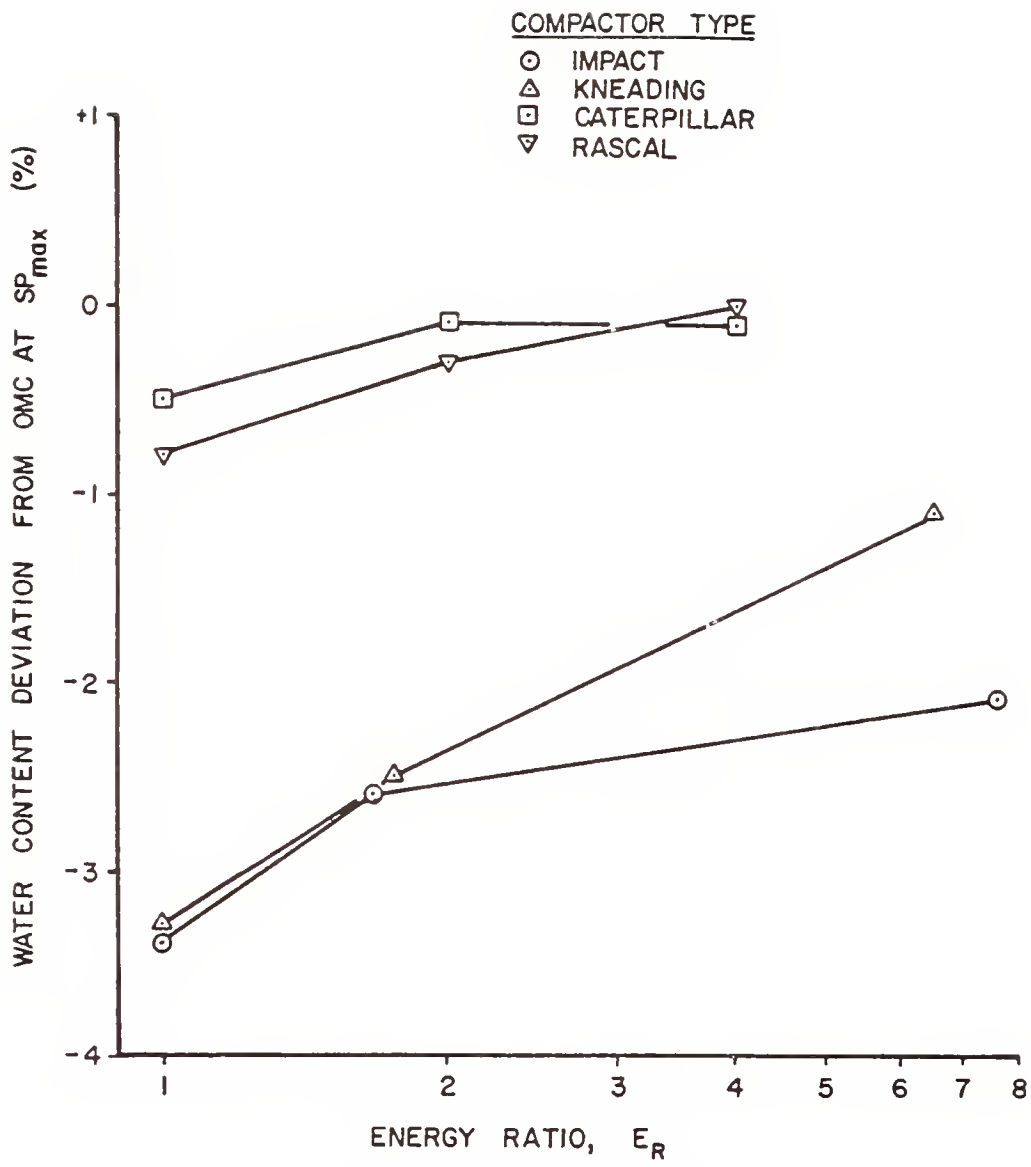

Figure 4.10 Water Content Deviation from OMC at SP_{max} Vs. Energy Ratio

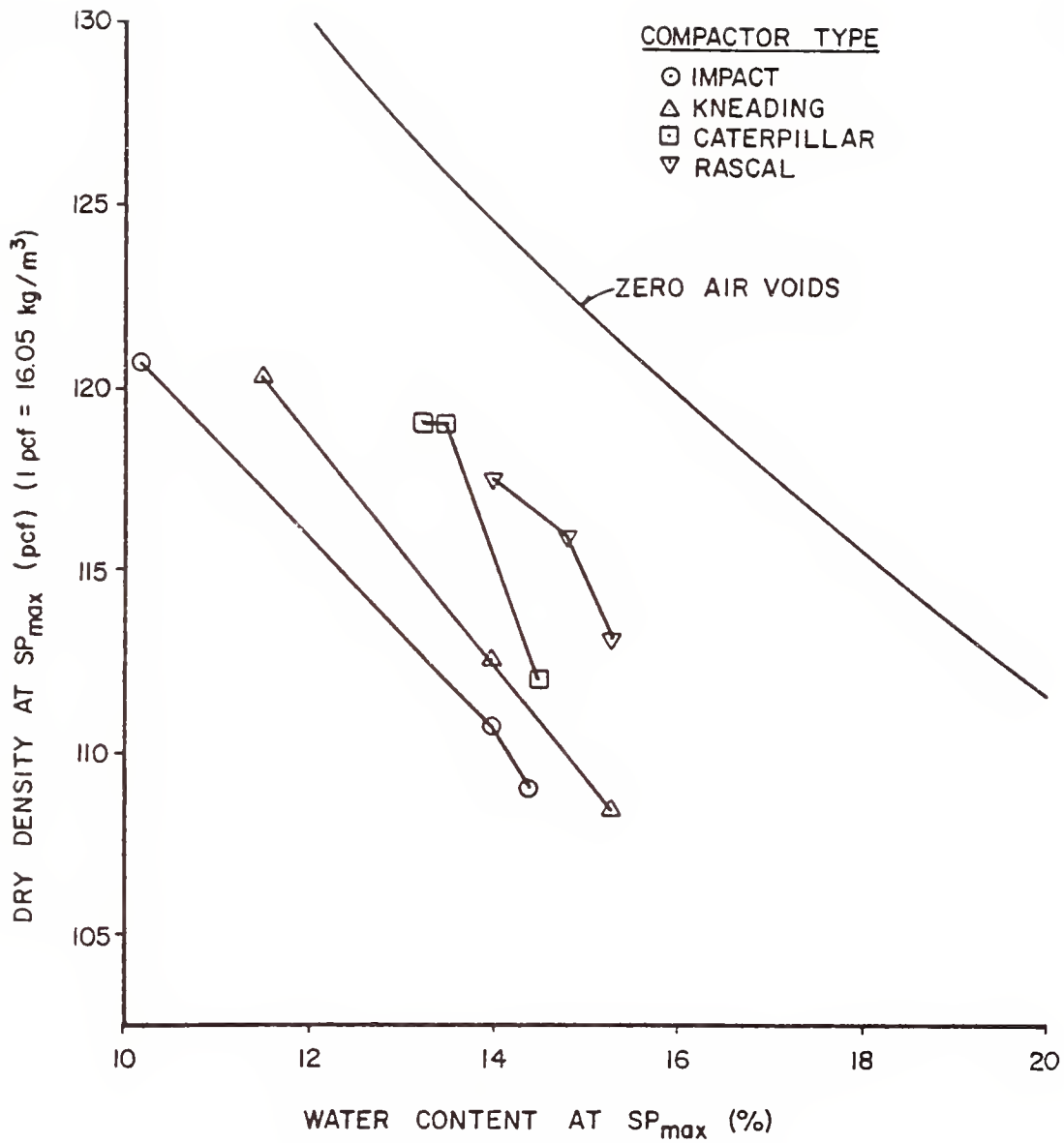

Figure 4.11 Dry Density at SP_{max} Vs. Water Content at SP_{max}

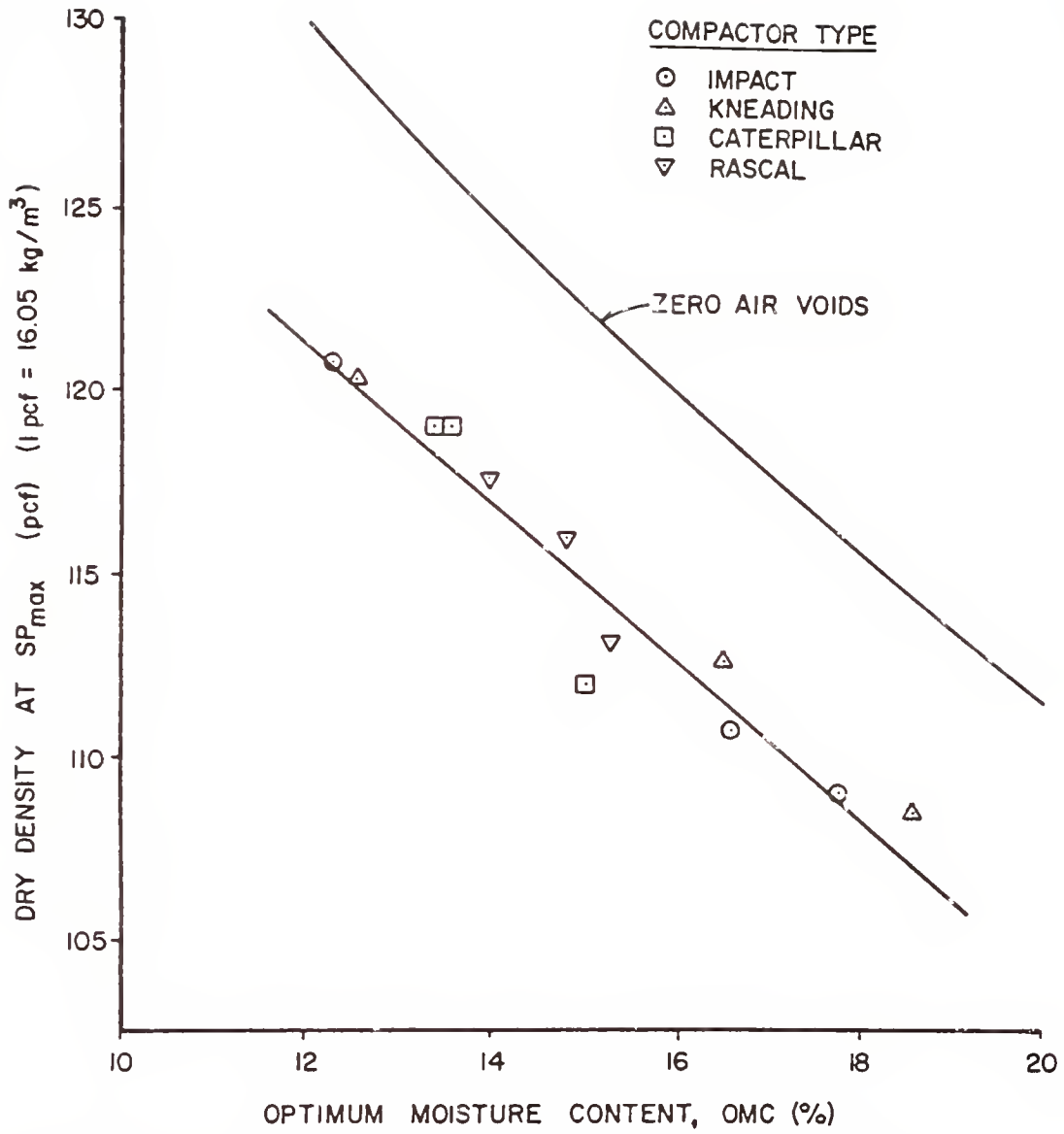

Figure 4.12 Dry Density at SP_{max} Vs. Optimum Moisture Content

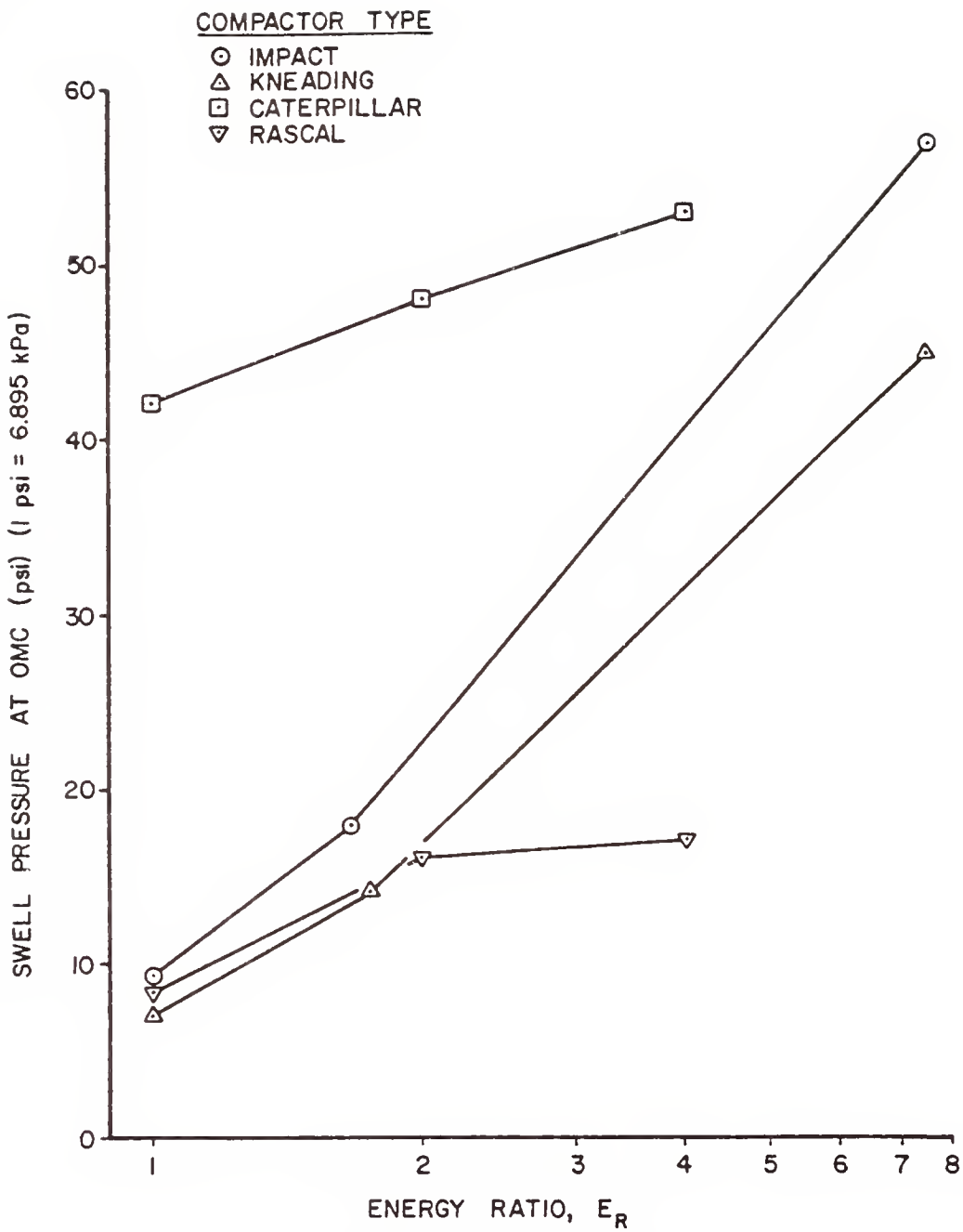

Figure 4.13 Swell Pressure at Optimum Moisture Content Vs. Energy Ratio

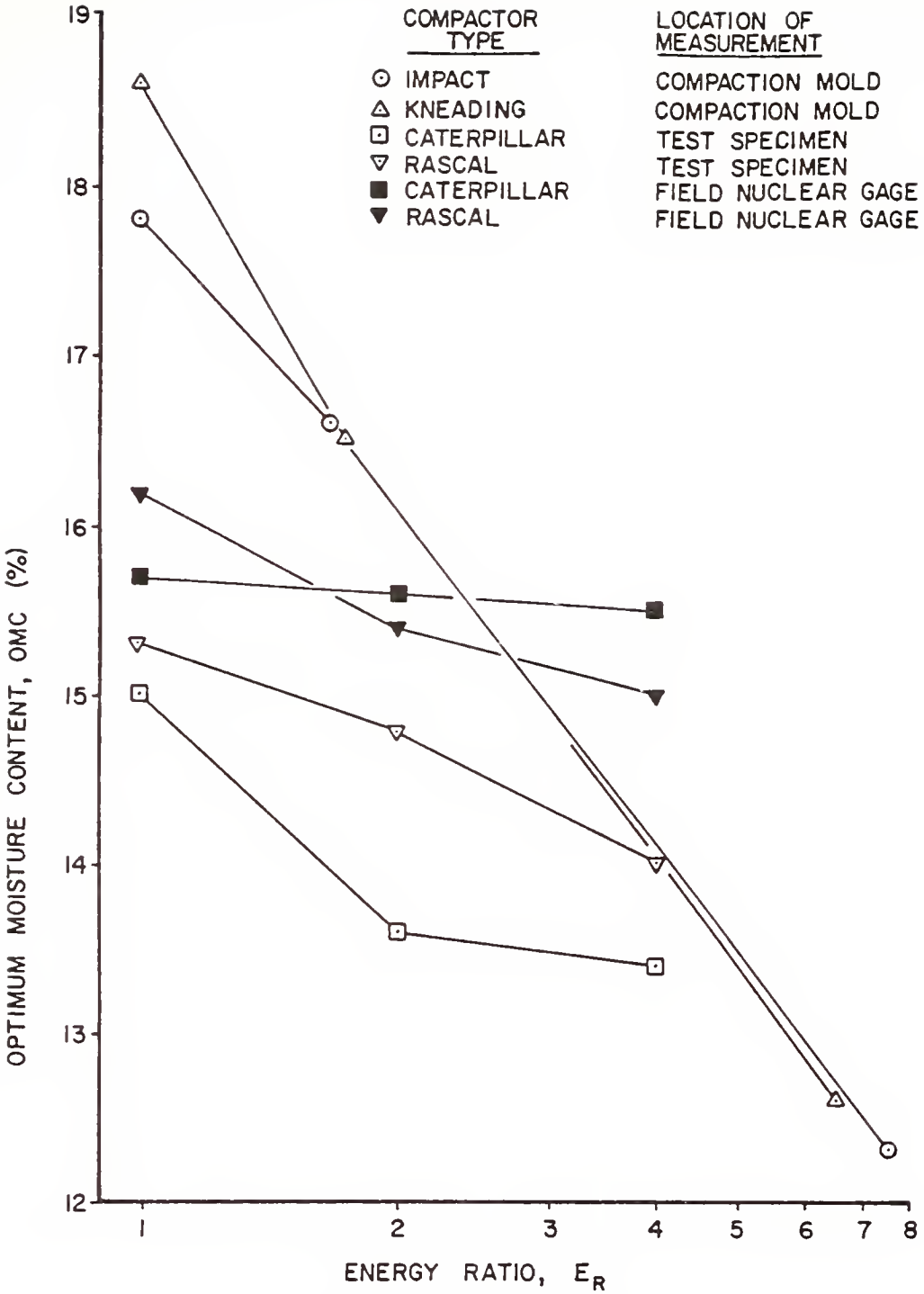

Figure 4.14 Optimum Moisture Content Vs. Energy Ratio

Prediction of Field Response from Laboratory Compacted Samples

One of the major goals of this study is the prediction of field swell pressure response from laboratory compacted samples. Several methods of prediction exist; however, not all appear to be applicable to this research. The following is a discussion of these methods and their potential for use in this work.

An ideal situation would occur if laboratory and field compacted samples produced identical response curves. This is not the case, as evidenced by Figures 4.15 and 4.16. These figures represent the laboratory impact response curves plotted with those for the Caterpillar and Rascal compactors, respectively. Similar results occur when the kneading curves are substituted for the impact curves. Price (1978) has also shown that lab and field responses are not identical.

Figures 4.15 and 4.16 also show that direct graphical comparisons cannot be done. Instead, one family of curves must be transformed graphically to simulate the other family of curves presented in the graph; direct comparisons can then be made. Another method of transformation requires a mathematical equation or set of equations that correlate the field results with laboratory responses. Such a transformation would be complicated and difficult to perform.

If laboratory and field compaction produced nearly identical sets of compaction curves, then the laboratory values could be directly substituted into the regression equations for field swell pressure. Since these sets of curves are dissimilar, the laboratory values would

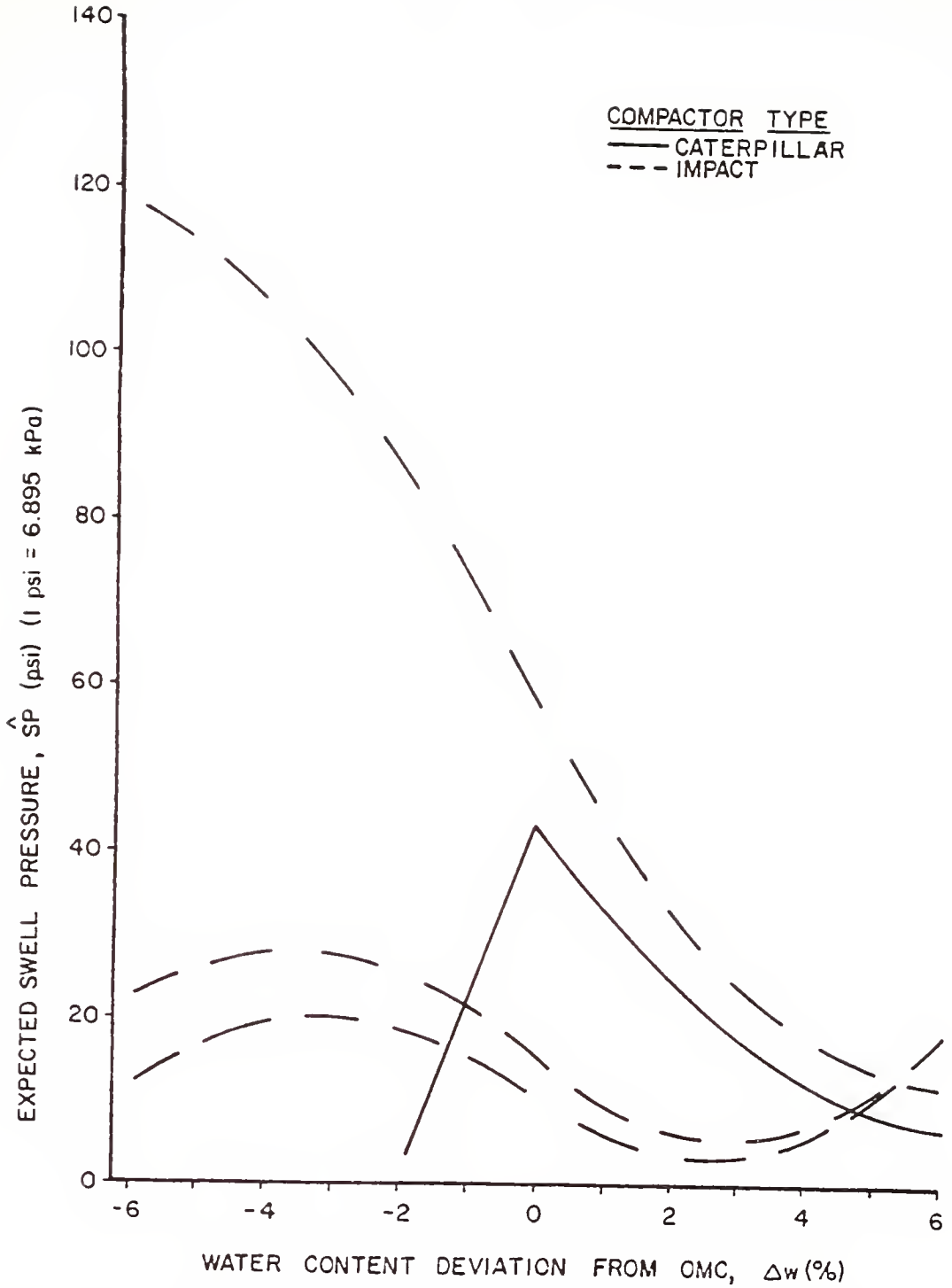

Figure 4.15 Comparison of Caterpillar and Impact Swell Pressure Relationships

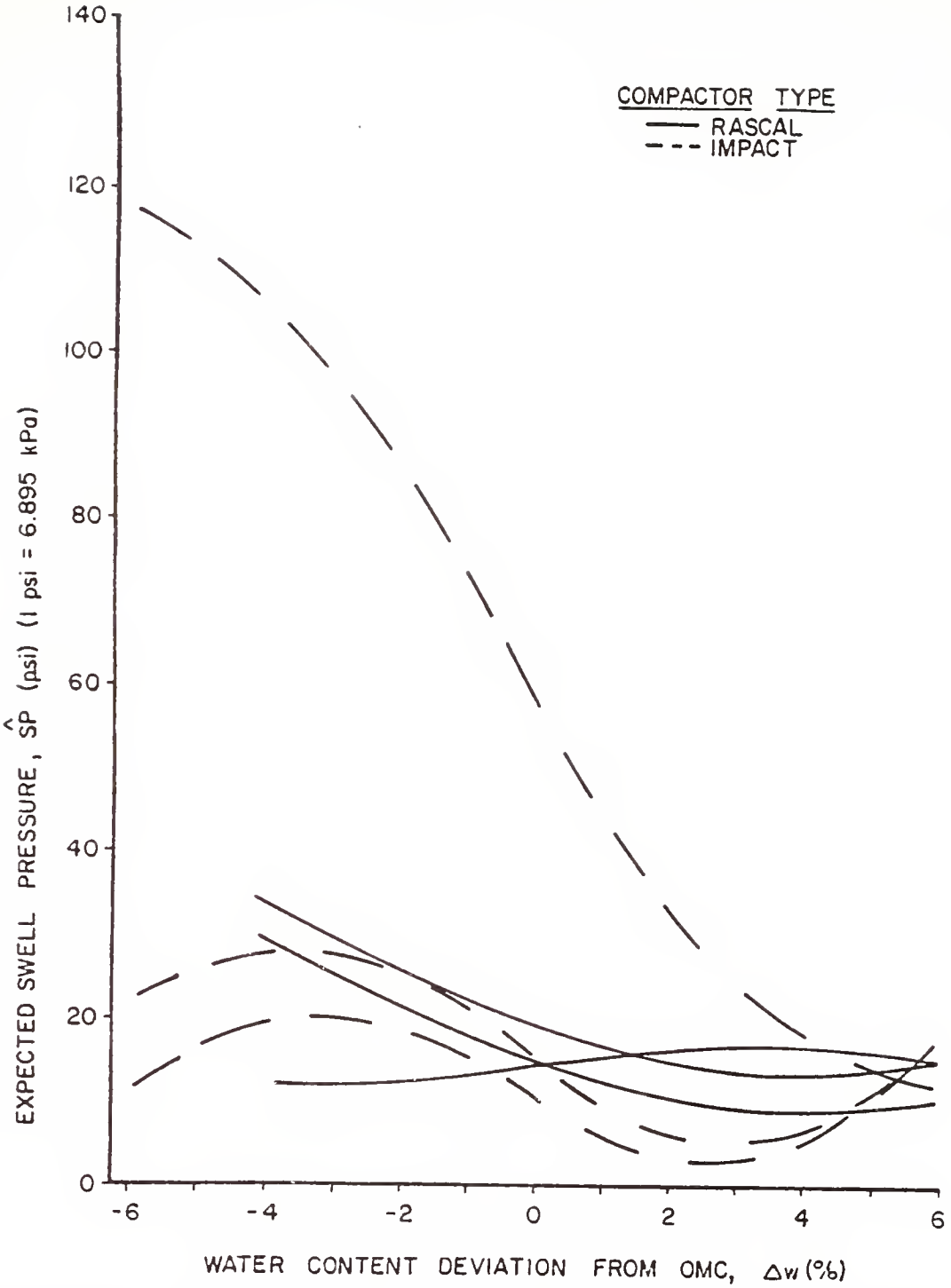

Figure 4.16 Comparison of Rascal and Impact Swell Pressure Relationships

require transformation before being used in the field response equations. This would also be a complicated mathematical process.

The approach used in this study is based upon relationships that were found between laboratory and field compaction results (viz. maximum dry densities and optimum moisture contents). These relationships have been obtained from the compaction curves shown in Figures 2.3, 2.4, 2.11, and 2.12 and are presented in the "Application of Results". They are used to predict the field maximum dry density and optimum moisture content from the results of Standard Proctor laboratory compaction performed upon the soil. It is assumed that these relationships are also valid for other soils in the A-6 classification.

The regression models for field dry density are used to predict the field compaction curves. In some cases, the models must be adjusted to correspond with the predicted maximum dry density. Because these adjustments are based upon relationships developed for the compaction curves (not for the regression models), discrepancies in γ_d might occur near OMC; judgment should be used in these cases.

The predicted values of γ_d and OMC can then be utilized to write a compaction specification which will predict and control the magnitude and variability of swell pressure that subsequently develop in the field. If the compaction specification has previously been written for a project, the predicted values of γ_d and OMC can be used for inspection testing and also to predict the swell pressure and its variability that will develop for the compaction procedure

specified. The complete prediction procedure is described in the following chapter.

5 - APPLICATION OF RESULTS

Design Engineering

This study presents evidence that large swell pressures can be induced by field compaction methods. These tendencies to swell can reduce the strength of the compacted soil, as well as cause damage to structures placed on or in the fill. To ensure proper performance of a compacted fill and the structures it supports, strength, compressibility, and swelling characteristics must be accounted for in the engineering design. If the borrow soil is located and identified well in advance of its placement, proper compaction specifications can be prepared to account for these three factors by use of such relations as are presented in this report.

This section is presented in order to illustrate how the relationships developed in this study can be used to create an appropriate specification to limit the swell pressures induced by compaction. These relationships can be utilized when an A-6 soil (i.e., one similar to the St. Croix clay of this study) is compacted in the field by one of the compactors used in this study. To begin the specification process, the engineer must decide what magnitude of maximum swell pressure can be tolerated in the design; this decision is a judgment based upon the requirements of the project under consideration.

The rest of the procedure is best presented in the form of the following example and commentary. Let us assume that a maximum swell pressure of 20 psi (138 kPa) can be tolerated in the design. As an upper permissible bound, this quantity is represented by the expected swell pressure (mean value) plus the expected variability in swell pressure that will occur with a particular set of compaction conditions (i.e., compactor type, E_R, Δw, and half-range variability of Δw). Figures 5.1 thru 5.4 can be used directly to obtain appropriate combinations of compaction conditions that, if used, will assure a maximum swell pressure of 20 psi (138 kPa).

A number of figures are presented herein to convey the various data developed in this study. Figure 5.1 is developed for the Caterpillar compactor over all energy levels and Figures 5.2 thru 5.4 represent the three energy levels for the Rascal roller. The expected maximum swell pressures, for different values of the half-range variability of Δw, are shown by the solid curves in the four figures; again, the expected maximum SP represents the sum of the expected mean SP and the expected variability of SP for the given conditions of compaction. The dashed curves indicate the expected mean swell pressure and are drawn within the limits of the gathered data. These limits should be observed when using all curves in these figures, as values outside these Δw bounds are an extrapolation of the data and are subject to error. Horizontal dashed lines appear in Figures 5.1 thru 5.3 wet of OMC. These are believed to be reasonable limiting values of expected swell pressures, rather than the large increases shown for the wet side. Reasons for indicating that these increases

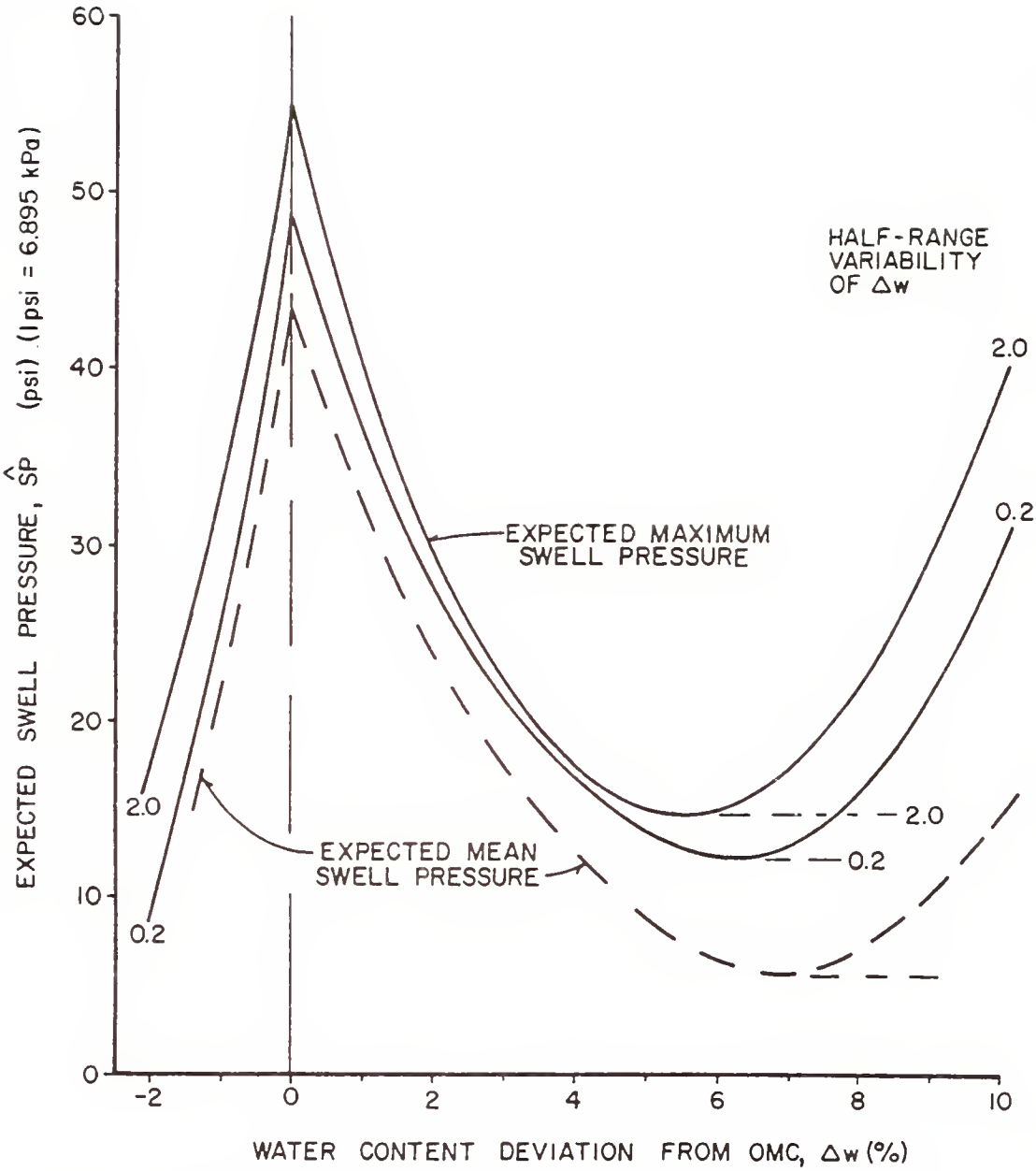

Figure 5.1 Caterpillar Swell Pressure Variability Relationships

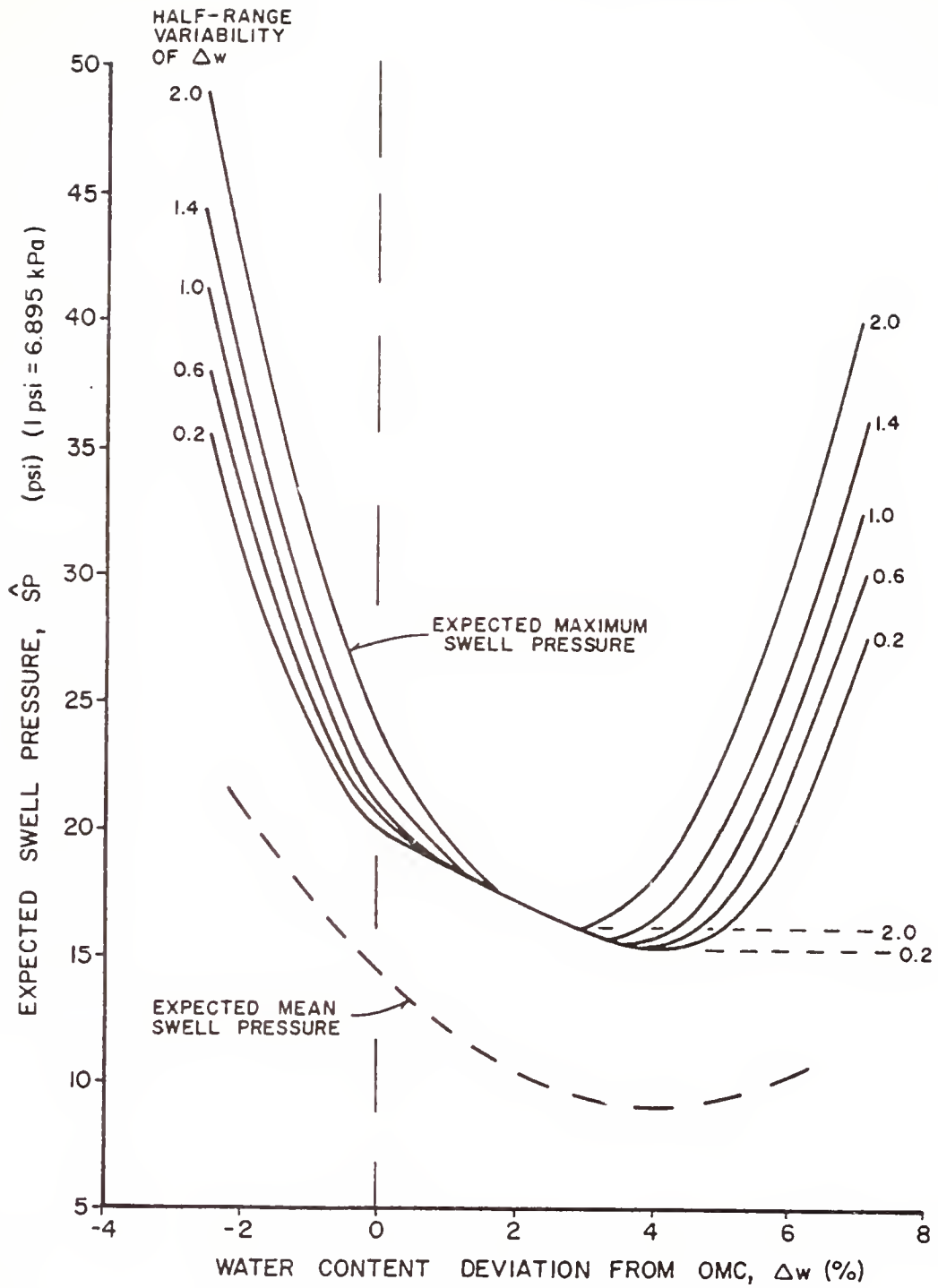

Figure 5.2 Rascal Swell Pressure Variability Relationships, A Energy Level

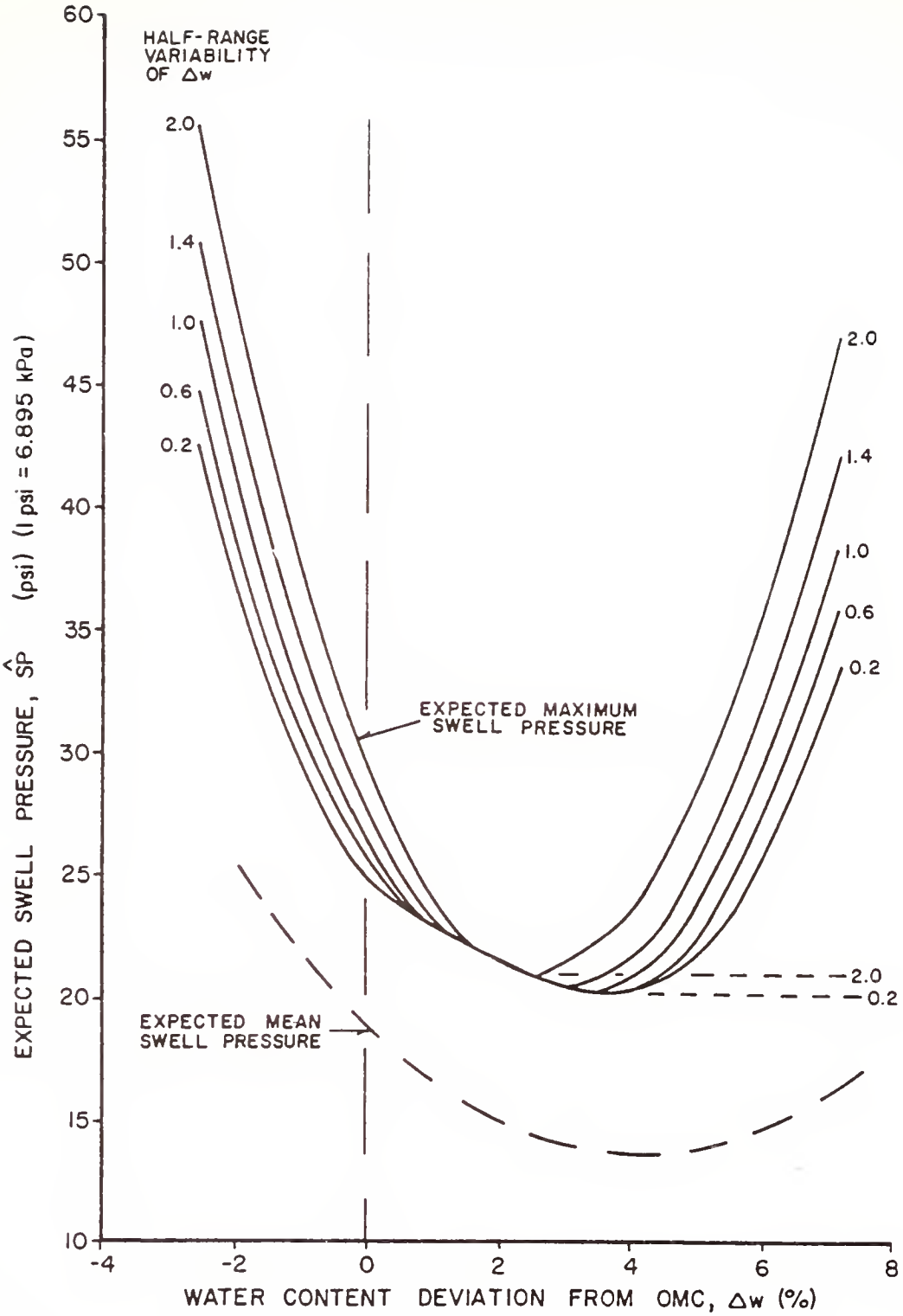

Figure 5.3 Rascal Swell Pressure Variability Relationships, B Energy Level

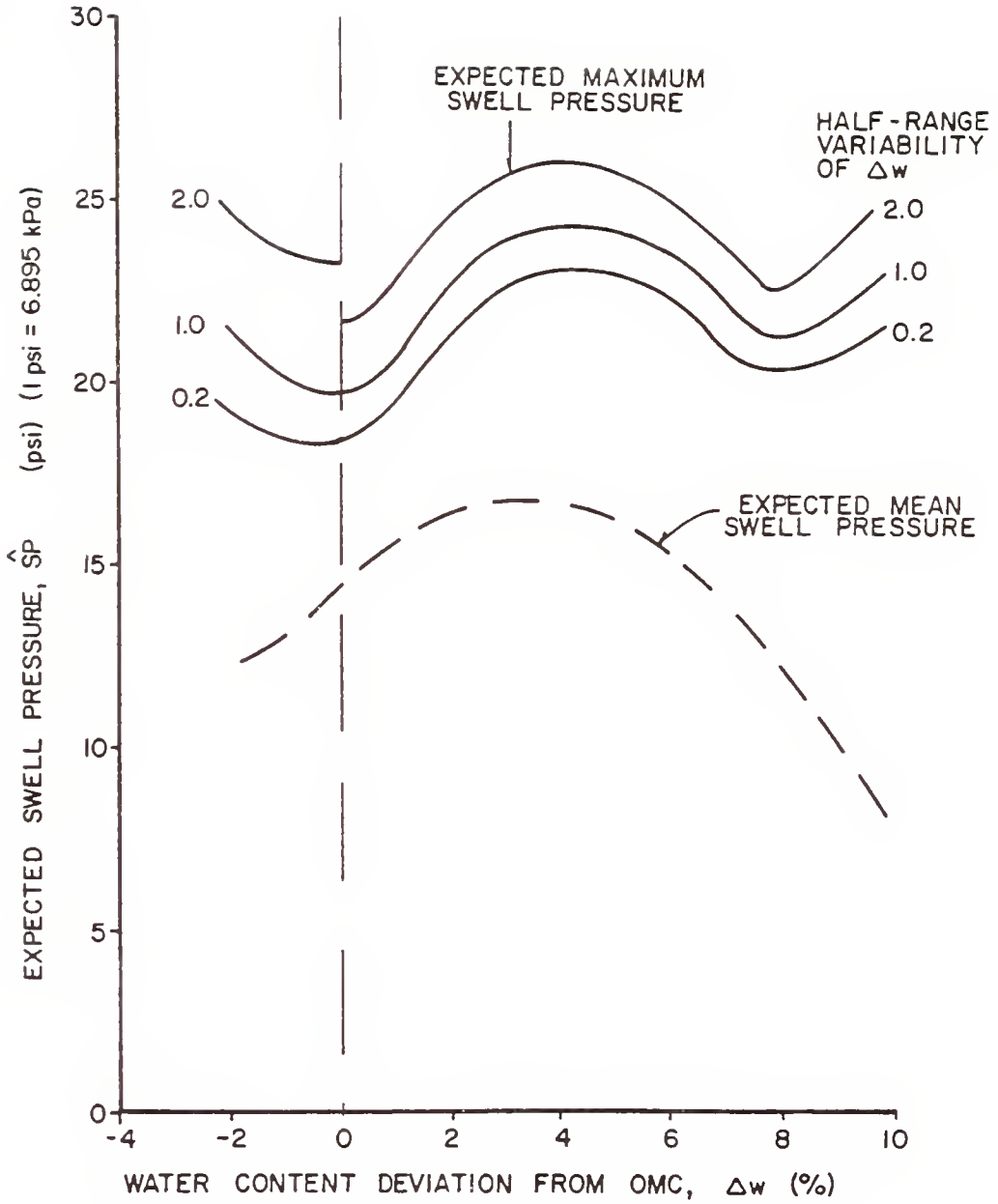

Figure 5.4 Rascal Swell Pressure Variability Relationships, C Energy Level

are not to be expected in the field are given in the "Discussion of Results" section.

Returning to the example, results obtained for the Caterpillar compactor (see Figure 5.1) indicate that this maximum swell pressure, 20 psi (138 kPa), will not be exceeded if the following conditions are met: (1) the number of passes ranges between four and sixteen (i.e., $1 \leq E_R \leq 4$); (2) the soil is compacted at least 3.3% wet of OMC with a half-range variability of Δw less than 0.2%; or (3) the soil is compacted at least 3.5% wet of OMC with a half-range variability of Δw less than 2.0%. Other possible combinations also exist for intermediate values of Δw variability which can be located by interpolation. Dry of OMC, maximum swell pressures less than 20 psi (138 kPa) can be achieved only outside the limits of the gathered data; therefore, no attempt is made here to denote these compaction conditions.

For the Rascal compactor, the maximum swell pressure will not be exceeded if four passes of the compactor are used between Δw of 0.0% to 8.0% with a half-range variability of Δw less than 0.2%. This may be expressed as (1, 0.0, 8.0, 0.2), i.e., (energy ratio = 1 = 4 passes; 0.0 = minimum value of Δw; 8.0 = maximum value of Δw; 0.2 = maximum half-range of variability of Δw). Using this manner of expression, and referring to Figure 5.2, the maximum swell pressure will not be exceeded with (1, 0.3, 8.0, 0.6), (1, 0.5, 8.0, 1.0), (1, 0.7, 8.0, 1.4), (1, 0.8, 8.0, 2.0). Figure 5.3 shows that the 20 psi (138 kPa) maximum swell pressure will always be exceeded if this soil is compacted at the B energy level (i.e., 8 passes).

From Figure 5.4 it can be seen that the maximum swell pressure will not be exceeded for the following combinations of variables (4, -2.0, 1.3, 0.2), (4, -0.7, 0.5, 1.0).

In the development of the project's specifications for compaction the above will control the swell pressure. However, strength, compressibility, and other requirements must also be considered as the engineer develops "trade-offs" for the in-service field behavior.

Since the results of this study are based on water content deviation from OMC, it is important to know where optimum moisture content and maximum dry density will occur in the field. If economies (of time and money) do not permit the construction of field test sections to determine OMC and γ_{dmax} directly, the following procedure can be used to predict these quantities. First, a laboratory compaction curve is generated for the soil with the Standard Proctor energy level; this can be done either by impact or kneading compaction. Compare these values of OMC and γ_{dmax} with those in Table 5.1. If the values are equal or nearly so, field values of OMC and γ_{dmax} can be taken directly from Table 5.1.

If the generated γ_{dmax} is different, then Figure 5.5 can be used to adjust the tabular value of maximum dry density to predict that which should be anticipated in the field. Figure 5.5 shows the ratios of maximum dry densities produced in this study (field nuclear gage to laboratory Standard Proctor values) versus field energy ratios. To use Figure 5.5 choose the curve which corresponds to the compactor types being used (e.g., impact and Rascal), determine the energy ratio at which the field compactor will be used (e.g., 4, which means 16

Table 5.1 Optimum Moisture Contents and Maximum Dry Densities Used for Predictions

Compactor Type	Location of Measurement	Energy Level	Energy Ratio*	OMC (%)	γ_{dmax} (pcf)
Impact	Compaction Mold	B (Standard Proctor)	1.67	16.6	113.8
Kneading	Compaction Mold	B (Standard Proctor)	1.75	16.5	114.9
Caterpillar	Field Nuclear Gage	A	1	15.7	105.5
		B	2	15.6	110.9
		C	4	15.5	111.5
Rascal	Field Nuclear Gage	A	1	16.2	103.7
		B	2	15.4	107.2
		C	4	15.0	110.6

*To obtain the number of passes for field compactors, multiply the energy ratio by 4.

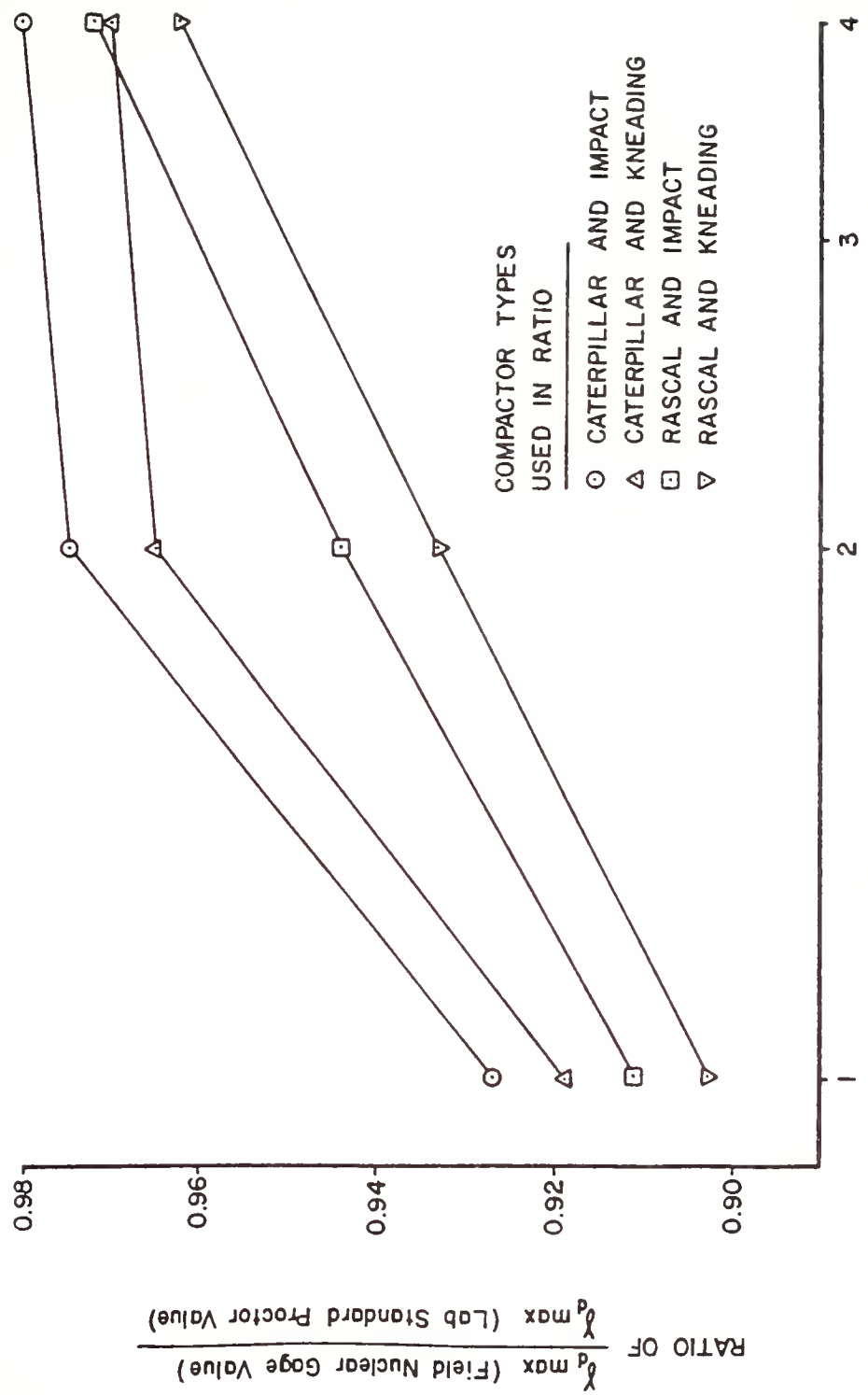

Figure 5.5 Ratio of Maximum Dry Densities Vs. Field Energy Ratio

passes), and locate their point of intersection. Obtain the ordinate of this point (ratio of γ_{dmax}; e.g., 0.972) and multiply the generated Standard Proctor maximum dry density by this value. This will yield the predicted value of maximum dry density in the field (γ_{pmax}).

To obtain the other values of dry density for the predicted field compaction curve the following procedure can be used. First, pick the appropriate field regression equation (see Table 3.3 or Figures 4.1 thru 4.4) and insert appropriate values of Δw for the E_R under consideration. Next, multiply each γ_d so obtained by the ratio:

$$\frac{\text{field } \gamma_{pmax} \text{ for the soil under consideration}}{\text{appropriate field } \gamma_{dmax} \text{ from Table 5.1}} .$$

Then, one more adjustment of this γ_d is necessary because the regression equations for field dry density were developed for test specimen values. This final adjustment is to multiply by 0.93 to yield the proper predicted field dry density (γ_p). The coefficient of 0.93 is the average ratio of:

$$\frac{\gamma_{dmax}(\text{field nuclear gage values})}{\gamma_{dmax}(\text{test specimen values})} .$$

The underlying assumption is that the field compaction curves are of the same general shape as the regression equation obtained for the test specimens.

If the generated Standard Proctor OMC is appreciably different from that shown in Table 5.1, the appropriate field OMC can be predicted in the following manner. First, calculate the ratio of the

generated Standard Proctor OMC to that obtained in this study. Then multiply the appropriate value of field OMC (given in Table 5.1) by this quantity to obtain the magnitude of the predicted field optimum moisture content (OMC_p).

As a continuation of the previous example, let us assume that Standard Proctor impact compaction on the soil under consideration produced a maximum dry density of 116 pcf and OMC of 15.0%. The engineer has accepted the Rascal compactor at an $E_R = 1.0$ (4 passes) and $\Delta w = +2.0\%$ (see Figure 5.2) to produce the allowable maximum swell pressure; the half-range variability of Δw will be controlled at 1.4%.

Using Figure 5.5, the appropriate ratio of

$$\frac{\gamma_{dmax} \text{ (field nuclear gage value)}}{\gamma_{dmax} \text{ (laboratory Standard Proctor value)}} \text{ is } 0.911.$$

Thus, the predicted field maximum dry density is:

$$\gamma_{pmax} = 116 \text{ pcf} \times 0.911 = 105.7 \text{ pcf}.$$

To predict the expected field dry density, insert the appropriate Δw and E_R into the proper regression equation (see Table 3.3, line 6):

$$\hat{\gamma}_d = -1.378 \times 2.0 + 1.044 \times 1.0 + 112.0 = 110.3 \text{ pcf}.$$

This value could also have been obtained from Figure 4.2. Next, multiply this quantity by the appropriate ratio of

$$\frac{\text{predicted field } \gamma_{dmax} \text{ (i.e., } \gamma_{pmax})}{\text{appropriate field } \gamma_{dmax} \text{ from Table 5.1}}$$

(which is $\frac{105.7 \text{ pcf}}{103.7 \text{ pcf}}$ here) and by 0.93:

$$\gamma_p = 110.3 \text{ pcf} \times \frac{105.7 \text{ pcf}}{103.7 \text{ pcf}} \times 0.93 = 104.5 \text{ pcf}.$$

To predict the field OMC, multiply the appropriate field OMC in Table 5.1 (16.2%) by the ratio

$$\frac{\text{generated Standard Proctor OMC}}{\text{Standard Proctor OMC from Table 5.1}} \quad (\text{i.e., } \frac{15.0\%}{16.6\%}).$$

Thus, the predicted field OMC is:

$$OMC_p = \frac{15.0\%}{16.6\%} \times 16.2\% = 14.6\%.$$

For the soil under consideration, the predicted values of field OMC_p, γ_{pmax}, and γ_p at $\Delta w = 2.0\%$ are 14.6%, 105.7 pcf, and 104.5 pcf, respectively.

Application of the results obtained in this study is dependent upon the OMC and γ_{dmax} which will be achieved in the field. Predicting the field OMC by methods described above allows the engineer to write a proper compaction specification; i.e., once the allowable average or maximum swell pressure and field OMC are determined, Figrues 5.1 thru 5.4 can be used to specify the allowable absolute values of field moisture content.

Quality Control

There are cases where the borrow soil to be used for compaction is not located and identified well in advance of construction. For these cases, the compaction specification may not contain the necessary provisions that will control the induced swell pressures to a tolerable level. However, it is still desirable to be able to predict

the maximum swell pressures for the resulting product. This section outlines a method for predicting swell pressures from inspection test results of compaction projects in progress.

Figures 5.1 thru 5.4 could be adapted for use by the quality control engineer, but they do not provide all of the necessary information. Computer printouts generated by the programs in Appendix B would be better suited for this purpose. Table 5.2 is a sample of the output produced by the Caterpillar program; it can be used for quality assurance testing and for prediction of the expected swell pressure magnitude and variability.

Before this table can be used, the field optimum moisture content and maximum dry density must be determined. If this cannot be established from the on-going field operation, these values can be predicted by methods described in the "Design Engineering" section; i.e., a laboratory Standard Proctor compaction test is performed, and γ_{pmax} and OMC_p are generated using the proper charts.

Next, obtain the number of passes of the compaction equipment and the fill water content and dry density for the lift being examined. A minimum of five to seven samples for w and γ_d must be taken to accommodate the approach used in this study. The average water content and dry density are then calculated for the group of samples. Also calculate the expected variabilities in the water content and dry density; these variabilities are equal to the half-range variation for each parameter, as calculated from the group of samples. Then Δw is calculated as the difference between the average water content and field OMC previously determined.

Table 5.2 Sample of Computer Output from Caterpillar Swell Pressure Variability Program

V(Δw) (%)	Δw (%)	No. of Passes	E_R	$\hat{\gamma}_d$ (pcf)	Field γ_p (pcr)	$V(\hat{\gamma}_d)$ (pcf)	$\hat{SP}$ (psi)	$V(\hat{SP})$ (psi)	$\hat{SP}_{max}$ (psi)
1.4	-2.0	4.0	1.0	106.6	99.1	13.3	.7	13.3	13.9
1.4	-1.5	4.0	1.0	109.5	101.8	11.1	11.5	11.1	22.6
1.4	-1.0	4.0	1.0	112.4	104.6	8.9	22.4	8.9	31.3
1.4	- .5	4.0	1.0	115.4	107.3	6.7	33.3	6.7	39.9
1.4	0	4.0	1.0	118.3	110.0	8.7	44.1	8.7	52.8
1.4	0	4.0	1.0	115.3	107.2	1.3	43.1	9.4	52.4
1.4	.5	4.0	1.0	114.5	106.5	1.2	37.8	7.6	45.5
1.4	1.0	4.0	1.0	113.7	105.7	1.1	33.0	6.1	39.1
1.4	1.5	4.0	1.0	112.9	105.0	1.0	28.6	4.8	33.4
1.4	2.0	4.0	1.0	112.1	104.2	1.0	24.5	4.0	28.6
1.4	2.5	4.0	1.0	111.3	103.5	1.0	20.9	4.3	25.2
1.4	3.0	4.0	1.0	110.5	102.7	1.1	17.7	4.6	22.2
1.4	3.5	4.0	1.0	109.7	102.0	1.2	14.8	4.8	19.6
1.4	4.0	4.0	1.0	108.9	101.2	1.3	12.4	5.0	17.4
1.4	4.5	4.0	1.0	108.1	100.5	1.4	10.4	5.3	15.7
1.4	5.0	4.0	1.0	107.3	99.8	1.5	8.7	5.8	14.5
1.4	5.5	4.0	1.0	106.5	99.0	1.6	7.5	6.3	13.8
1.4	6.0	4.0	1.0	105.7	98.3	1.7	6.7	7.1	13.8

With the above data, proceed into the appropriate section of the table using the measured half-range of the water content, $V(\Delta w)$, as the variability measurement. This value appears in the left-hand column (1) of the table; Table 5.2 is based upon the average water content variability found for the St. Croix test pad test specimens (1.4%). Next, locate the proper value of Δw in column two, and the appropriate number of passes in the third column from the left; energy ratio (E_R) is presented in column four.

On the appropriate line for the combination of these compaction variables, column five contains the expected dry density ($\hat{\gamma}_d$ in pcf) for test specimens. Contents of column five are used in the variability analyses and are consistently higher than values measured in the field by nuclear devices. The predicted field dry density (γ_p in pcf) is given in column six and should be used for comparisons with inspection test results. If the appropriate γ_{dmax} in Table 5.1 (lab or field, depending on how it is determined for the borrow material) is different from that achieved for the borrow soil, the values in column six should be adjusted by methods given in the "Design Engineering" section to provide a more reliable basis for comparisons with inspection tests results. Column seven shows the expected dry density variability ($V(\hat{\gamma}_d)$ in pcf); this is appropriate for use with both measures of dry density presented in the table.

The expected swell pressure ($\hat{SP}$ in psi) appears in the eighth column, and its expected variability ($V(\hat{SP})$ in psi) is given in column nine. The last column in the table presents the expected maximum swell pressure ($\hat{SP}_{max}$ in psi), which is the sum of the entries in columns

eight and nine. The values in these last three columns should be compared with the wet side limiting values (horizontal dashed lines) presented in Figures 5.1 thru 5.4. The limiting values should be used, in their applicable ranges of Δw, to predict the field swell pressures.

Of particular interest are columns six, seven, eight, and ten. Columns six and seven can be used as a check for the compaction process, i.e., as a check against gross errors being made in establishing the compaction variables. If large discrepancies exist, the predictions will be questionable. Columns eight and ten represent the best estimate of the swell pressure and its variability for the compacted soil. If the measured dry density variability is greater than the value shown in column seven, the values in columns nine and ten may be in slight error. Again, swell pressure variability is relatively insensitive to small changes in dry density or its associated variability.

The tabular form of the regression results provides the quality control engineer with a convenient means of evaluating field inspection tests, predicting subsequent swell behavior, and determining when corrective action is required in the field. It can also be used to assess the application of these results to other projects and soil types.

The computer programs in Appendix B generate tables for a wide variety of compaction conditions, of which Table 5.2 is a small sample. These programs can easily be modified to assess conditions not presented herein. However, the results should be used only within the limits of the data (compactor type, Δw, E_R) gathered in this study.

6 - CONCLUSIONS

For the residual medium plastic St. Croix clay and methods of compaction used in this study, the following conclusions can be drawn:

1. Soil compacted by the Caterpillar compactor exhibits the following relationships:

   a. The magnitude of dry density is governed by the water content deviation from OMC (Δw) for conditions dry of OMC. Wet of OMC, both Δw and energy ratio (E_R) contribute toward the resulting magnitude.

   b. Swell pressure magnitude is defined by Δw dry of OMC, while both Δw and Δw^2 are important wet of OMC.

2. For soil compacted by the Rascal compactor, the following relationships exist:

   a. Dry density magnitude is most influenced by Δw and E_R both wet and dry of OMC.

   b. Swell pressure magnitude is divided into two subsets; the A and B energy levels form one subset and the C level comprises the other. For the former subset, Δw^2, E_R, and the interaction term $\Delta w \gamma_d$ produce the best relationships, even though Δw^2 and E_R are not statistically significant. No significant relation exists for the C energy level, but Δw and $\Delta w \gamma_d$ generate reasonable magnitudes.

3. For soil compacted by the laboratory impact and kneading methods used in this study, the following relationships are obtained:

   a. The two compactor types produce similar compaction curves, with Δw and E_R being the most important descriptors of dry density magnitude both wet and dry of OMC.

   b. The variables contributing most to the resultant swell pressure magnitude are Δw, E_R, and $\Delta w \gamma_d$. Swell pressure response curves are also similar for the two compactor types, with impact samples generating slightly larger swell pressures.

4. The following relationships occur for the variability of dry density and swell pressure for field compacted samples:

   a. The magnitude of SP variability is large and is generally higher for the Rascal compactor.

   b. The magnitudes of the γ_d and SP variabilities of both compactors are reduced if the water content variability is reduced.

   c. Due to the inherent variability of a compacted soil mass, the average of a number of samples (a minimum of 5 to 7) must be used to compute the measured values of field water content and dry density.

5. Field test specimens exhibit higher and less variable values of dry density than those measured in the field by nuclear devices. This is probably caused by the occurrence of drying during storage as well as differences in the location and volume of the material within the measurement, rather than by trimming and testing procedures.

6. A method has been devised that is believed to reasonably predict the field optimum moisture content, dry density, and swell pressure response from laboratory compaction data.

7 - RECOMMENDATIONS FOR FUTURE STUDIES

1. Verify the field dry density prediction relations presented in this study. This should be done for St. Croix clay as well as other A-6 soils at future compaction project sites.

2. Verify the field swell pressure prediction relations presented herein for this and other A-6 soils. Predictions could be made for future embankments or those now in-service; field samples could be obtained and tested to verify the relations. This could also include the development of methods for measuring the in situ field swell pressure.

3. Develop prediction relations for field dry density, swell pressure, and other mechanical properties for different compactors and soil types.

4. Develop better methods to measure and control the sources of variability in field compaction processes. Application of these results is necessary to improve the overall uniformity of a compacted soil mass.

5. Determine if the associated relationships presented in this study are valid for other soils and compactor types.

6. Develop and standardize swell pressure tests that will produce the specific information desired for a particular project. These include:

a. For CVS tests, develop a rigid testing appratus that will ensure constant volume and provide a simpler testing procedure than that required for a consolidometer.

b. Perform swell tests in a triaxial cell and determine the loss in shear strength due to swelling tendencies. This apparatus can also be used to measure three-dimensional (or lateral) swell pressures and volume changes.

c. Using a consolidometer, apply various surcharge loads on the soil samples before inundation. This may better simulate field loading conditions and allow the appropriate amount of volume change to occur, and can be used to relate volume change to the reduction in swell pressure as compared to the CVS condition.

7. Determine the effects of drying on susequent swell behavior, and compare with results from samples that remain at their as-compacted water content.

8. Determine if there is a relationship between the as-compacted pore size distribution and the swell pressure that develops. Also compare pore size data taken from samples before and after swelling has occurred.

BIBLIOGRAPHY

BIBLIOGRAPHY

Ahmed, S., Lovell, C. W., and Diamond, S. (1974), "Pore Sizes and Strength of Compacted Clay," Journal of the Geotechnical Engineering Division, ASCE, Vol. 100, GT4, April, pp. 407-425.

Aitchison, G. D. and Richards, B. G. (1969), "The Fundamental Mechanisms Involved in Heave and Soil Moisture Movement and the Engineering Properties of Soils which are Important in Such Movement," Proceeedings of the Second International Research and Engineering Conference on Expansive Clay Soils, College Station, Texas, pp. 66-84.

Barber, E. S. (1956), Discussion of "Engineering Properties of Expansive Clays," Transaction, ASCE, Vol. 121, pp. 669-673.

Barden, L. and Sides, G. R. (1969), "The Influence of Structure on the Collapse of Compacted Clay," Proceedings of the Second International Research and Engineering Conference on Expansive Clay Soils, College Station, Texas, pp. 317-326.

Barden, L., Madedor, A. O. and Sides, G. R. (1969), "Volume Change Characteristics of Unsaturated Clay," Journal of the Soil Mechanics and Foundations Division, ASCE, Vol. 95,No. SM1, January, pp. 33-51.

Barden, L. and Sides, G. R. (1970), "Engineering Behavior and Structure of Compacted Clay," Journal of the Soil Mechanics and Foundations Division, ASCE, Vol. 96, No. SM4, July, pp. 1171-1200.

Bhasin, R. N. (1975), "Pore Size Distribution of Compacted Soils After Critical Region Drying," Ph.D. Thesis, Purdue University, West Lafayette, Indiana, May, 222 pp.

Bolt, G. H. (1956), "Physico-Chemical Analysis of the Compressibility of Pure Clays," Geotechnique, Vol. 6, No. 2, June, pp. 86-93.

Brackley, I. J. A. (1975a), "Swell Under Load," Proceedings of the Sixth Regional Conference for Africa on Soil Mechanics and Foundation Engineering, Durban, South Africa, pp. 65-70.

Brackley, I. J. A. (1975b), "A Model of Unsaturated Clay Structure and Its Application to Swell Behavior," Proceedings of the Sixth Regional Conference for Africa on Soil Mechanics and Foundation Engineering, Durban, South Africa, pp. 71-79.

Dawson, R. F. (1956), Discussion of "Engineering Properties of Expansive Clays," Transactions, ASCE, Vol. 121, pp. 664-666.

Diamond, S. (1970), "Pore Size Distribution in Clays," Clays and Clay Minerals, Vol. 18, pp. 7-23.

_____. (1971), "Macrostructure and Pore Structure of Impact Compacted Clays," Clays and Clay Minerals, Vol. 19, pp. 239-249.

DiBernardo, A. (1979), "The Effect of Laboratory Compaction on the Compressibility of a Compacted Highly Plastic Clay," MSCE Thesis, Purdue University, West Lafayette, Indiana, February, 187 pp.

Escario, V. (1969), "A New Method for In Situ Measurement of Pore Water Tension," Proceedings of the Second International Research and Engineering Conference on Expansive Clay Soils, College Station, Texas, pp. 194-206.

Essigman, M. F., Jr. (1976), "An Examination of the Variability Resulting from Soil Compaction," MSCE Thesis, Purdue University, West Lafayette, Indiana, August, 108 pp.

Fredlund, D. G. (1969), "Consolidometer Test Procedural Factors Affecting Swell Properties," Proceedings of the Second International Research and Engineering Conference on Expansive Clay Soils, College Station, Texas, pp. 435-456.

Garcia-Bengochea, I. (1978), "The Relation Between Permeability and Pore Size Distribution of Compacted Clayey Silts," MSCE Thesis, Purdue University, West Lafayette, Indiana, 179 pp.

Gau, F. L. and Olson, R. E. (1971), "Uniformity of Specimens of a Compacted Clay," Journal of Materials, JMLSA, Vol. 6, No. 4, December, pp. 874-888.

Gaudette, N. G., Jr. (1960), "Application of Kneading Compactor and Hveem Stabilometer to Bituminous Concrete Design in Indiana," MSCE Thesis, Purdue University, West Lafayette, Indiana, December, 238 pp.

Gromko, G. J. (1969), "Planned Field Testing of Expansive Clay Soil," Proceedings of the Second International Research and Engineering Conference on Expansive Clay Soils, College Station, Texas, pp. 235-249.

Gromko, G. J. (1974), "Review of Expansive Soils," Journal of the Geotechnical Engineering Division, ASCE, Vol. 100, No. GT6, June, pp. 667-687.

Hodek, R. J. (1972), "Mechanism for the Compaction and Response of Kaolinite," Ph.D. Thesis, Purdue University, West Lafayette, Indiana, December, 269 pp.

Holtz, W. G. and Gibbs, H. J. (1956), "Engineering Properties of Expansive Clays," Transactions, ASCE, Vol. 121, pp. 641-677.

Johnson, J. M. (1979), "The Effect of Laboratory Compaction on the Shear Behavior of a Highly Plastic Clay after Saturation and Consolidation," MSCE Thesis,Purdue University, West Lafayette, Indiana, July, 269 pp.

Johnson, L. D. (1977), "Evaluation of Laboratory Suction Tests for Prediction of Heave in Foundation Soils," Technical Report S-77-7, U.S. Army Engineer WES, Vicksburg, Miss., August, 92 pp.

Kassiff, G. and Baker, R. (1971), "Aging Effects on Swell Potential of Compacted Clay," Journal of the Soil Mechanics and Foundation Division, ASCE, Vol. 97, No. SM3, March, pp. 529-540.

Katti, R. K., Kulkarni, U. V., Bhangale, E. S. and Divashikar, D. G. (1979), "Shear Strength Development in Expansive Black Cotton Soil Media With and Without a Cohesive Non-Swelling Soil Surcharge, Application to Stability of Canals in Cuts and Embankments," Final Report, Indian Institute of Technology, Bombay, 329 pp.

Komornik, A. and David, D. (1969), "Prediction of Swelling Pressure of Clays," Journal of the Soil Mechanics and Foundations Division, ASCE, Vol. 95, No. SM1, January, pp. 209-225.

Ladd, C. C. (1959), "Mechanisms of Swelling by Compacted Clay," Highway Research Board Bulletin 245, pp. 10-26.

Ladd, C. C. and Lambe, T. W. (1961), "The Identification and Behavior of Compacted Expansive Clays," Proceedings of the Fifth International Conference on Soil Mechanics and Foundation Engineering, Vol. 1, Paris, pp. 201-206.

Lambe, T. W. (1960), "Compacted Clay, A Symposium--Structure and Engineering Behavior," Transactions, ASCE, Vol. 125, pp. 681-756.

_____. (1961), "Residual Pore Pressure in Compacted Clay," Proceeding of the Fifth International Conference on Soil Mechanics and Foundation Engineering, Vol. 1, Paris, pp. 207-212.

Leonards, G. A. (1962), "Engineering Properties of Soils, "Chapter 2 of Foundation Engineering, edited by G. A. Leonards, McGraw-Hill, New York, pp. 66-240.

Mishu, L. P. (1963), "Collapse in One-Dimensional Compression of Compacted Clay Upon Wetting," MSCE Thesis, Purdue University, West Lafayette, Indiana, August, 105 pp.

Mitchell, J. K. (1976), Fundamentals of Soil Behavior, John Wiley and Sons, New York, 422 pp.

Nalezny, C. L. and Li, M. C. (1967), "Effect of Soil Structure and Thixotropic Hardening on the Swelling Behavior of Compacted Clay Soils," Highway Research Record, No. 209, pp. 1-22.

Neter, J. and Wasserman, W. (1974), Applied Linear Statistical Models, Richard D. Irwin, Inc., Homewood, 842 pp.

Nevels, J. B., Jr. and Laguros, J. G. (1979), "Swelling Characteristics of Compacted B-Horizon Oklahoma Soils," Transportation Research Record, No. 733, pp. 91-94.

Nie, N. H. et al. (1975), SPSS Statistical Package for the Social Sciences, 2nd edition, McGraw-Hill, New York, 675 pp.

Olson, R. E. (1963), "Effective Stress Theory of Soil Compaction," Journal of the Soil Mechanics and Foundations Division, ASCE, Vol. 89, No. SM2, March, pp. 27-45.

Parcher, J. V. and Liu, P. C. (1965), "Some Swelling Characteristics of Compacted Clays." Journal of the Soil Mechanics and Foundations Division, ASCE, Vol. 91, No. SM3, May, pp. 1-17.

Price, J. T. (1978), "Soil Compaction Specification Procedure for Desired Field Strength Response," MSCE Thesis, Purdue University, West Lafayette, Indiana, June, 151 pp.

Proctor, R. R. (1933), "Fundamental Principles of Soil Compaction," Engineering News-Record, Vol. 3, No. 9, August 31, pp. 245-248.

Reed, M. A., Lovell, C. W., Altschaeffl, A. G. and Wood, L. E. (1980), "Frost-Heaving Rate Predicted from Pore Size Distribution," Canadian Geotechnical Journal, Vol. 16, No. 3, pp. 463-472.

Ring, G. W., III (1965), "Shrink-Swell Potentials of Soils," Public Roads, Vol. 33, No. 6, February, pp. 97-105.

Schmertmann, J. H. (1969), "Swell Sensitivity," Geotechnique, Vol. 19, No. 4, December, pp. 530-533.

Scott, J. C. (1977), "Examination of the Variability of the Soaked Strength of a Laboratory Compacted Clay," MSCE Thesis, Purdue University, West Lafayette, Indiana, June, 97 pp.

Seed, H. B. and Chan, C. K. (1961), "Structure and Strength Characteristics of Compacted Clays," Transactions, ASCE, Vol. 126, Part 1, pp. 1343-1407.

Seed, H. B., Lundgren, R. and Chan, C. K. (1954), "Effect of Compaction Method on Stability and Swell Pressure of Soils," Highway Research Board Bulletin 93, pp. 33-48.

Seed, H. B., Mitchell, J. K. and Chan, C. K. (1961), "Studies of Swell and Swell Pressure Characteristics of Compacted Clays," Highway Research Board Bulletin 313, pp. 12-39.

Seed, H. B., Woodward, R. J. and Lundgren, R. (1962), "Prediction of Swelling Potential for Compacted Clays," Journal of the Soil Mechanics and Foundations Division, ASCE, Vol. 88, No. SM3, June, pp. 53-87.

Sridharan, A., Altschaeffl, A. G. and Diamond, S. (1971), "Pore Size Distribution Studies," Journal of the Soil Mechanics and Foundations Division, ASCE, Vol. 97, SM5, pp. 771-787.

Terzaghi, K. (1956), Correspondence, Geotechnique, Vol. 6, No. 4, December, pp. 191-192.

Terzaghi, K. and Peck, R. B. (1967), Soil Mechanics in Engineering Practice, Second edition, John Wiley and Sons, New York, 729 pp.

Uppal, H. L. (1969), "The Laboratory Testing of Expansive Soils," Proceedings of the Second International Research and Engineering Conference on Expansive Clay Soils, College Station, Texas, pp. 121-124.

Weitzel, D. W. (1979), "The Effect of Laboratory Compaction on the Unconsolidated-Undrained Strength Behavior of a Highly Plastic Clay," MSCE Thesis, Purdue University, West Lafayette, Indiana, September, 218 pp.

White, D. M. (1980), "The Fabric of a Medium Plastic Clay Compacted in the Laboratory and in the Field," MSCE Thesis, Purdue University, West Lafayette, Indiana, August, 101 pp.

Woodsum, H. C. (1951), "The Compressibility of Two Compacted Clays," MSCE Thesis, Purdue University, West Lafayette, Indiana, June, 69 pp.

Yevnin, A. and Zaslavsky, D. (1970), "Some Factors Affecting Compacted Clay Swelling," Canadian Geotechnical Journal, Vol. 7, No. 1, February, pp. 79-91.

Yong, R. N. and Sheeran, D. E. (1973), "Fabric Unit Interaction and Soil Behavior," Proceedings of the International Symposium on Soil Structure, Swedish Geotechnical Society, Gothenburg, pp. 176-183.

Yong, R. N. and Warkentin, B. P. (1969), "Flow of Water in Partially Saturated Expansive Soils," Proceedings of the Second International Research and Engineering Conference on Expansive Clay Soils, College Station, Texas, pp. 85-97.

APPENDICES

Appendix A

Presentation of Field and Laboratory Compacted Sample Data

FIELD COMPACTED SAMPLE DATA

-CATERPILLAR COMPACTOR-

SAMPLE NO.	ENERGY RATIO	LIQUID LIMIT (PERCENT)	TEST SPECIMEN WATER CONTENT (PERCENT)	TEST SPECIMEN DRY DENSITY (PCF)	SWELL PRESSURE (PSI)
C1A3	1.0	45.8	15.6	111.7	41.3
C1A4	1.0	42.7	15.7	114.3	30.9
C1A6	1.0	39.1	16.0	110.6	17.3
C2A4	1.0	32.6	18.1	111.7	8.0
C2A5	1.0	41.0	14.0	111.2	19.1
C3A2	1.0	42.5	14.7	111.5	48.0
C3A4	1.0	39.6	15.2	116.0	20.2
C3A5	1.0	32.9	14.7	116.2	13.8
C4A1	1.0	38.3	20.0	106.3	5.6
C4A2	1.0	43.9	17.7	110.5	15.5
C4A3	1.0	39.7	19.1	107.9	6.6
C5A1	1.0	46.0	17.0	112.3	41.2
C5A2	1.0	44.9	16.0	111.1	26.3
C5A6	1.0	41.9	17.4	112.2	14.3
C1B1	2.0	37.1	13.4	119.7	45.6
C1B2	2.0	42.8	13.4	116.9	49.2
C1B4	2.0	38.0	13.5	120.2	49.2
C1B5	2.0	42.0	14.2	117.2	42.6
C1B6	2.0	43.6	13.4	115.7	36.2
C2B2	2.0	38.3	15.0	115.8	33.8
C2B3	2.0	38.8	14.5	116.4	39.9
C2B6	2.0	32.5	12.7	119.4	32.0
C3B4	2.0	41.0	12.0	106.9	15.4
C4B1	2.0	42.8	18.5	111.1	12.5
C4B4	2.0	41.0	17.3	111.5	13.0
C4B5	2.0	44.0	15.4	113.3	30.6
C5B2	2.0	46.1	15.7	115.3	30.0
C5B4	2.0	42.5	18.6	109.1	14.1
C5B5	2.0	42.1	16.7	109.2	15.4
C1C1	4.0	39.6	13.4	119.2	53.2
C1C2	4.0	42.3	14.6	118.1	43.8
C1C5	4.0	38.4	12.7	115.6	17.3
C2C1	4.0	43.0	14.1	117.1	48.0
C2C5	4.0	45.5	13.1	113.3	24.5
C3C2	4.0	39.7	20.4	107.0	6.6
C3C4	4.0	30.0	15.7	117.0	7.2
C3C5	4.0	36.5	14.0	114.3	19.7
C4C3	4.0	44.5	19.0	108.5	8.2
C4C5	4.0	43.5	16.6	112.8	17.1
C4C6	4.0	41.9	15.4	113.9	24.2
C5C1	4.0	45.9	18.5	108.8	18.9
C5C3	4.0	43.0	23.7	101.4	13.8
C5C4	4.0	33.6	17.7	111.4	12.0
C5C5	4.0	41.0	16.2	112.4	17.5

FIELD COMPACTED SAMPLE DATA

-RASCAL COMPACTOR-

SAMPLE NO.	ENERGY RATIO	LIQUID LIMIT (PERCENT)	TEST SPECIMEN WATER CONTENT (PERCENT)	TEST SPECIMEN DRY DENSITY (PCF)	SWELL PRESSURE (PSI)
R1A1	1.0	36.6	13.7	111.6	22.2
R1A3	1.0	37.0	14.1	110.2	11.4
R1A4	1.0	37.2	13.5	110.9	19.9
R1A6	1.0	36.2	14.4	110.6	15.3
R2A1	1.0	34.0	14.1	112.6	12.5
R2A5	1.0	36.1	15.4	109.6	7.0
R2A6	1.0	35.6	15.0	111.4	11.3
R3A2	1.0	40.8	15.9	106.0	5.4
R3A5	1.0	38.0	16.0	111.6	12.0
R3A6	1.0	39.8	14.4	113.2	33.6
R4A2	1.0	51.8	19.5	108.1	15.5
R4A3	1.0	34.0	15.9	113.3	2.6
R4A4	1.0	43.5	19.3	108.6	17.5
R4A5	1.0	45.6	20.9	104.3	7.5
R4A6	1.0	43.4	17.9	108.7	16.8
R5A1	1.0	44.6	20.2	107.2	5.2
R5A3	1.0	36.4	21.0	106.0	8.7
R5A5	1.0	43.0	20.5	105.3	24.0
R5A6	1.0	41.2	19.4	109.7	4.8
R1B1	2.0	33.6	14.2	113.8	25.3
R1B2	2.0	36.4	13.6	113.0	24.7
R1B4	2.0	37.0	16.3	112.5	12.5
R2B1	2.0	38.4	15.7	114.1	10.7
R2B3	2.0	36.5	14.9	116.9	16.0
R2B6	2.0	34.3	15.3	112.8	11.7
R3B4	2.0	39.4	13.8	115.8	37.3
R3B5	2.0	39.2	14.0	113.6	26.0
R4B2	2.0	44.0	16.1	112.9	9.4
R4B3	2.0	42.5	17.0	111.8	13.3
R4B4	2.0	45.2	18.4	111.4	19.5
R5B2	2.0	41.4	21.8	103.0	5.1
R5B4	2.0	42.4	18.9	109.7	15.4
R5B6	2.0	46.6	18.0	110.6	17.3
R1C3	4.0	34.8	15.8	114.8	11.5
R1C4	4.0	37.0	15.0	117.5	17.0
R1C6	4.0	34.2	11.8	111.4	19.8
R2C1	4.0	31.1	12.9	119.6	14.6
R2C2	4.0	37.4	12.6	114.1	11.6
R2C3	4.0	33.0	14.3	114.5	12.8
R2C4	4.0	37.3	14.1	109.0	6.9
R2C5	4.0	37.2	14.0	117.3	15.7
R3C3	4.0	39.8	18.9	110.3	26.9
R3C6	4.0	37.0	14.7	119.0	17.5
R4C1	4.0	47.4	17.6	112.4	19.4
R4C4	4.0	40.7	12.3	114.8	11.4
R4C5	4.0	40.5	18.8	109.4	8.8
R5C3	4.0	42.4	17.2	110.3	15.3
R5C4	4.0	34.6	22.4	102.9	11.6
R5C6	4.0	46.8	23.1	101.9	5.4

LABORATORY COMPACTED SAMPLE DATA

-IMPACT COMPACTOR-

SAMPLE NO.	ENERGY RATIO	TEST SPECIMEN WATER CONTENT (PERCENT)	TEST SPECIMEN DRY DENSITY (PCF)	COMPACTION MOLD WATER CONTENT (PERCENT)	COMPACTION MOLD DRY DENSITY (PCF)	SWELL PRESSURE (PSI)
I1A1	1.00	12.9	101.0	13.2	101.3	11.4
I1A2	1.00	12.6	104.8	12.2	103.7	19.7
I2A1	1.00	14.6	107.6	15.3	104.9	18.0
I2A2	1.00	13.8	106.5	14.2	105.6	16.0
I2A3	1.00	14.5	109.7	14.3	106.2	19.7
I3A2	1.00	16.6	111.1	16.4	110.1	14.7
I3A1	1.00	17.3	110.2	17.8	109.1	9.3
I4A1	1.00	18.1	109.5	18.6	108.5	8.8
I5A1	1.00	19.6	107.0	20.7	107.0	4.5
I6A1	1.00	-0	-0	22.8	102.2	-0
I1B1	1.67	12.8	107.2	13.3	108.1	25.3
I1B2	1.67	12.2	109.9	12.3	108.9	29.3
I2B2	1.67	14.2	112.8	14.5	112.1	24.0
I2B3	1.67	14.4	109.5	14.1	111.6	20.0
I2B1	1.67	15.0	114.6	15.4	112.7	25.3
I3B2	1.67	16.5	113.1	16.6	113.8	17.9
I2'B1	1.67	16.8	111.9	17.1	113.6	10.1
I3B1	1.67	17.0	112.3	17.4	113.2	10.1
I4B1	1.67	17.9	110.5	18.4	111.7	7.7
I5B1	1.67	19.4	107.6	20.5	108.4	4.9
I0*C1	7.58	8.3	118.4	8.1	120.6	102.3
I0C1	7.58	9.4	120.2	9.8	121.6	112.3
I1C2	7.58	7.5	115.7	7.5	119.5	80.6
I2C2	7.58	8.8	117.0	8.6	118.3	96.3
I3C2	7.58	10.2	120.7	9.9	123.3	123.6
I0'C1	7.58	10.8	121.2	10.8	123.6	89.0
I1*C1	7.58	12.1	122.0	12.2	124.9	57.6
I1C1	7.58	12.7	122.6	13.4	123.7	43.9
I2C1	7.58	15.2	116.7	15.3	120.4	18.7
I3C1	7.58	16.6	113.0	17.3	115.0	9.3
I4C1	7.58	17.8	110.8	18.2	113.1	7.5

LABORATORY COMPACTED SAMPLE DATA

-KNEADING COMPACTOR-

SAMPLE NO.	ENERGY RATIO	TEST SPECIMEN WATER CONTENT (PERCENT)	TEST SPECIMEN DRY DENSITY (PCF)	COMPACTION MOLD WATER CONTENT (PERCENT)	COMPACTION MOLD DRY DENSITY (PCF)	SWELL PRESSURE (PSI)
K1A1	1.00	12.9	97.2	13.1	99.1	10.6
K1A2	1.00	12.0	95.6	11.9	98.8	7.7
K2A1	1.00	14.9	103.4	14.8	102.7	12.0
K2A2	1.00	14.3	100.0	14.2	102.5	10.4
K3A2	1.00	15.5	105.0	15.4	103.6	14.4
K3A1	1.00	16.7	108.6	16.8	107.2	10.6
K4A1	1.00	18.1	109.7	18.5	110.6	7.5
K5A1	1.00	19.7	106.6	20.1	108.5	4.0
K6A1	1.00	-0	-0	21.7	104.7	-0
K1B1	1.75	12.8	106.0	12.7	108.9	22.4
K1B2	1.75	11.9	106.3	12.1	105.9	16.5
K2B2	1.75	14.0	110.4	14.0	109.0	24.8
K2B3	1.75	14.1	109.2	14.1	110.0	20.5
K2B1	1.75	15.0	111.2	14.8	112.8	18.6
K3B1	1.75	16.7	112.9	16.7	114.7	10.2
K3B2	1.75	15.8	113.6	15.9	113.1	18.6
K4B1	1.75	18.1	110.2	18.2	113.2	8.0
K5B1	1.75	19.2	107.7	19.1	110.1	3.2
K0*C1	6.50	8.1	113.5	8.1	114.9	71.5
K0C1	6.50	9.8	116.1	9.8	117.6	84.2
K0'C1	6.50	11.0	117.5	10.9	119.7	78.6
K0'C2	6.50	10.4	117.7	10.2	119.2	74.9
K1C2	6.50	7.6	110.1	7.2	114.1	50.5
K2C2	6.50	9.0	112.2	8.8	113.9	77.0
K3C2	6.50	11.5	120.4	11.3	120.6	91.3
K1C1	6.50	12.5	122.6	12.6	124.1	44.7
K2C1	6.50	14.4	118.3	14.4	121.6	17.1

Appendix B

Computer Programs for Evaluating Swell Pressure Variability

An Example of the Computer Programs' Use

The computer programs presented in this appendix are used to evaluate the magnitude and variability of the dry density and swell pressure for field compacted samples. The three programs presented herein are for the Caterpillar compactor, the Rascal A and B energy levels, and the Rascal C energy level, respectively. Programs for laboratory compacted samples were developed but are not included because they are not necessary to implement the procedures developed in this study.

The statistical methods and parameters used in these three programs are discussed and explained in the "Analysis of Data" chapter. Comment cards in the programs also explain the names of variables used and steps taken during the evaluation process. The following is an example of the programs' use.

GIVEN: Statistical prediction models for the dry density and swell pressure of a medium plastic clay. These are developed for the Caterpillar and Rascal compactors used in this study.

DESIRED: Having reviewed the requirements of the project, the design engineer specifies that the soil is to be compacted with 8 passes of the Rascal compactor (E_R = 2.0) 1% wet of the field OMC, with a maximum half-range variability of water content of 1.6%. The engineer wishes to predict the expected and maximum swell pressures to be encountered in the embankment.

ANALYSIS: The engineer selects the computer program for the Rascal A and B energy levels. This program may be used as presented, or the initial values may be changed to include only the values under

consideration (i.e., $\Delta w = +1.0$, $V(\Delta w) = 1.6$, and $E_R = 2.0$). The magnitudes of dry density and swell pressure are evaluated by the program using the appropriate regression equations:

$$\hat{\gamma}_d = -1.378\ \Delta w + 1.044\ E_R + 112.0$$

$$\hat{SP} = 0.2919\ \Delta w^2 + 4.593\ E_R - 0.02357\ \Delta w\ \gamma_d + 9.908\ .$$

To evaluate the variabilities of $\hat{\gamma}_d$ and $\hat{SP}$, the program utilizes the values of $[X'X]^{-1}$ derived from the data sets of this study. See the "Analysis of Data" chapter for a complete explanation of the variability formula and the statistical parameters used. $V(\hat{\gamma}_d)$ is calculated at $\Delta w \pm V(\Delta w)$ and the largest value of $V(\hat{\gamma}_d)$ is chosen. For swell pressure variability, the following conditions are assessed:

Δ	$\hat{\gamma}_d$	$V(\hat{SP})$
$\Delta w + 1.6$	$\hat{\gamma}_d + V(\hat{\gamma}_d)$	$V(\hat{SP})_1$
$\Delta w + 1.6$	$\hat{\gamma}_d - V(\hat{\gamma}_d)$	$V(\hat{SP})_2$
$\Delta w - 1.6$	$\hat{\gamma}_d + V(\hat{\gamma}_d)$	$V(\hat{SP})_3$
$\Delta w - 1.6$	$\hat{\gamma}_d - V(\hat{\gamma}_d)$	$V(\hat{SP})_4$

and the largest value of $V(\hat{SP})$ is selected as the appropriate measure of variability.

SOLUTION: From the computer output:

$$\hat{\gamma}_d{}^{*} = 112.7 \text{ pcf}$$

$$V(\hat{\gamma}_d) = 1.5 \text{ pcf}$$

$$\hat{SP} = 16.7 \text{ psi}$$

---

*This value of $\hat{\gamma}_d$ may need to be adjusted to give the proper value expected in the field. See the "Application of Results".

$$V(\hat{SP}) = 6.7 \text{ psi}$$

$$\hat{SP}_{max} = \hat{SP} + V(\hat{SP}) = 23.5 \text{ psi}$$

Therefore, for the conditions of compaction specified, the average expected swell pressure will be 16.7 psi and the maximum expected swell pressure will be 23.5 psi in the compacted fill.

If these values of swell pressure are not desirable for the project under consideration, the engineer can change the imput values of Δw, $V(\Delta w)$, or E_R until a more suitable swell pressure is attained. As written, the programs automatically increment Δw, $V(\Delta w)$, and E_R; however, if the programs are used to evaluate a single set of Δw, $V(\Delta w)$, and E_R, these values must be changed manually for each run of the program. In this manner the engineer can obtain compaction conditions and values of swell pressure that are compatible with other requirements of the project.

If the engineer wishes to control the expected or maximum swell pressure to some predetermined value, he can obtain the appropriate compaction conditions by using the methods outlined in the "Design Engineering" section. Figures 5.1 thru 5.4 in that section are generated from the data produced by the computer programs presented in this appendix. If he wishes to use the programs to control the allowable swell pressure he must run the programs in their entirety, select the desired values of swell pressure from the output, and choose the conditions of compaction (also presented in the output) which are most appropriate for the project at hand.

The programs presented also generate data which are applicable to quality control work; the "Quality Control" section explains such usage. Some additional notes about the programs are now included.

At OMC ($\Delta w = 0.0$) all parameters are evaluated twice - once using the dry-side regression equations and once using those for the wet side.

For the Caterpillar program, the values of $\hat{SP}$ and $V(\hat{SP})$ do not change for different values of E_R, all other variables remaining constant. This is because the swell pressure is a function of Δw only. The magnitude and variability of dry density wet of OMC do change with E_R, and the output contains these values for quality control work.

These programs should produce sufficient information for most projects. However, if intermediate values of Δw, $V(\Delta w)$, or E_R are required, the programs can be changed to include them. This can be done by changing the initial values, size of the increments, or number of iterations. It must be noted that use of these parameters outside the ranges given in each program constitutes an extrapolation, and must be used with caution.

```
COMPUTER PROGRAM FOR EVALUATING SWELL PRESSURE VARIABILITY, CATERPILLAR
C
C
C  WCO=WATER CONTENT DEVIATION FROM OMC
C  VWCO=EXPECTED WATER CONTENT VARIABILITY (HALF RANGE)
C
C  AD=(X'X)-1 FOR DRY DENSITY, DRY OF OMC
C
C  AW=(X'X)-1 FOR DRY DENSITY, WET OF OMC
C  XDD=VECTOR OF INDEPENDENT VARIABLES FOR DRY DENSITY, DRY OF OMC
C  XDW=VECTOR OF INDEPENDENT VARIABLES FOR DRY DENSITY, WET OF OMC
C  TDD=T-STATISTIC FOR DRY DENSITY, DRY OF OMC
C  TDW=T-STATISTIC FOR DRY DENSITY, WET OF OMC
C  MSEDD=MEAN SQUARE ERROR FOR DRY DENSITY, DRY OF OMC
C  MSEDW=MEAN SQUARE ERROR FOR DRY DENSITY, WET OF OMC
C  VDD=EXPECTED DRY DENSITY VARIABILITY
C
C  BD=(X'X)-1 FOR SWELL PRESSURE, DRY OF OMC
C
C  BW=(X'X)-1 FOR SWELL PRESSURE, WET OF OMC
C  XSD=VECTOR OF INDEPENDENT VARIABLES FOR SP, DRY OF OMC
C  XSW=VECTOR OF INDEPENDENT VARIABLES FOR SP, WET OF OMC
C  TSD=T-STATISTIC FOR SWELL PRESSURE, DRY OF OMC
C  TSW=T-STATISTIC FOR SWELL PRESSURE, WET OF OMC
C  MSESD=MEAN SQUARE ERROR FOR SWELL PRESSURE, DRY OF OMC
C  MSESW=MEAN SQUARE ERROR FOR SWELL PRESSURE, WET OF OMC
C  VSP=EXPECTED SWELL PRESSURE VARIABILITY
C
      REAL MSEDD,MSEDW,MSESD,MSESW
      DIMENSION XDD(2),XDW(3),AD(2,2),AW(3,3),XSD(2),
     $XSW(3),BD(2,2),BW(3,3)
    1 FORMAT(9X,5F10.7/F10.4)
    2 FORMAT(9X,6F10.7,F10.4/F10.4)
    3 FORMAT(///2(24X,2F12.7/)//24X,2F12.4)
    4 FORMAT(///3(24X,3F12.7/)//24X,2F12.4/////)
    5 FORMAT(/X,10F8.1)
C
C  READ DATA
C
      READ  1,AD(1,1),AD(1,2),AD(2,1),AD(2,2),MSEDD,TDD
      READ  2,AW(1,1),AW(1,2),AW(1,3),AW(2,2),AW(2,3),AW(3,3),MSEDW,TDW
      READ  1,BD(1,1),BD(1,2),BD(2,1),BD(2,2),MSESD,TSD
      READ  2,BW(1,1),BW(1,2),BW(1,3),BW(2,2),BW(2,3),BW(3,3),MSESW,TSW
C
C  ASSEMBLE SYMMETRIC MATRICIES
C
      AW(2,1)=AW(1,2)
      AW(3,1)=AW(1,3)
      AW(3,2)=AW(2,3)
      BW(2,1)=BW(1,2)
      BW(3,1)=BW(1,3)
      BW(3,2)=BW(2,3)
      PRINT 3,AD,MSEDD,TDD
      PRINT 4,AW,MSEDW,TDW
      PRINT 3,BD,MSESD,TSD
      PRINT 4,BW,MSESW,TSW
```

```
C
C  SET INITIAL VALUES
C
      XDD(1)=1.0
      XDW(1)=1.0
      XSD(1)=1.0
      XSW(1)=1.0
      DO 30 I=1,3
      IF (I .EQ. 1) ER=1.0
      IF (I .EQ. 2) ER=2.0
      IF (I .EQ. 3) ER=4.0
      PASS=4*ER
      WWCO=0.0
      DO 20 J=1,10
      WWCO=WWCO+0.2
      WCO=-2.5
      DO 10 N=1,27
      WCO=WCO+0.5
C
C  CALCULATE DRY DENSITY VARIABILITY, DRY OF OMC
C
      IF (WCO .GT. 0.0) GO TO 100
      ADD1=ADD2=0.0
      XDD(2)=WCO-WWCO
      ADD1=XDD(1)*AD(1,1)+XDD(2)*AD(2,1)
      ADD2=XDD(1)*AD(1,2)+XDD(2)*AD(2,2)
      SDDSO1=MSEDD*(ADD1*XDD(1)+ADD2*XDD(2))
      SDD1=SQRT(SDDSO1)
      VDD1=SDD1*TDD
      ADD1=ADD2=0.0
      XDD(2)=XDD(2)+(2.0*WWCO)
      ADD1=XDD(1)*AD(1,1)+XDD(2)*AD(2,1)
      ADD2=XDD(1)*AD(1,2)+XDD(2)*AD(2,2)
      SDDSO2=MSEDD*(ADD1*XDD(1)+ADD2*XDD(2))
      SDD2=SQRT(SDDSO2)
      VDD2=SDD2*TDD
      VDD=VDD2
      IF (VDD1 .GT. VDD2) VDD=VDD1
C
C  EVALUATE REGRESSION EQUATION FOR DRY DENSITY, DRY OF OMC
C
      DD=5.853*WCO+118.3
      DDF=0.93*DD
C
C  CALCULATE SWELL PRESSURE VARIABILITY, DRY OF OMC
C
      BSD1=BSD2=0.0
      XSD(2)=WCO-WWCO
      BSD1=XSD(1)*BD(1,1)+XSD(2)*BD(2,1)
      BSD2=XSD(1)*BD(1,2)+XSD(2)*BD(2,2)
      SSDSO1=MSESD*(BSD1*XSD(1)+BSD2*XSD(2))
      SSD1=SQRT(SSDSO1)
      VSD1=SSD1*TSD
      BSD1=BSD2=0.0
      XSD(2)=XSD(2)+(2.0*WWCO)
      BSD1=XSD(1)*BD(1,1)+XSD(2)*BD(2,1)
      BSD2=XSD(1)*BD(1,2)+XSD(2)*BD(2,2)
      SSDSO2=MSESD*(BSD1*XSD(1)+BSD2*XSD(2))
      SSD2=SQRT(SSDSO2)
      VSD2=SSD2*TSD
      VSP=VSD2
      IF (VSD1 .GT. VSD2) VSP=VSD1
C
C  EVALUATE REGRESSION EQUATION FOR SWELL PRESSURE, DRY OF OMC
C
      SP=21.72*WCO+44.12
      SPMAX=SP+VSP
      GO TO 200
```

```
C
C  CALCULATE DRY DENSITY VARIABILITY, WET OF OMC
C
  100 IF (N .EQ. 6) WCO=0.0
      ADW1=ADW2=ADW3=0.0
      XDW(2)=WCO-UWCO
      XDW(3)=ER
      ADW1=XDW(1)*AW(1,1)+XDW(2)*AW(2,1)+XDW(3)*AW(3,1)
      ADW2=XDW(1)*AW(1,2)+XDW(2)*AW(2,2)+XDW(3)*AW(3,2)
      ADW3=XDW(1)*AW(1,3)+XDW(2)*AW(2,3)+XDW(3)*AW(3,3)
      SDWSQ1=MSEDW*(ADW1*XDW(1)+ADW2*XDW(2)+ADW3*XDW(3))
      SDW1=SQRT(SDWSQ1)
      VDW1=SDW1*TDW
      ADW1=ADW2=ADW3=0.0
      XDW(2)=XDW(2)+(2.0*UWCO)
      ADW1=XDW(1)*AW(1,1)+XDW(2)*AW(2,1)+XDW(3)*AW(3,1)
      ADW2=XDW(1)*AW(1,2)+XDW(2)*AW(2,2)+XDW(3)*AW(3,2)
      ADW3=XDW(1)*AW(1,3)+XDW(2)*AW(2,3)+XDW(3)*AW(3,3)
      SDWSQ2=MSEDW*(ADW1*XDW(1)+ADW2*XDW(2)+ADW3*XDW(3))
      SDW2=SQRT(SDWSQ2)
      VDW2=SDW2*TDW
      VDD=VDW2
      IF (VDW1 .GT. VDW2) VDD=VDW1
C
C  EVALUATE REGRESSION EQUATION FOR DRY DENSITY, WET OF OMC
C
      DD=-1.609*WCO+1.006*ER+114.3
      DDF=0.93*DD
C
C  CALCULATE SWELL PRESSURE VARIABILITY, WET OF OMC
C
      BSW1=BSW2=BSW3=0.0
      XSW(2)=WCO-UWCO
      XSW(3)=XSW(2)**2
      BSW1=XSW(1)*BW(1,1)+XSW(2)*BW(2,1)+XSW(3)*BW(3,1)
      BSW2=XSW(1)*BW(1,2)+XSW(2)*BW(2,2)+XSW(3)*BW(3,2)
      BSW3=XSW(1)*BW(1,3)+XSW(2)*BW(2,3)+XSW(3)*BW(3,3)
      SSWSQ1=MSESW*(BSW1*XSW(1)+BSW2*XSW(2)+BSW3*XSW(3))
      SSW1=SQRT(SSWSQ1)
      VSW1=SSW1*TSW
      BSW1=BSW2=BSW3=0.0
      XSW(2)=XSW(2)+(2.0*UWCO)
      XSW(3)=XSW(2)**2
      BSW1=XSW(1)*BW(1,1)+XSW(2)*BW(2,1)+XSW(3)*BW(3,1)
      BSW2=XSW(1)*BW(1,2)+XSW(2)*BW(2,2)+XSW(3)*BW(3,2)
      BSW3=XSW(1)*BW(1,3)+XSW(2)*BW(2,3)+XSW(3)*BW(3,3)
      SSWSQ2=MSESW*(BSW1*XSW(1)+BSW2*XSW(2)+BSW3*XSW(3))
      SSW2=SQRT(SSWSQ2)
      VSW2=SSW2*TSW
      VSP=VSW2
      IF (VSW1 .GT. VSW2) VSP=VSW1
C
C  EVALUATE REGRESSION EQUATION FOR SWELL PRESSURE, WET OF OMC
C
      WCO2=WCO*WCO
      SP=-10.87*WCO+0.7998*WCO2+43.08
      SPMAX=SP+VSP
  200 PRINT 5,UWCO,WCO,PASS,ER,DD,DDF,VDD,SP,VSP,SPMAX
   10 CONTINUE
   20 CONTINUE
   30 CONTINUE
      END
```

```
C
C  THE PRINTED DATA MATRICIES FOLLOW
C
```

```
 .1784300    .1967400
 .1967400    .4070600

   9.9970      2.2280

 .1555000   -.0109300   -.0386600
-.0109300    .0066660   -.0030680
-.0386600   -.0030680    .0192100

   2.7190      2.0420
```

```
 .1784300    .1967400
 .1967400    .4070600

   9.9970      2.2280

 .0837600   -.0385100    .0033470
-.0385100    .0311400   -.0033620
 .0033470   -.0033620    .0004353

  74.0580      2.0340
```

```
COMPUTER PROGRAM FOR EVALUATING SWELL PRESSURE VARIABILITY, RASCAL A+B
C
C
C  WCO=WATER CONTENT DEVIATION FROM OMC
C  VWCO=EXPECTED WATER CONTENT VARIABILITY (HALF RANGE)
C
C  AD=(X'X)^-1 FOR DRY DENSITY, DRY OF OMC
C
C  AW=(X'X)^-1 FOR DRY DENSITY, WET OF OMC
C  XDD=VECTOR OF INDEPENDENT VARIABLES FOR DRY DENSITY, DRY OF OMC
C  XDW=VECTOR OF INDEPENDENT VARIABLES FOR DRY DENSITY, WET OF OMC
C  TDD=T-STATISTIC FOR DRY DENSITY, DRY OF OMC
C  TDW=T-STATISTIC FOR DRY DENSITY, WET OF OMC
C  MSEDD=MEAN SQUARE ERROR FOR DRY DENSITY, DRY OF OMC
C  MSEDW=MEAN SQUARE ERROR FOR DRY DENSITY, WET OF OMC
C  VDD=EXPECTED DRY DENSITY VARIABILITY
C
C  B=(X'X)^-1 FOR SWELL PRESSURE
C  XS=VECTOR OF INDEPENDENT VARIABLES FOR SWELL PRESSURE
C  TSP=T-STATISTIC FOR SWELL PRESSURE
C  MSESP=MEAN SQUARE ERROR FOR SWELL PRESSURE
C  VSP=EXPECTED SWELL PRESSURE VARIABILITY
C
      REAL MSEDD,MSEDW,MSESP
      DIMENSION XDD(3),XDW(3),AD(3,3),AW(3,3),XS(4),B(4,4)
    1 FORMAT(9X,6F10.7,F10.4/F10.4)
    2 FORMAT(9X,4F15.11/5F15.11/F15.11,F10.4/F10.4)
    3 FORMAT(///3(24X,3F12.7/)//24X,2F12.4)
    4 FORMAT(///4(24X,4F15.10/)//24X,2F15.4/////)
    5 FORMAT(/X,10F8.1)
C
C  READ DATA
C
      READ  1,AD(1,1),AD(1,2),AD(1,3),AD(2,2),AD(2,3),AD(3,3),MSEDD,TDD
      READ  1,AW(1,1),AW(1,2),AW(1,3),AW(2,2),AW(2,3),AW(3,3),MSEDW,TDW
      READ  2,B(1,1),B(1,2),B(1,3),B(1,4),B(2,2),B(2,3),B(2,4),B(3,3),
     $B(3,4),B(4,4),MSESP,TSP
C
C  ASSEMBLE SYMMETRIC MATRICIES
C
      AD(2,1)=AD(1,2)
      AD(3,1)=AD(1,3)
      AD(3,2)=AD(2,3)
      AW(2,1)=AW(1,2)
      AW(3,1)=AW(1,3)
      AW(3,2)=AW(2,3)
      B(2,1)=B(1,2)
      B(3,1)=B(1,3)
      B(3,2)=B(2,3)
      B(4,1)=B(1,4)
      B(4,2)=B(2,4)
      B(4,3)=B(3,4)
      PRINT 3,AD,MSEDD,TDD
      PRINT 3,AW,MSEDW,TDW
      PRINT 4,B,MSESP,TSP
```

```
C
C  SET INITIAL VALUES
C
      XDD(1)=1.0
      XDW(1)=1.0
      XS(1)=1.0
      DO 30 I=1,2
      IF (I .EQ. 1) ER=1.0
      IF (I .EQ. 2) ER=2.0
      PASS=4*ER
      VWCO=0.0
      DO 20 J=1,10
      VWCO=VWCO+0.2
      WCO=-3.0
      DO 10 N=1,21
      WCO=WCO+0.5
C
C  CALCULATE DRY DENSITY VARIABILITY, DRY OF OMC
C
      IF (WCO .GT. 0.0) GO TO 100
      ADD1=ADD2=ADD3=0.0
      XDD(2)=WCO-VWCO
      XDD(3)=ER
      ADD1=XDD(1)*AD(1,1)+XDD(2)*AD(2,1)+XDD(3)*AD(3,1)
      ADD2=XDD(1)*AD(1,2)+XDD(2)*AD(2,2)+XDD(3)*AD(3,2)
      ADD3=XDD(1)*AD(1,3)+XDD(2)*AD(2,3)+XDD(3)*AD(3,3)
      SDDSQ1=MSEDD*(ADD1*XDD(1)+ADD2*XDD(2)+ADD3*XDD(3))
      SDD1=SQRT(SDDSQ1)
      VDD1=SDD1*TDD
      ADD1=ADD2=ADD3=0.0
      XDD(2)=XDD(2)+(2.0*VWCO)
      ADD1=XDD(1)*AD(1,1)+XDD(2)*AD(2,1)+XDD(3)*AD(3,1)
      ADD2=XDD(1)*AD(1,2)+XDD(2)*AD(2,2)+XDD(3)*AD(3,2)
      ADD3=XDD(1)*AD(1,3)+XDD(2)*AD(2,3)+XDD(3)*AD(3,3)
      SDDSQ2=MSEDD*(ADD1*XDD(1)+ADD2*XDD(2)+ADD3*XDD(3))
      SDD2=SQRT(SDDSQ2)
      VDD2=SDD2*TDD
      VDD=VDD2
      IF (VDD1 .GT. VDD2) VDD=VDD1
C
C  EVALUATE REGRESSION EQUATION FOR DRY DENSITY, DRY OF OMC
C
      DD=1.906*WCO+1.390*ER+112.5
      DDF=0.93*DD
      GO TO 200
C
C  CALCULATE DRY DENSITY VARIABILITY, WET OF OMC
C
  100 IF (N .EQ. 7) WCO=0.0
      ADW1=ADW2=ADW3=0.0
      XDW(2)=WCO-VWCO
      XDW(3)=ER
      ADW1=XDW(1)*AW(1,1)+XDW(2)*AW(2,1)+XDW(3)*AW(3,1)
      ADW2=XDW(1)*AW(1,2)+XDW(2)*AW(2,2)+XDW(3)*AW(3,2)
      ADW3=XDW(1)*AW(1,3)+XDW(2)*AW(2,3)+XDW(3)*AW(3,3)
      SDWSQ1=MSEDW*(ADW1*XDW(1)+ADW2*XDW(2)+ADW3*XDW(3))
      SDW1=SQRT(SDWSQ1)
      VDW1=SDW1*TDW
      ADW1=ADW2=ADW3=0.0
      XDW(2)=XDW(2)+(2.0*VWCO)
      ADW1=XDW(1)*AW(1,1)+XDW(2)*AW(2,1)+XDW(3)*AW(3,1)
      ADW2=XDW(1)*AW(1,2)+XDW(2)*AW(2,2)+XDW(3)*AW(3,2)
      ADW3=XDW(1)*AW(1,3)+XDW(2)*AW(2,3)+XDW(3)*AW(3,3)
      SDWSQ2=MSEDW*(ADW1*XDW(1)+ADW2*XDW(2)+ADW3*XDW(3))
      SDW2=SQRT(SDWSQ2)
      VDW2=SDW2*TDW
      VDD=VDW2
      IF (VDW1 .GT. VDW2) VDD=VDW1
```

```
C
C  EVALUATE REGRESSION EQUATION FOR DRY DENSITY, WET OF OMC
C
      DD=-1.378*WCO+1.044*ER+112.0
      DDF=0.93*DD

C
C  EVALUATE REGRESSION EQUATION FOR SWELL PRESSURE
C
  200 WD=WCO*DD
      WCO2=WCO*WCO
      SP=0.2919*WCO2+4.593*ER-0.02357*WD+9.908
C
C  CALCULATE SWELL PRESSURE VARIABILITY
C
      Z1=Z2=Z3=Z4=0.0
      XS(2)=(WCO+UWCO)**2
      XS(3)=(WCO+UWCO)*(DD+UDD)
      XS(4)=ER
      Z1=XS(1)*B(1,1)+XS(2)*B(2,1)+XS(3)*B(3,1)+XS(4)*B(4,1)
      Z2=XS(1)*B(1,2)+XS(2)*B(2,2)+XS(3)*B(3,2)+XS(4)*B(4,2)
      Z3=XS(1)*B(1,3)+XS(2)*B(2,3)+XS(3)*B(3,3)+XS(4)*B(4,3)
      Z4=XS(1)*B(1,4)+XS(2)*B(2,4)+XS(3)*B(3,4)+XS(4)*B(4,4)
      SSPSQ1=MSESP*(Z1*XS(1)+Z2*XS(2)+Z3*XS(3)+Z4*XS(4))
      SSP1=SQRT(SSPSQ1)
      U1=SSP1*TSP
      Z1=Z2=Z3=Z4=0.0
      XS(2)=(WCO+UWCO)**2
      XS(3)=(WCO+UWCO)*(DD-UDD)
      Z1=XS(1)*B(1,1)+XS(2)*B(2,1)+XS(3)*B(3,1)+XS(4)*B(4,1)
      Z2=XS(1)*B(1,2)+XS(2)*B(2,2)+XS(3)*B(3,2)+XS(4)*B(4,2)
      Z3=XS(1)*B(1,3)+XS(2)*B(2,3)+XS(3)*B(3,3)+XS(4)*B(4,3)
      Z4=XS(1)*B(1,4)+XS(2)*B(2,4)+XS(3)*B(3,4)+XS(4)*B(4,4)
      SSPSQ2=MSESP*(Z1*XS(1)+Z2*XS(2)+Z3*XS(3)+Z4*XS(4))
      SSP2=SQRT(SSPSQ2)
      U2=SSP2*TSP
      Z1=Z2=Z3=Z4=0.0
      XS(2)=(WCO-UWCO)**2
      XS(3)=(WCO-UWCO)*(DD+UDD)
      Z1=XS(1)*B(1,1)+XS(2)*B(2,1)+XS(3)*B(3,1)+XS(4)*B(4,1)
      Z2=XS(1)*B(1,2)+XS(2)*B(2,2)+XS(3)*B(3,2)+XS(4)*B(4,2)
      Z3=XS(1)*B(1,3)+XS(2)*B(2,3)+XS(3)*B(3,3)+XS(4)*B(4,3)
      Z4=XS(1)*B(1,4)+XS(2)*B(2,4)+XS(3)*B(3,4)+XS(4)*B(4,4)
      SSPSQ3=MSESP*(Z1*XS(1)+Z2*XS(2)+Z3*XS(3)+Z4*XS(4))
      SSP3=SQRT(SSPSQ3)
      U3=SSP3*TSP
      Z1=Z2=Z3=Z4=0.0
      XS(2)=(WCO-UWCO)**2
      XS(3)=(WCO-UWCO)*(DD-UDD)
      Z1=XS(1)*B(1,1)+XS(2)*B(2,1)+XS(3)*B(3,1)+XS(4)*B(4,1)
      Z2=XS(1)*B(1,2)+XS(2)*B(2,2)+XS(3)*B(3,2)+XS(4)*B(4,2)
      Z3=XS(1)*B(1,3)+XS(2)*B(2,3)+XS(3)*B(3,3)+XS(4)*B(4,3)
      Z4=XS(1)*B(1,4)+XS(2)*B(2,4)+XS(3)*B(3,4)+XS(4)*B(4,4)
      SSPSQ4=MSESP*(Z1*XS(1)+Z2*XS(2)+Z3*XS(3)+Z4*XS(4))
      SSP4=SQRT(SSPSQ4)
      U4=SSP4*TSP
      USP=U4
      IF(U1.GE.U2.AND.U1.GE.U3.AND.U1.GE.U4) USP=U1
      IF(U2.GE.U1.AND.U2.GE.U3.AND.U2.GE.U4) USP=U2
      IF(U3.GE.U1.AND.U3.GE.U2.AND.U3.GE.U4) USP=U3
      SPMAX=SP+USP
      PRINT 5,UWCO,WCO,PASS,ER,DD,DDF,UDD,SP,USP,SPMAX
   10 CONTINUE
   20 CONTINUE
   30 CONTINUE
      END
```

```
C
C  THE PRINTED DATA MATRICIES FOLLOW
C
```

```
 .4563000    .2148000   -.0702000
 .2148000    .2167000    .0126500
-.0702000    .0126500    .0385600

   2.9610      2.1600


 .1694000   -.0141700   -.0416900
-.0141700    .0049280   -.0001762
-.0416900   -.0001762    .0179400

   5.4380      2.0400


 .3196000000   -.0048720000    .0001175000   -.1871000000
-.0048720000    .0009815000   -.0000388300    .0019670000
 .0001175000   -.0000388300    .0000019580   -.0000740000
-.1871000000    .0019670000   -.0000740000    .1280000000

     55.4250         2.6830
```

```
COMPUTER PROGRAM FOR EVALUATING SWELL PRESSURE VARIABILITY, RASCAL C
C
C
C  WCO=WATER CONTENT DEVIATION FROM OMC
C  VWCO=EXPECTED WATER CONTENT VARIABILITY (HALF RANGE)
C
C  AD=(X'X)^-1 FOR DRY DENSITY, DRY OF OMC
C
C  AW=(X'X)^-1 FOR DRY DENSITY, WET OF OMC
C  XDD=VECTOR OF INDEPENDENT VARIABLES FOR DRY DENSITY, DRY OF OMC
C  XDW=VECTOR OF INDEPENDENT VARIABLES FOR DRY DENSITY, WET OF OMC
C  TDD=T-STATISTIC FOR DRY DENSITY, DRY OF OMC
C  TDW=T-STATISTIC FOR DRY DENSITY, WET OF OMC
C  MSEDD=MEAN SQUARE ERROR FOR DRY DENSITY, DRY OF OMC
C  MSEDW=MEAN SQUARE ERROR FOR DRY DENSITY, WET OF OMC
C  VDD=EXPECTED DRY DENSITY VARIABILITY
C
C  B=(X'X)^-1 FOR SWELL PRESSURE
C  XS=VECTOR OF INDEPENDENT VARIABLES FOR SWELL PRESSURE
C  TSP=T-STATISTIC FOR SWELL PRESSURE
C  MSESP=MEAN SQUARE ERROR FOR SWELL PRESSURE
C  VSP=EXPECTED SWELL PRESSURE VARIABILITY
C
      REAL MSEDD,MSEDW,MSESP
      DIMENSION XDD(3),XDW(3),AD(3,3),AW(3,3),XS(3),B(3,3)
    1 FORMAT(9X,6F10.7,F10.4/F10.4)
    2 FORMAT(9X,6F10.7,F10.4/F10.4)
    3 FORMAT(///3(24X,3F12.7/)//24X,2F12.4)
    4 FORMAT(///3(24X,3F12.7/)//24X,2F12.4/////)
    5 FORMAT(/X,10F8.1)
C
C  READ DATA
C
      READ  1,AD(1,1),AD(1,2),AD(1,3),AD(2,2),AD(2,3),AD(3,3),MSEDD,TDD
      READ  1,AW(1,1),AW(1,2),AW(1,3),AW(2,2),AW(2,3),AW(3,3),MSEDW,TDW
      READ  2,B(1,1),B(1,2),B(1,3),B(2,2),B(2,3),B(3,3),MSESP,TSP
C
C  ASSEMBLE SYMMETRIC MATRICIES
C
      AD(2,1)=AD(1,2)
      AD(3,1)=AD(1,3)
      AD(3,2)=AD(2,3)
      AW(2,1)=AW(1,2)
      AW(3,1)=AW(1,3)
      AW(3,2)=AW(2,3)
      B(2,1)=B(1,2)
      B(3,1)=B(1,3)
      B(3,2)=B(2,3)
      PRINT 3,AD,MSEDD,TDD
      PRINT 3,AW,MSEDW,TDW
      PRINT 4,B,MSESP,TSP
C
C  SET INITIAL VALUES
C
      XDD(1)=1.0
      XDW(1)=1.0
      XS(1)=1.0
      ER=4.0
      PASS=4*ER
      VWCO=0.0
      DO 20 J=1,10
      VWCO=VWCO+0.2
      WCO=-2.5
      DO 10 N=1,25
      WCO=WCO+0.5
```

```
C
C  CALCULATE DRY DENSITY VARIABILITY, DRY OF OMC
C
      IF (WCO .GT. 0.0) GO TO 100
      ADD1=ADD2=ADD3=0.0
      XDD(2)=WCO-UWCO
      XDD(3)=ER
      ADD1=XDD(1)*AD(1,1)+XDD(2)*AD(2,1)+XDD(3)*AD(3,1)
      ADD2=XDD(1)*AD(1,2)+XDD(2)*AD(2,2)+XDD(3)*AD(3,2)
      ADD3=XDD(1)*AD(1,3)+XDD(2)*AD(2,3)+XDD(3)*AD(3,3)
      SDDSQ1=MSEDD*(ADD1*XDD(1)+ADD2*XDD(2)+ADD3*XDD(3))
      SDD1=SQRT(SDDSQ1)
      VDD1=SDD1*TDD
      ADD1=ADD2=ADD3=0.0
      XDD(2)=XDD(2)+(2.0*UWCO)
      ADD1=XDD(1)*AD(1,1)+XDD(2)*AD(2,1)+XDD(3)*AD(3,1)
      ADD2=XDD(1)*AD(1,2)+XDD(2)*AD(2,2)+XDD(3)*AD(3,2)
      ADD3=XDD(1)*AD(1,3)+XDD(2)*AD(2,3)+XDD(3)*AD(3,3)
      SDDSQ2=MSEDD*(ADD1*XDD(1)+ADD2*XDD(2)+ADD3*XDD(3))
      SDD2=SQRT(SDDSQ2)
      VDD2=SDD2*TDD
      VDD=VDD2
      IF (VDD1 .GT. VDD2) VDD=VDD1
C
C  EVALUATE REGRESSION EQUATION FOR DRY DENSITY, DRY OF OMC
C
      DD=1.906*WCO+1.390*ER+112.5
      DDF=0.93*DD
      GO TO 200
C
C  CALCULATE DRY DENSITY VARIABILITY, WET OF OMC
C
  100 IF (N .EQ. 6) WCO=0.0
      ADW1=ADW2=ADW3=0.0
      XDW(2)=WCO-UWCO
      XDW(3)=ER
      ADW1=XDW(1)*AW(1,1)+XDW(2)*AW(2,1)+XDW(3)*AW(3,1)
      ADW2=XDW(1)*AW(1,2)+XDW(2)*AW(2,2)+XDW(3)*AW(3,2)
      ADW3=XDW(1)*AW(1,3)+XDW(2)*AW(2,3)+XDW(3)*AW(3,3)
      SDWSQ1=MSEDW*(ADW1*XDW(1)+ADW2*XDW(2)+ADW3*XDW(3))
      SDW1=SQRT(SDWSQ1)
      VDW1=SDW1*TDW
      ADW1=ADW2=ADW3=0.0
      XDW(2)=XDW(2)+(2.0*UWCO)
      ADW1=XDW(1)*AW(1,1)+XDW(2)*AW(2,1)+XDW(3)*AW(3,1)
      ADW2=XDW(1)*AW(1,2)+XDW(2)*AW(2,2)+XDW(3)*AW(3,2)
      ADW3=XDW(1)*AW(1,3)+XDW(2)*AW(2,3)+XDW(3)*AW(3,3)
      SDWSQ2=MSEDW*(ADW1*XDW(1)+ADW2*XDW(2)+ADW3*XDW(3))
      SDW2=SQRT(SDWSQ2)
      VDW2=SDW2*TDW
      VDD=VDW2
      IF (VDW1 .GT. VDW2) VDD=VDW1
C
C  EVALUATE REGRESSION EQUATION FOR DRY DENSITY, WET OF OMC
C
      DD=-1.378*WCO+1.044*ER+112.0
      DDF=0.93*DD
```

```
C
C  EVALUATE REGRESSION EQUATION FOR SWELL PRESSURE
C
  200 WD=WCO*DD
      SP=-16.08*WCO+0.1501*WD+14.50
C
C  CALCULATE SWELL PRESSURE VARIABILITY
C
      Z1=Z2=Z3=0.0
      XS(2)=WCO+VWCO
      XS(3)=(WCO+VWCO)*(DD+VDD)
      Z1=XS(1)*B(1,1)+XS(2)*B(2,1)+XS(3)*B(3,1)
      Z2=XS(1)*B(1,2)+XS(2)*B(2,2)+XS(3)*B(3,2)
      Z3=XS(1)*B(1,3)+XS(2)*B(2,3)+XS(3)*B(3,3)
      SSPSQ1=MSESP*(Z1*XS(1)+Z2*XS(2)+Z3*XS(3))
      SSP1=SQRT(SSPSQ1)
      V1=SSP1*TSP
      Z1=Z2=Z3=0.0
      XS(2)=WCO+VWCO
      XS(3)=(WCO+VWCO)*(DD-VDD)
      Z1=XS(1)*B(1,1)+XS(2)*B(2,1)+XS(3)*B(3,1)
      Z2=XS(1)*B(1,2)+XS(2)*B(2,2)+XS(3)*B(3,2)
      Z3=XS(1)*B(1,3)+XS(2)*B(2,3)+XS(3)*B(3,3)
      SSPSQ2=MSESP*(Z1*XS(1)+Z2*XS(2)+Z3*XS(3))
      SSP2=SQRT(SSPSQ2)
      V2=SSP2*TSP
      Z1=Z2=Z3=0.0
      XS(2)=WCO-VWCO
      XS(3)=(WCO-VWCO)*(DD+VDD)
      Z1=XS(1)*B(1,1)+XS(2)*B(2,1)+XS(3)*B(3,1)
      Z2=XS(1)*B(1,2)+XS(2)*B(2,2)+XS(3)*B(3,2)
      Z3=XS(1)*B(1,3)+XS(2)*B(2,3)+XS(3)*B(3,3)
      SSPSQ3=MSESP*(Z1*XS(1)+Z2*XS(2)+Z3*XS(3))
      SSP3=SQRT(SSPSQ3)
      V3=SSP3*TSP
      Z1=Z2=Z3=0.0
      XS(2)=WCO-VWCO
      XS(3)=(WCO-VWCO)*(DD-VDD)
      Z1=XS(1)*B(1,1)+XS(2)*B(2,1)+XS(3)*B(3,1)
      Z2=XS(1)*B(1,2)+XS(2)*B(2,2)+XS(3)*B(3,2)
      Z3=XS(1)*B(1,3)+XS(2)*B(2,3)+XS(3)*B(3,3)
      SSPSQ4=MSESP*(Z1*XS(1)+Z2*XS(2)+Z3*XS(3))
      SSP4=SQRT(SSPSQ4)
      V4=SSP4*TSP
      VSP=V4
      IF(V1.GE.V2.AND.V1.GE.V3.AND.V1.GE.V4) VSP=V1
      IF(V2.GE.V1.AND.V2.GE.V3.AND.V2.GE.V4) VSP=V2
      IF(V3.GE.V1.AND.V3.GE.V2.AND.V3.GE.V4) VSP=V3
      SPMAX=SP+VSP
      PRINT 5,VWCO,WCO,PASS,ER,DD,DDF,VDD,SP,VSP,SPMAX
   10 CONTINUE
   20 CONTINUE
      END
```

```
C  THE PRINTED DATA MATRICIES FOLLOW
C
```

.4563000	.2148000	-.0702000
.2148000	.2167000	.0126500
-.0702000	.0126500	.0385600

2.9610	2.1600

.1694000	-.0141700	-.0416900
-.0141700	.0049280	-.0001762
-.0416900	-.0001762	.0179400

5.4380	2.0400

.0846000	.0131500	-.0002302
.0131500	2.4095000	-.0228100
-.0002302	-.0228100	.0002165

24.3200	2.5680

COVER DESIGN BY ALDO GIORGINI